Development of the silique of Arabidopsis Thaliana

Jacqueline Spence

ABSTRACT

Using the silique of *Arabidopsis* as a model system, we are studying fruit development by a combination of cytological, cytochemical and molecular techniques. Within the floral bud the early gynoecium develops with differentiation of two major vascular bundles and two meristematic regions. The latter give rise to the ovules and combine to form the septum which separates the two loculi of the maturing fruit. Development of the carpel walls results in the differentiation of three specific layers, the endocarp, the mesocarp and the exocarp. After fertilisation absicission zones form between the carpel walls and the major vascular supplies to the developing ovules. The patterns of differentiation result in the dehiscence mechanism which disperses seeds from the shattering fruit. Such fruit shatter and seed dispersal mechanisms represent significant problems in a number of agricultural crops causing loss of seed yield and the distribution of volunteers.

We have described the cytological events associated with the differentiation of the major tissue types associated with carpel and septal development, and identified a number of probes which act, by immunocytochemistry, *in situ* hybridisation or enzymecytochemistry, as appropriate markers for specific phases of differentiation. We have compared the development of the meristic *clv1* mutant, which shows anomalies in gynoecial development, with that of wild type, and are screening EMS-mutated stock for other variants of fruit development.

DEVELOPMENT OF THE SILIQUE OF *ARABIDOPSIS THALIANA*

Student Jaqueline Spence

Supervisor Dr.N.Harris

Submitted for the Degree of Master of Science
Department of Biological Sciences
University of Durham

CONTENTS

ACKNOWLEDGEMENTS 1
LIST OF FIGURES 2
LIST OF TABLES 2
MEMORANDUM 3
INTRODUCTION 4
ARABIDOPSIS THALIANA 5
FLORAL DEVELOPMENT 6
THE FLOWER 6
THE INFLORESCENCE 9
SIMILAR SYSTEMS 10
FRUIT DEVELOPMENT 10
PRE-FERTILISATION 11
POST-FERTILISATION 12
PROJECT AIMS 13
ABBREVIATIONS 15
MATERIALS AND METHODS 17
STANDARD SOLUTIONS 18
PLANT MATERIAL 20
TISSUE PREPARATION 20
ALDEHYDE FIXATION 20
DEHYDRATION 20
TISSUE EMBEDDING 20
PEG 1000 20
WAX 21
LR WHITE 21
SCANNING ELECTRON MICROSCOPY (SEM) 21
SECTIONING 22
SLIDE PREPARATION 22
EMBEDDED MATERIAL 22
CRYOSECTIONING 22
DEWAXING 22
HISTOCHEMISTRY 23
ACRIDINE ORANGE 23
ALKALINE PHOSPHATASE 23
GENERAL ESTERASE 23
METHYL GREEN PYRONIN 23
PHENOL OXIDASE 23
TOLUIDINE BLUE 24
IMMUNOCYTOCHEMISTRY 24
MONOCLONAL ANTIBODIES 24
FLUORESCENT DETECTION 24
IMMUNOGOLD/SILVER DETECTION 24
MOLECULAR HISTOCHEMISTRY 25
PLASMID PREPARATION 25
PREPARATION OF AT53 PLASMID USING PROMEGA MAGIC MINIPREP 25
PREPARATION OF BIN19 PLASMID USING QIAGEN TIP 25
RESTRICTION DIGEST OF PLASMID DNA 26
PHENOL/CHLOROFORM EXTRACTION OF DNA 26
LABELLING dsDNA PROBES USING BOEHRINGER MANHEIM DIG LABELLING KIT 27
IN-SITU HYBRIDISATION 27
RESULTS 29
DEVELOPMENT OF THE ARABIDOPSIS GYNOECIUM 29
HISTOCHEMISTRY OF THE PRE-FERTILISED FRUIT 40

ESTERASE 40
PHENOL OXIDASE 40
IMMUNOCYTOCHEMISTRY OF THE PRE-FERTILISED FRUIT 43
PECTIN ANTIBODIES 43
GLYCOPROTEIN ANTIBODIES 43
AGP ANTIBODIES 43
PROTEASE 46
RUBISCO (RIBULOSE 1, 5, BIS PHOSPHATE CARBOXYLASE) 46
MOLECULAR HISTOCHEMISTRY OF THE PRE-FERTILISED FRUIT 46
CELLULASE (ß 1, 4, GLUCONASE) 46
PECTINESTERASE 49
POLYGALACTURONASE 49
DEVELOPMENT OF THE ARABIDOPSIS SILIQUE 52
HISTOCHEMISTRY OF THE POST FERTILISED FRUIT 63
ESTERASE 63
PHENOL OXIDASE 63
IMMUNOCYTOCHEMISTRY OF THE POST-FERTILISED FRUIT 63
PECTIN ANTIBODIES 63
GLYCOPROTEIN ANTIBODIES 68
AGP ANTIBODIES 68
PROTEASE 68
RUBISCO 71
MOLECULAR HISTOCHEMISTRY OF THE POST-FERTILISED FRUIT 71
CELLULASE 71
PECTINESTERASE 71
POLYGALACTURONASE 74
DEVELOPMENT OF THE CLAVATA1 (CLV1) MUTANT SILIQUE 79
MODEL DEVELOPMENT OF THE CLV1 SILIQUE 79
GYNOECIAL FASCIATIONS 84
THE VESTIGIAL GYNOECIUM 89
EMS GENERATED MUTANTS 97
MUTANT 003 97
MUTANT 006 100
MUTANT 007 100
DISCUSSION 106
APPENDIX 1 112
TISSUE PREPARATION 113
DETECTION METHODS 114
REFERENCES 115

ACKNOWLEDGEMENTS

This thesis would not have been possible without the support of the following people. My sincere and heartfelt thanks go to all of them.

Special thanks to my supervisor Dr. Nick Harris for his confidence, patience, expertise and guidance throughout this project.

Mr. J. Davies, Mrs. L. Edwards and Dr. Y. Vercher for their boundless enthusiasm, terrible jokes and for helping me get to grips with the subject of botany.

Dr. W. Schuch for providing the cellulase and polygalacturonase cDNA probes, Dr. J. Gatehouse and Mr. D. Bown for providing the pectinesterase cDNA probe and Dr. M. Cercos for providing the Protease and Rubisco antibodies.

Finally special thanks to my family and friends for their encouragement and support and for keeping my feet so firmly on the ground (it often felt as if they were nailed!).

LIST OF FIGURES

Figure 1. Early stages of gynoecial development. 33
Figure 2. Mid stages of gynoecial development. 35
Figure 3. Late stages of gynoecial development 38
Figure 4 The mature gynoecium 41
Figure 5 Histochemistry of the pre-fertilised fruit, esterase 44
Figure 6 Histochemistry of the pre-fertilised fruit, phenol oxidase and JIM13. 47
Figure 7 Histochemistry of the pre-fertilised fruit, cellulase and pectinesterase. 50
Figure 8 Gross morphology of wild type Arabidopsis thaliana. 53
Figure 9 Early stages of silique development 56
Figure 10 Carpel wall and septum structure of the young silique. 59
Figure 11 The mature silique and dehiscence zones. 61
Figure 12 Carpel wall and septum structure of the mature silique. 65
Figure 13 Histochemistry of the post fertilised fruit, esterase. 67
Figure 14 Histochemistry of the post-fertilised fruit, phenol oxidase. 69
Figure 15 Histochemistry of the post-fertilised fruit, JIM13. 72
Figure 16 Histochemistry of the post-fertilised silique, Protease and Rubisco. 75
Figure 17 Histochemistry of the mature silique, cellulase and pectinesterase. 78
Figure 18 Gross morphology of the clavata mutant plant. 80
Figure 19 Early stages of clv1 gynoecial development. 83
Figure 20 Late stages of clv1 gynoecial development. 85
Figure 21 Late stages of clv1 silique development. 88
Figure 22 Anomalies in clv1 gynoecial development. 90
Figure 23 Anomalies in clv1 silique development. 93
Figure 24 The vestigial gynoecium. 95
Figure 25 The 'inferior septum'. 98
Figure 26 EMS generated mutants. 101
Figure 27 Mutant 003. 104
Figure 28 Mutant 006. 107

LIST OF TABLES

Table 1. Ontogeny of wild type Arabidopsis flower. 7
Table 2. Brief summary of gynoecial development. 29
Table 3. Brief summary of silique development. 52

MEMORANDUM

The work in this thesis was carried out by myself in the Department of Biological Sciences at the University of Durham. I declare that this work has not been submitted previously for a degree at this or any other University. This thesis is a report of my own work, except where acknowledged by reference. The copyright of this thesis rests with the author. No quotation should be published without her written consent, and information derived from it should be acknowledged.

INTRODUCTION

ARABIDOPSIS THALIANA

The small crucifer *Arabidopsis thaliana* belongs to the dicotyledenous Brassicaceae family. This large family of plants, commonly called the mustard family, contains about 3000 species in about 375 genera and occurs predominantly in northern temperate latitudes. Most cruciferous plants are herbs with 4 petalled flowers in the shape of a cross borne in a raceme. Many crucifers are important crop plants and include cauliflower, turnip and oilseed rape. *Arabidopsis* is a self-fertilising, flowering plant which grows to a height of 20-30cm at maturity. The flowers develop on the stem in a raceme, a single plant has mature fruits (siliques) at the bottom and floral primordia at the top. *Arabidopsis* has various properties which make it an ideal system for morphological, genetic and molecular studies (Redei 1975, Meyerowitz & Pruitt 1985, Estelle & Somerville 1986, Haughn & Somerville 1988, Meyerowitz 1989). Each silique contains about 50 seeds each the product of a separate fertilisation event. The diploid chromosome number is 5 pairs, and the small genome ($7x10^7$ base pairs per haploid genome), about one hundredth of the size of most higher plants, contains few repetitive sequences. This allows easy screening of genomic libraries and makes chromosome walking an attractive option. The small size of the plant, its short generation time (about 5 weeks) and its requirements for only moist simple soil mixtures and fluorescent light means that it can easily be propagated in a small space. *Arabidopsis* seeds are easily mutagenised by either soaking in chemical mutagens such as ethyl methanesulphonate (EMS) or irradiating imbibed seeds. As the plant typically self fertilises (*Arabidopsis* spontaneously outcrosses at a low frequency of about 10^{-4}) homozygous mutations are easily obtained. Cross pollination can also be easily effected to obtain multiple mutants and male sterile lines are available as an alternative to hand emasculation.

Mutations affecting various morphological or biochemical aspects of the plant have been identified and in some instances the genes responsible isolated and cloned. The former are usually visible, with phenotypes affecting every part of the plant including; pigmentation (*chlorina, chloretica, albina*), trichrome morhology (*glaborous, distorted*), growth habit (*erecta* and *compacta*) and the many floral mutants (*agamous, apetala, pistillata, clavata*) (Haughn *et al.* 1988). Mutants in which a biochemical lesion has been demonstrated or inferred are however the most extensively studied. Biochemical mutations can often be selected by the presence or absence of normal function. This can be achieved simply in some instances, by the direct assay of individual plant organs for the presence or absence of specific metabolic or enzyme activity, without killing the whole plant. In other instances

direct selection may be an alternative. An example of this method, first adapted for use in *Arabidopsis*, is the isolation of mutants lacking nitrate reductase activity. These mutants are chlorate resistant due to an inability to reduce chlorate to chlorite, a cell toxin; *Arabidopsis* has a relatively large number of chlorate resistant mutants, the majority falling into the chl1 complementation group (Estelle & Sommerville 1986). When there is no biochemical information on the gene product, molecular cloning can be achieved by chromosome walking or transposon tagging, two methods initially developed using micro-organisms. Chromosome walking involves recovering the required mutation by starting at a nearby cloned DNA fragment and isolating successive overlapping DNA segments. *Arabidopsis* is especially suited to this method of analysis due to its unique genetic characteristics. Transposon tagging involves the insertion of an active mobile element, for which probes are available, that cause genetic mutations. Having identified a transposon-induced mutation, the transposon and adjoining gene can be recovered from a library of DNA from the mutant line.

FLORAL DEVELOPMENT

THE FLOWER

Much recent work on *Arabidopsis* has focused on the genetic control factors involved in floral organ development. Mutations that specifically affect floral morphogenesis have been extensively characterised and in some instances the genes mapped, isolated and cloned (Komaki *et al.* 1988, Bowman *et al.* 1989, Hill & Lord 1989, Kunst *et al.* 1989, Yanofsky *et al.* 1990, Hong Ma *et al.* 1991). Floral development in *Arabidopsis* begins when florally induced cells on the apical meristem grow to form a buttress which is then separated from the rest of the meristem by an indentation. The medial then lateral sepals are the first primordia to form followed by petals and stamens: the medial sepals grow to cover the inner developing organs. The ovary develops interior to the stamens from a dome of cells which become a cylinder as those on the periphery grow (Miksche & Brown 1965, Bowman *et al.* 1989, Hill & Lord 1989, Smyth *et al.* 1990). This pattern of development differs from that of a number of other crucifers including *Brassica napus* in which inception of the stamen primordia precedes that of the petals (Polowick & Sawhney 1986). Smyth *et al.* (1990) performed a detailed analysis of the ontogeny of the wild type *Arabidopsis* flower and divided it into 12 stages based on distinct histological events see Table 1.

STAGE	DESCRIPTION
1	Floral buttress arises on apical meristem
2	Buttress is separated by an indentation
3	Sepal primordia develop on flanks
4	Medial sepals elongate
5	Petal and stamen primordia develop
6	Sepals grow to cover other organs; long stamens become distinct
7	Stamens develop stalks; gynoecium begins to develop
8	Stamens develop lobes; petals elongate; gynoecium elongates
9	Petals develop stalks; gynoecium begins to close at top
10	Petals and short stamens reach same height; gynoecium closes at top
11	Gynoecium develops stigmatic papillae
12	Petals reach same height as long stamens

Table 1: ontogeny of wild type Arabidopsis flower

The heirachy of genetic control involves regulatory genes determining when and for how long the housekeeping or structural genes specific to each cell are turned on. Heterochronic or timing genes are likely regulatory elements as they affect the sequence and duration of events. Mutations in homeotic genes are however the most extensively studied. Homeosis in zoological terms is the replacement of one organ type with that of another however, in botanical terms it has been expanded to include mosaic organs which are often found in plants. The *Arabidopsis* flower consists of four concentric whorls; sepals, petals, stamens and carpels and many of the homeotic mutants so far isolated affect adjacent whorls of organs. The floral mutations apetela (ap), pistillata (pi) and agamous (ag) have been shown to be involved in the differentiation of floral organs (Bowman *et al.* 1989, Hill & Lord 1989, Kunst *et al.* 1989, Irish & Sussex 1990). Ap1 flowers show transformations in the first and second whorls of sepals to bracts with the formation of a new floral bud in the axil of each bract, petals are totally absent. Ap2 flowers also show transformations in the first and second whorls of sepals to leaves and petals to mosaic petaloid stamens, although a wide range of phenotypes are observed some of which are temperature sensitive. In ap3 flowers the second and third whorls are affected with transformations of petals to sepals and stamens to carpelloid stamens. Pi flowers show transformations in three whorls; petals are mosaic organs of sepaloid petals and the stamens are incompletely formed and fused to the gynoecium, which as a result, is also abnormal. In ag flowers there are no stamens or carpels so again two whorls are affected. Transformations are of stamens to petals (so ten petals are formed) and carpels to a new round of sepals

and petals giving the phenotype of a flower within a flower. In fact up to up to seventy organs may be found within one ag flower.

Analysis of the phenotypes of single, double and triple mutants has lead to models of how homeotic genes specify organ position and identity. The sequential model assumes that floral organ identity genes are expressed in a temporal sequence and therefore the floral organs arise in a temporal sequence, sepals, petals, stamens, carpels. It also assumes that the development of an inner whorl is dependant on the correct differentiation of its outer whorl (Jack *et al.* 1992, Lord 1991) The most widely adopted theory assumes that there are three overlapping fields in which genes may be active and can specify the four whorls of floral organs and these fields can be specified at the same time. In this spatial model the development of each whorl is independent of the development of others (Jack *et al.* 1992, Coen & Meyerowitz 1991). Whilst the model is incomplete, it is sufficient to allow the prediction of the phenotypes of mutant combinations of the genes involved and states; if AP2 alone is present sepals are formed but if AP2, AP3 and PI are present together petals are formed. If AG alone is present carpels are formed but if AG, AP3 and Pi are present stamens are formed. Evidence to support this theory has come from a detailed study of the AGAMOUS gene by Meyerowitz's laboratory. Using an RNA probe hybridisation studies have shown that AG RNA is first detectable in whorls three and four between late stage two and early stage three wild type flowers. As AG activity can be detected before stamen and gynoecial primordia are initiated it is thought to be involved in specifying the identity of whorls three and four. Similar experiments using ap2 mutant flowers showed AG RNA to be present in the primordia of all floral whorls suggesting that AP2 prevents AG activity in the first and second whorls (Drews *et al.* 1991). AG expression is limited to specific cell types within the stamens and carpels later in flower development and is unlikely dependent on AP2 activity (Bowman *et al.* 1991). Sequence analysis of the AG gene showed it encodes a transcription factor with similar DNA binding domains to MCM1, a transcription regulator of mating type specific genes in yeast, to DefA, a homeotic floral gene in *Antirrhinum majus*, and to SRF, serum response factor in humans (Sommer *et al.* 1990, Yanofsky *et al.* 1990, Hong Ma *et al.* 1991, Schwartz-Sommer *et al.* 1992) although which genes are controlled is unknown. The conserved domain has been called the MADS box (MCM1, AG, DEFA, SRF). Floral development is complex and likely to require many regulatory proteins to control temporal and spacial events. Several other AGAMOUS like (AGL) genes containing this conserved sequence have been isolated from *Arabidopsis thaliana* (Hong Ma *et al.* 1991) and some of them

have been found to be flower specific although their temporal and spacial expression differs from that of AG.

Ap1, 2, and 3 flowers have distinctly different phenotypes therefore AP1, AP2 and AP3 have different functions. However AP1 and AP2 show functional similarities being active before AP3 and possibly interacting in a common developmental pathway to produce a determinate pattern of growth. Interactions between AP1 and AP2 with that of AG may be involved in establishing a determinate floral pattern (Irish & Sussex 1990). Homeotic floral mutations do not always affect two whorls of organs. Flo 10 mutant flowers have normal sepals, petals and stamens but the gynoecium is replaced by two to eight stamens or staminoid carpels (Schultz *et al.* 1991). Phenotypic analysis of flo 10 double mutants suggest that the FLO 10 gene negatively regulates the expression of AP3 and PI in the gynoecium.

THE INFLORESCENCE

The *Arabidopsis* shoot apical meristem produces stem, cauline leaves and lateral branches prior to the induction of the inflorescence meristem. The inflorescence meristem consists of a central and peripheral zone; floral primordia develop in a spiral pattern around the central zone, which gives rise to the stem, and this produces the floral racaemic pattern. In addition to the homeotic genes which affect organ identity in flower development there is also a class of homeotic genes termed meristic which affect the identity of meristems or change the number of parts of an organ. In plants possessing the terminal flower (tfl) mutation, the meristic region normally giving rise to the stem is converted, probably early in the floral transition, into a floral meristem (Shannon & Meeks-Wagner 1991). This produces a terminal flower at the point where stem elongation would normally occur. Plants possessing the mutation lfy1 in the LEAFY1 (LFY1) gene do not produce flowers. Instead primordia in the inflorescence that would normally give rise to flowers produce indeterminate shoots (Schultz & Haughn 1991). These shoots develop in a spiral phyllotaxy therefore the LFY gene is likely necessary to positively regulate the switch from a shoot to a floral meristem. Meristic mutations also occur within the flower itself. A good example of this is clavata (clv) in which the number of carpel primordia in the gynoecium is increased from two to four (Haughn & Somerville 1988, Komaki *et al.* 1988) but all the other organs are normal. This results in a silique with four locules. Flo 82 is similar to clv forming three or more carpels in the gynoecium (it can also form 2 gynoecia), but the number of organs in the other whorls may also increase (Komaki *et al.* 1988). Ag can be classed as a meristic as

well as a homeotic mutant as the number of organs is increased and flo 10, like ag, can also fall into both categories.

SIMILAR SYSTEMS

Detailed studies on the genetic control of flower development have not been limited to *Arabidopsis*. Homeotic mutants of *Antirrhinum majus* have also been extensively characterised. *Antirrhinum* also has various properties which make it an ideal system for study, although they differ from those of *Arabidopsis*. *Antirrhinum* is easy to propagate and has large flowers that are easy to emasculate and cross. It also has well characterised transposable elements enabling easy isolation of the mutant genes. *Antirrhinum* flowers, like those of *Arabidopsis*, comprise four concentric whorls of organs. Whorl one comprises five sepals, whorl two has five petals which are united for part of their length to form a tube, whorl three initiates five stamens although the uppermost stamen aborts giving the adult flower four, and whorl four the gynoecium which comprises a bilocular ovary.

Many of the floral mutants of *Antirrhinum* show similar phenotypes to those of *Arabidopsis*. Meristic mutations include floricaula (flo) which like lfy1 produces indeterminate shoots instead of flowers on the inflorescence meristem and centroradialis which produces a terminal flower like tfl (Coen *et al.* 1990). As with *Arabidopsis* more detailed studies have been made on the floral homeotic genes which affect whorl identity and in *Antirrhinum* these also affect adjacent whorls. The model applied to the *Arabidopsis* homeotic mutants ap2, ap3, pi and ag can also be applied to *Antirrhinum* mutants. Ovulata (ovl) affects whorls one and two like ap2, deficiens (def) and globosa (glo) affect whorls two and three like ap3 and pi and pleniflora (pleni) like ag affects whorls three and four (Schwartz-Sommer *et al.* 1990, Coen *et al.* 1991). Recent research (Jack *et al.* 1992) has shown that AP3 and DEFA are cognate homologues. The similarity seen in the mutants of these two species suggest that the mechanisms which control floral morphogenesis have been highly conserved in evolution.

FRUIT DEVELOPMENT

Plant development involves growth, pattern formation, and differentiation of specific cell types, and is characterised by a series of histological and cytological changes ultimately producing specific plant organs. Cytologically plant cell differentiation can be observed by a change in the shape of the cell or thickening of the cell wall.

Development also involves changes in the biochemical composition of for example intracellular components, cell membranes and the secreted extracellular matrix or cell wall. The formation of tissue patterns with associated and subsequent differentiation requires cells to recognise their spatial identity within the meristem and may be consequences of cell lineage and spatial interactions.

PRE-FERTILISATION

Arabidopsis fruit development begins with gynoecial initiation in the floral meristem. The gynoecium is first visible as a raised cylinder of tissue which produces two inner opposing placentae. These eventually fuse to form a partition or septum (Hill & Lord 1989, Okada *et al.* 1989). A row of ovules develops on each side of the two placentae. The open end of the cylinder eventually closes and stigmatic papillae develop, the centre of the septum contains the transmitting tissue. Recently Okada *et al.* (1989) proposed a "pistil", or for convention "carpel-forming unit" to explain the structure of various floral mutants of *Arabidopsis* showing variations in the gynoecium. This unit consists of a carpel wall with marginal ovular placentae and one central and two marginal vascular bundles. The margins of the two carpels are fused and the marginal bundles are shared. Although this successfully explains the vasculature and position of the ovules in the gynoecium, it does not attempt to describe the presence of the septal tissue. Development of the septum can be more easily explained if each carpel possesses a central placenta from which a septum possessing a row of ovules on each side develops. If the margins of each carpel are fused, growth of the septa towards each other would result in a false partition. It is also possible for each carpel to possess a placenta along one margin, from which the septum and two rows of ovules develop. The two carpels would in this instance be fused in a laterally opposed orientation. There are conflicting hypotheses concerning the number of carpels which constitute the gynoecium (Saunders 1929, Hill & Lord 1989, Kunst *et al.* 1989, Okada *et al.* 1989). However, as this controversy is not a main concern of this thesis, for simplicity and in keeping with others (Hill & Lord 1989, Kunst *et al.* 1989, Okada *et al.* 1989) the gynoecium is considered to consist simply of two carpels each possessing two rows of ovules.

The general plant cell wall is made up of cellulose, hemicellulose, pectin and protein and there is no reason to presume that the *Arabidopsis* cell is any different. How these components are controlled, interact and change during cell differentiation is still a subject of great controversy. Recently molecular biological techniques have been used to study enzyme activity during fruit development. Hydrolytic enzymes and cell

wall hydrolases have long been associated with fruit ripening and abscission (Sexton & Roberts 1982, Fisher & Bennett 1991). The ripening process in tomato has been extensively studied and the genes for pectinesterase and polygalacturonase have been isolated and cloned (Markovic & Jornvall 1986, Ray *et al.* 1988, Taylor *et al.* 1990). Pectinesterase makes the cell wall pectin more susceptible to degradation by polygalacturonase, which is the main cell wall softening enzyme, and genetic manipulation of these genes has lead to the firmer longer lasting tomato on the supermarket shelf. A more recently isolated pectinesterase gene from *Brassica napus* shows homology to that from the tomato fruit but it is active in the pollen of *Brassica* (Albani *et al.* 1991) therefore the enzyme may have different functions in these two tissue types.

Within plant meristems biochemical markers have been identified which indicate that cells within the meristem are committed to differentiate early on before cytological changes are evident. Esterase has been described as a good biochemical marker for early stelar differentiation (Gahan 1981) and cell elongation (Vercher & Harris in press) Recent research (Knox *et al.* 1989, 1990, Pennell *et al.* 1989, Schopfer 1990, Stacey *et al.* 1990) has shown that arabinogalactan proteins or AGP's may be good indicators of positional effects and subsequent differentiation in plants. AGP's belong to a diverse class of proteins which are rich in the uncommon imino acid hydroxyproline (Marcus *et al.* 1991), and are found throughout the plant kingdom in the cell plasma membrane and cell wall. They may be peripheral and located on the surface of the membrane or integral and embedded in the lipid bilayer. The chemical mechanism for cell-cell recognition is not fully understood however, identification of markers of early pattern or cell identity will aid in understanding how these patterns are established.

POST-FERTILISATION

After fertilisation the gynoecium develops into a dry, dehiscing fruit or silique. The silique is a relatively simple structure composed of only ten basic cell types of which not more than seven are associated with the dehiscence mechanism. The mature silique comprises two locules separated by a septum which possesses two vascular bundles, one on either side. Adjacent to each bundle are two rows of seeds. Dehiscence zones form on each side of the two main vascular bundles. Formation of these zones produces two valves which can split away and detach from the silique leaving the seeds exposed. Silique dehiscence or "pod shatter" is a major problem in

the agricultural industry as the consequent seed loss inevitably lowers yields. Due to commercial implications dehiscence in oil seed rape, another member of the Brassicacea, has been quite extensively studied (Jossefson 1968, Tayto *et al.* 1979, Kadkol *et al.* 1986, Macmillan 1986, Polowick *et al.* 1986, Meakin *et al.* 1990 a, 1990 b). In oilseed rape the dehiscence zone consists of a layer of cells, 1-3 cells wide, on either side of the replum extending from the locule to the pericarp. The dehiscence zones are enclosed by thickened tissues of the adjacent valve and replar vascular bundles. Following lignification of the thickened tissues, the dehiscence zone cells show progressive degradation which is primarily due to middle lamellar breakdown (Meakin & Roberts 1990 a). This weakens valve attachment although physical stresses and dessication are also necessary for pod shatter.

Dehiscence of the *Arabidopsis* silique has many features in common with the dehiscence of rape pods and with the abscission of leaves and floral organs for example which occurs in many plant species. Abscission is a very precisely, temporally and spacially controlled process which results in cell separation. Various hormones such as auxins, gibberellins and ethylene have been implicated in the temporal control of abscission (Sexton & Roberts 1982), and dehiscence of oilseed rape (Meakin & Roberts 1990 b). Hydrolytic enzymes such as cellulase and polygalacturonase have been associated with abscission, however, there are different forms of cellulase; that associated with abscission has a basic isoelectric point of 9.5 and is referred to as 9.5 cellulase. In *Phaseolus vulgaris* (bean) leaf 9.5 cellulase is found in the separation layer cells of the abscission zone and adjacent vascular tissues (Campillo *et al.* 1990). *In situ* hybridization experiments have revealed that all classes of living cell associated with the abscission layer of bean leaves synthesise 9.5 cellulase mRNA (Tucker *et al.* 1991). The substrate upon which 9.5 cellulase acts is as yet unknown. In rape pods the increase in cellulase activity in the dehiscence zone cells is preceded by an increase in ethylene production suggesting ethylene may have a regulatory role (Meakin & Roberts 1990 b). Although Meakin & Roberts (1990 b) found no correlation between rape dehiscence and polygalacturonase activity, a zone specific rise in the enzyme has been found in the abscission zones of tomato leaves. Taylor *et al.* (1990) found that the polygalacturonase protein associated with tomato leaf abscission is different to that associated with tomato fruit ripening, although both enzymes may have similar biochemical roles and share the same regulators.

PROJECT AIMS

The aim of this project was to identify and describe the histological development of the major tissue types of the fruit of *Arabidopsis thaliana* from gynoecial initiation until silique dehiscence. Using a number of well-established histochemical techniques, and a number of novel probes, we hoped to identify appropriate markers for specific phases of differentiation. The meristic *clavata* mutant, which shows anomalies only in gynoecial development, was chosen as a comparable system and the development of the *clv1* mutant is also described and compared to that of the wild type. EMS treated seeds were planted on a regular basis and screened for mutants which showed anomalies in silique development that can be used for future work carried out on silique development in this laboratory.

ABBREVIATIONS

∝	alpha
a	anther
Acetic acid	ethanoic acid
AP	alkaline phosphatase
ß	beta
BCIP	5-bromo-4-chloro-3-indolyl phosphate
BSA	bovine serum albumin (Fraction V)
c	carpel
clv	clavata
cDNA	complementary DNA
cpm	counts per minute
DEPC	diethylpyrocarbonate
DIG	digoxigenin
DMF	dimethyl formamide
DMSO	dimethyl sulphoxide
DNA	deoxyribonucleic acid
DNase	deoxyribonuclease
EDTA	(ethylenedinitrilo) tetraacetic acid
en	endocarp
ex	exocarp
Fast Red TR	4-chloro-2-methylbenzene-diazonium salt
FITC	fluorescein isothiocyanate
g	gram
gc	guard cell
gr	pollen grain
gt	goat
gy	gynoecium
HEPES	N-2-hydroxy ethyl piperazine-N'-2-ethane sulphonic acid
if	inferior septum
IGSS	immuno`-gold silver staining
l	litre
L.M.	light microscopy
lme	lignified mesocarp
M	molar
me	mesocarp

MES 2-(N-morpholino) ethane sulphonic acid

mg milligram

MOPS 3-(N-morpholino) propane sulphonic acid

mRNA messenger ribonucleic acid

MW molecular weight

NAMP naphthol AS-MX phosphate disodium salt

NBT nitro blue tetrazolium

ov ovule

p placenta

PBS phosphate-buffered saline

pe petal

PEG polyethylene glycol

PVP polyvinyl pyrollidone

rb rabbit

RNA ribonucleic acid

RNase ribonuclease

rpm revolutions per minute

R.T. Room temperature

s septum

se sepal

SEM scanning electron microscopy

SDS sodium dodecyl sulphate

st stigma

TBS Tris-buffered saline

TESPA 3-aminopropyl triethoxysilane

Tris 2-amino-2-(hydroxymethyl)-1,3-propanediol

vb vascular bundle

vg vestigial gynoecium

(v/v) volume:volume ratio

wt wild type

(w/v) weight:volume ratio

MATERIALS AND METHODS

STANDARD SOLUTIONS

Acetate buffer:
30% (v/v) 0.2 M acetic acid
70% (v/v) 0.2 M sodium acetate

BSA diluent:
5% (w/v) BSA (Fraction V) in TBS

Denhardt's (50 x):

1% (w/v)	BSA
1% (w/v)	Ficoll
1% (w/v)	PVP

DNase-free RNase: Pancreatic RNase A was dissolved at 10 mg/ml in 10 mM Tris/HCl pH 7.5, 15 mM NaCl, heated to 100°C for 15 min and allowed to cool slowly to room temperature. The solution was then aliquoted and stored at -20°C.

Developing buffer:

0.1 M	NaCl
0.1 M	Tris/HCl pH 9.6
10 mM	$MgCl_2$

PBS (10 x):

0.1 M	Sodium phosphate pH 7.5
1.3 M	NaCl

Phosphate citrate buffer:

37.4 mls	0.5M sodium phosphate
21.3 mls	0.5M citric acid

SSC (20 x):

3.0 M	NaCl
0.3 M	Na_3citrate

SSPE (20 x):

3.6 M	NaCl
0.2 M	Sodium phosphate pH 7.7
2.0 mM	EDTA disodium salt

TAE (50 x):

2.0 M	Tris/acetate
1.0 M	acetic acid
50 mM	EDTA

TBS (10 x):	1.0 M	Tris/HCl pH 8.0
	1.5 M	NaCl
TE:	10 mM	Tris/HCl pH 8.0
	1.0 mM	EDTA

All solutions were sterilised by autoclaving (>20 min at 121°C) or ultrafiltration (0.22 μm) as appropriate.

All reagents were of BDH laboratory reagent grade or better. For critical applications, and for all work involving RNA, Sigma or Boehringer-Mannheim molecular biology-grade reagents were employed. Immunochemicals were supplied by Sigma.

PLANT MATERIAL

Plants were grown in either Levingtons F2 standard pH compost or J. Arthur Bowes all purpose seed and potting compost. Seeds were suspended in 0.5% (sloppy) agar (0.5 g of agar in 100ml distilled water) and dispensed through a 10ml syringe onto the compost surface. Plants were grown in 24 hour daylight at 25°C. and the compost kept moist by watering from below every 2-3 days.

TISSUE PREPARATION

ALDEHYDE FIXATION

Tissues were excised and immediately placed in a freshly prepared solution containing 3% paraformaldehyde and 1.25% gluteraldehyde in 50mM phosphate buffer pH 7.0 and infiltrated for 12 hours at R.T. and pressure with gentle agitation using a 45° rotating platform at 2 r.p.m..

DEHYDRATION

Dehydration table

% solution	25%	50%	75%	90%	100%	100%
Time mins	60	60	60	60	60	60

Times for dehydration in the table are in minutes (mins) and refer to all protocols where dehydration was required, however, dry ethanol (using molecular sieves) was substituted for the last 100% stage when wax or PEG embedding the tissue.

Dehydration was carried out at R.T. on a 45° rotating platform at 2 r.p.m. and the solutions were changed every 30 minutes.

TISSUE EMBEDDING

PEG 1000

An equal volume of polyethylene glycol 1000 (MW _ 950 - 1050), melted at 42°C, was added to the dehydrated samples under dry ethanol. The solutions were mixed thoroughly and incubated overnight at ± 2°C. The 50:50 PEG 1000:ethanol

mixture was then replaced with molten PEG 1000 alone and incubation took place at 42°C for a further 4 hours. The PEG 1000 was replaced twice daily until the tissues were judged to be fully infiltrated.

WAX

An equal volume of Histoclear was added to the dehydrated samples under dry ethanol and infiltrated at R.T. for 1 hour. Samples were then placed in 100% Histoclear and infiltrated overnight, fresh Histoclear was added and the samples infiltrated for a further 12 hours on a 45° rotating platform at 2 r.p.m.. An equal volume of molten Paraplast Plus wax was added and the samples infiltrated overnight at 60°C. Samples were then placed in 100% wax and infiltrated for 24 hours (wax was changed twice daily)

LR WHITE

All manipulations involving LR White acrylic resin were performed in a fume-hood. The resin was stored at 4°C and allowed to equilibrate at room temperature before opening to prevent the absorption of atmospheric water.

An equal volume of LR White acrylic resin (medium grade) was added to the dehydrated samples under 100% ethanol. The solutions were mixed thoroughly and incubated overnight, with gentle agitation at R.T.. The 50:50 resin:ethanol mixture was then replaced by resin alone and incubated at R.T. for a further 4 hours. The resin was then replaced twice daily until the tissues were judged to be fully infiltrated. Resin blocks were polymerised overnight at 65°C.

SCANNING ELECTRON MICROSCOPY (SEM)

Specimens were dehydrated as described in the above table in a graded series of acetone. Specimens were then critical point dried in liquid carbon dioxide in an E 3100 Jumbo Critical Point Drier then mounted on stubs and dissected using glass needles. Specimens were then gold coated and viewed on a Cambridge S600 SEM at 25 kv.

SECTIONING

SLIDE PREPARATION

Microscope slides (76 x 26 x 0.8-1.0mm) with frosted ends were washed in detergent then rinsed thoroughly in distilled water. The slides were then dipped for 10 seconds in a 2% solution of aminopropyltriethoxysilane (TESPA) in acetone, rinsed twice in acetone then rinsed in distilled water. The slides were then air dried at R.T. in a dust free environment.

EMBEDDED MATERIAL

Wax and PEG infiltrated material were embedded in suitably sized plastic moulds and cut on a Leitz 1512 microtome. Wax sections were floated out onto distilled or DEPC treated water at 50°C in a water bath and picked up on TESPA coated microscope slides, PEG sections were floated onto a drop of water on the slide. Sections were allowed to dry down overnight at 40°C on a hotplate.

LR White infiltrated material was embedded in suitably sized polypropylene embedding capsules and cut on a Sorvall MT2-B ultra microtome using glass knives.

CRYOSECTIONING

Fresh tissue was excised and placed on a cryostat chuck with a drop of Brights Cryo-M-Bed and frozen using pressurised CO_2. Frozen sections were then cut using a Bright OTF cryostat.

DEWAXING

All wax embedded sections were dewaxed by the following method; slides were placed in histoclear for a minimum of 2 minutes, rinsed in fresh histoclear then rinsed twice in 100% ethanol

HISTOCHEMISTRY

ACRIDINE ORANGE

LR White (1μm) or wax-embedded (10μm) sections were incubated 2-3 minutes at R.T. in freshly filtered 0.01% (w/v) acridine orange. Sections were then rinsed in distilled water and mounted in Citifluor.

ALKALINE PHOSPHATASE

Wax-embedded (10μm) sections were dewaxed and rehydrated to distilled water. Sections were rinsed in developing buffer then incubated in freshly prepared substrate solution (0.5mM NAMP and 2mM fast red TR in 0.1M Tris buffer pH 8) in darkness at R.T. until colour development was judged satisfactory. Sections were rinsed in developing buffer then mounted in Citifluor.

GENERAL ESTERASE

Frozen (10μm) sections were washed in distilled water to remove the embedding medium. Sections were rinsed in 0.2M Tris/HCl buffer pH 6.5 then incubated in substrate solution (0.1 mg/ml naphthol AS-D acetate, 0.6 mg/ml Fast Blue BB salt in 0.1M Tris/HCl pH 6.5) in darkness at R.T. until colour development was judged to be satisfactory. Sections were then rinsed in buffer then mounted in Citifluor. (After Gahan 1981).

METHYL GREEN PYRONIN

Wax-embedded (10μm) sections were dewaxed and rehydrated to distilled water. Sections were then rinsed in Walpoles buffer pH 4.8 (0.2M sodium acetate buffer pH 4.8) then stained in freshly filtered (0.45μm) methyl green pyronin solution (0.36% (w/v) methyl green, 0.16% (w/v) pyronin Y, 28% glycerol in 92mM acetate buffer pH 4.8) for 25 minutes at R.T.. Sections were then rinsed in buffer, blotted dry then rinsed twice in histoclear and mounted in DPX.

PHENOL OXIDASE

Frozen (10μm) sections were washed in distilled water to remove the embedding medium. Sections were rinsed in phosphate citrate buffer pH 4.5 then incubated in

substrate solution (0.5 mg/ml naphthol, 0.5 mg/ml 4, aminodiphenylenediamine in phosphate citrate buffer pH 4.5) in darkness at R.T. until colour development was judged to be satisfactory. Sections were then rinsed in buffer then mounted in Citifluor.

TOLUIDINE BLUE

Wax-embedded (10μm) sections were dewaxed and rehydrated to distilled water, LR White embedded sections were placed on a hot plate for 2 minutes to ensure adhesion of the sections to the microscope slides. Sections were then stained in freshly filtered (0.45μm) 0.1% toluidine blue in 1% boric acid at R.T.. to give optimal staining as determined empirically, rinsed in distilled water, air dried then mounted in DPX.

IMMUNOCYTOCHEMISTRY

MONOCLONAL ANTIBODIES

Wax-embedded (10μm) sections were dewaxed and rehydrated to distilled water.

Sections were rinsed in TBS pH 8.0 then incubated for up to 12 hours R.T. in primary antibody using 5% BSA as the diluent. Sections were rinsed for 15 minutes in TBS (fresh TBS was added every 5 minutes)

FLUORESCENT DETECTION

Sections were incubated in FITC-labelled secondary antibody for 2 hours at R.T. (diluted as per manufacturers recommendations using 5% BSA diluent). Sections were then thoroughly rinsed in TBS for 30 minutes (fresh TBS was added every 5 minutes) then mounted in Citifluor.

IMMUNOGOLD/SILVER DETECTION

Sections were incubated in 5nm gold-labelled secondary antibody for 2 hours at R.T. (diluted as per manufacturers recommendations using 5% BSA diluent). Sections were then rinsed in three changes of TBS then distilled water then Milli-Q (heavy metal-free) water. Sections were then silver enhanced for 1-3 minutes (the reaction was microscopically controlled) using Amersham IntenSE M following

manufacturers instructions. The sections were then rinsed in Milli-Q water, air dried and mounted in DPX.

MOLECULAR HISTOCHEMISTRY

PLASMID PREPARATION

The cellulase probe was cloned into the HINDIII sites of the plasmid pBIN19 and maintained in E. coli TG-2. The pectinesterase and polygalacturonase probes were cloned into the PST1 sites of the plasmid pAT153 and maintained in E. coli 600. E. coli TG-2 was plated out and grown overnight at 37°C on LB solid media containing kanamycin antibiotic. E. coli 600 was plated out and grown overnight at 37°C on LB solid media containing tetracyclin antibiotic. A single colony was removed and grown overnight at 37°C with agitation on LB liquid media containing the appropriate antibiotic.

PREPARATION OF AT53 PLASMID USING PROMEGA MAGIC MINIPREP

The bacterial suspension was microcentrifuged at 13000 r.p.m.. for 1 minute and the supernatant discarded. The pellet was resuspended in resuspension buffer (50mM tris pH 7.5, 10mM EDTA, 100μg/ml RNase A) by vortexing then the bacteria were lysed by addition of lysis buffer (200mM NaCl, 1% SDS). The suspension was neutralised by addition of neutralisation buffer (2.55M Potassium acetate) and microcentrifuged at 13000 r.p.m.. for 5 minutes. The supernatant was removed to a fresh tube and resin added. The resultant slurry was syringed slowly through a Magic Miniprep column, and the column was washed with buffer (0.2M NaCl, 20mM tris pH 7.5, 5mM EDTA, 50 % ethanol). The column was then centrifuged for 20 seconds to remove excess buffer. The DNA was eluted with TE at 70°C.

PREPARATION OF BIN19 PLASMID USING QIAGEN TIP

The bacterial suspension was centrifuged at 16,000 r.p.m. for five minutes and the supernatant discarded. The pellet was resuspended in P1 buffer (50mM tris/HCl 100μg/ml RNase A, 10mM EDTA pH 8.0) at 4°C by vortexing and the bacteria lysed by addition of buffer P2 (200mM NaOH, 1% SDS). The suspension was incubated at R.T.. for 5 minutes then neutralised by addition of buffer P3 (2.55M

potassium acetate) at 4°C. The suspension was incubated on ice for 20 minutes then centrifuged at 4°C for 30 minutes at 16,000r.p.m.. The supernatant was placed in the Qiagen tip column (equilibrated with 750mM NaCl, 50mM MOPS, 15% ethanol pH 7.0, 0.15% triton x-100) and allowed to run through. The column was washed with QC buffer (1.0M NaOH, 50mM MOPS, 15% ethanol pH 7.0) and the DNA eluted with QF buffer (1.25M NaCl, 50mM MOPS, 15% ethanol pH 8.2). 0.7 volume of isopropyl alcohol was added and the sample centrifuged at 4°C for 30 minutes at 16,000 r.p.m.. The DNA pellet was washed in 70% ethanol, air dried and resuspended in TE.

RESTRICTION DIGEST OF PLASMID DNA

50μl of solution containing the plasmid DNA was used for the digests. 6μl of X10 one-phor-all buffer, 3μl of PST1 and 1μl of water was added to the plasmids pAT153. 6μl of X10 one-phor-all buffer, 3μl of HINDIII and 1μl of water was added to the plasmid pBIN19. The digestion was carried out overnight at 37°C then sample buffer (0.25% bromophenol blue, 30% glycerol) was added and the fragments separated by gel electrophoresis using low melting point agarose gel. The gel was run at 50v for 4 hours. The appropriate band was cut out of the gel and an equal volume of gel elution buffer (0.1M tris acetate pH 7.5, 0.5M NaCl, 5mM EDTA) was added and the sample melted by incubating at 65°C for 5 minutes.

PHENOL/CHLOROFORM EXTRACTION OF DNA

The phenol and chloroform used for the extraction were first equilibrated with gel elution buffer.

An equal volume of phenol was added to the sample and mixed by vortexing, this was then microcentrifuged for 5 minutes at 13000 r.p.m.. The aqueous phase was pipetted into a fresh tube and the sample incubated on ice for 30 minutes, then microcentrifuged for 5 minutes. An equal volume of phenol/chloroform (1 : 1 ratio) was added to the sample and mixed by vortexing. This was microcentrifuged at 13000 r.p.m. for 5 minutes and the aqueous phase pipetted into a fresh tube and microcentrifuged for 5 minutes at 13000 r.p.m.. An equal volume of chloroform/ isoamylalcohol (24 : 1 ratio) was added to the sample and mixed by vortexing. This was microcentrifuged for 5 minutes at 13000 r.p.m.. and the aqueous phase pipetted into a fresh tube. The DNA was precipitated by adding 2/3 volume 7.5M ammonium acetate and 2 volumes -20°C ethanol and incubating the solution at -

20°C overnight. The solution was microcentrifuged for 5 minutes at 13,000 r.p.m. and the supernatant discarded. The pellet was washed with 70% ethanol, air dried and resuspended in TE.

LABELLING dsDNA PROBES USING BOEHRINGER MANHEIM DIG LABELLING KIT

These reactions were carried out following manufacturers instructions. Briefly, 10μl of solution containing the probe DNA was denatured by heating to 95°C for 5 minutes and cooled in an ice/NaCl bath. 2μl of hexonucleotides, 2μl of dNTP, 1μl of Klenow and 5μl of DEPC treated water were added and the solution incubated at 37°C overnight. The labelled probe was then precipitated overnight at -20° C by addition of 4M LiCl and 2 volumes of ethanol. The probe was washed with 70% ethanol, air dried and then resuspended in TE. The labelled probe was stored at -20°C.

IN-SITU HYBRIDISATION

Wax-embedded 10μm sections were dewaxed in Histoclear and rehydrated to DEPC treated water.

The DIG labelled probe was denatured by incubating for 10 mins at 95°C and cooled in an ice/NaCl bath. The denatured probe was added to the hybridisation buffer (50% deionised formamide, 4X SSC, 1X Denhardts, 500μg/ml sonicated denatured salmon sperm DNA, 250μg/ml yeast tRNA, 10% dextran sulphate) to a final concentration of 1μg/ml. Sections were incubated overnight under siliconised coverslips in a humid chamber at 42°C

Coverslips were removed by immersing the slides in a solution containing 4X SSC, 50% formamide at 42°C. Sections were rinsed twice in buffer (2X SSC, 0.1% SDS) at RT for 15 mins each then twice at 42°C for 15 mins each. Sections were dehydrated in a graded ethanol series buffered with 300mM ammonium acetate then allowed to air dry.

Sections were incubated in 2% sheep serum in buffer 1 (100mM Tris pH 7.5, 150mM NaCl) for 30 mins Sections were incubated in a 1:500 dilution of alkaline phosphatase conjugated polyclonal sheep anti-digoxygenin antibody in buffer 1 for 2 hours at RT then rinsed in buffer 1 for 60 mins (fresh buffer was added every 15 mins). Sections were then incubated in darkness at RT in freshly prepared substrate

solution containing 0.5mM naphthol AS-MX phosphate, 2.0mM fast red TR in Tris buffer pH 8.0. Colour development was microscopically controlled. Sections were given a final distilled water rinse then air dried and mounted in DPX.

RESULTS

DEVELOPMENT OF THE *ARABIDOPSIS* GYNOECIUM

The gynoecium forms the innermost whorl of the *Arabidopsis* flower and, based on the twelve stages of *Arabidopsis* floral development according to Smith *et al.* (1990), the gynoecium is the last floral organ to begin developing at stage seven. We have divided the development of the fruit into two sections; development of the pre-fertilised fruit or gynoecium, and development of the post-fertilised fruit or silique. Development has been divided into a number of stages based on distinct histological events. The first five stages of fruit development are concerned with the development of the gynoecium and are briefly summarised in Table 2. Stages one to five of silique development correspond to stages seven to twelve of flower development which are briefly summarised in Table 1.

The gynoecium is first visible as a small dome of meristematic cells interior to the stamens, and these begin to differentiate at stage one to form an elliptical, open ended cylinder, comprising about six concentric layers of small uniform cells. The cylinder has a deep, narrow, central fissure which is lined with two layers of slightly darker staining meristematic cells (Fig. 1A), which also extend around the top of the cylinder (Fig. 1C). Within the cylinder wall there is a combination of meristematic and vacuolate cells. Two radially opposed rudimentary vascular bundles can just be discerned in Fig. 1A; these we have termed primary bundles.

STAGE	KEY EVENTS
1	gynoecium arises as open ended cylinder with central fissure, primary vascular bundles appear
2	2 opposing placentae develop
3	4 ovule primordia develop, carpel wall differentiates into 3 layers
4	placentae fuse to form septum, endocarp differentiates to form 2 layers
5	transmitting tissue develops, stigmatic papillae develop

Table 2: Brief Summary Of Gynoecial Development

During the second stage of development, there is a general increase in the size of the gynoecium. The increase in diameter is achieved by anticlinal divisions in gynoecial cell wall layers (Fig. 1D); the number of cell layers does not increase. Periclinal divisions at the tip of the gynoecium increase the length.

Figure 1. Early stages of gynoecial development.

The sections are stained with toluidine blue and photographed under bright field illumination.

[A] Transverse section of a stage 1 gynoecium. Small arrows indicate the central fissure and large arrows indicate the rudimentary primary vascular bundles (vb).

[B] Transverse section of a stage 2 gynoecium showing the placentae (p) bulging into the central fissure. The vascular bundles (vb) are very distinct.

[C] Longitudinal section of a young gynoecium (gy) showing the darker staining meristematic cells which line the central fissure; (a) anther.

[D] Longitudinal section of the tip of a young gynoecium showing the patterns of cell division, indicated by arrows, in the outer and inner tissue layers.

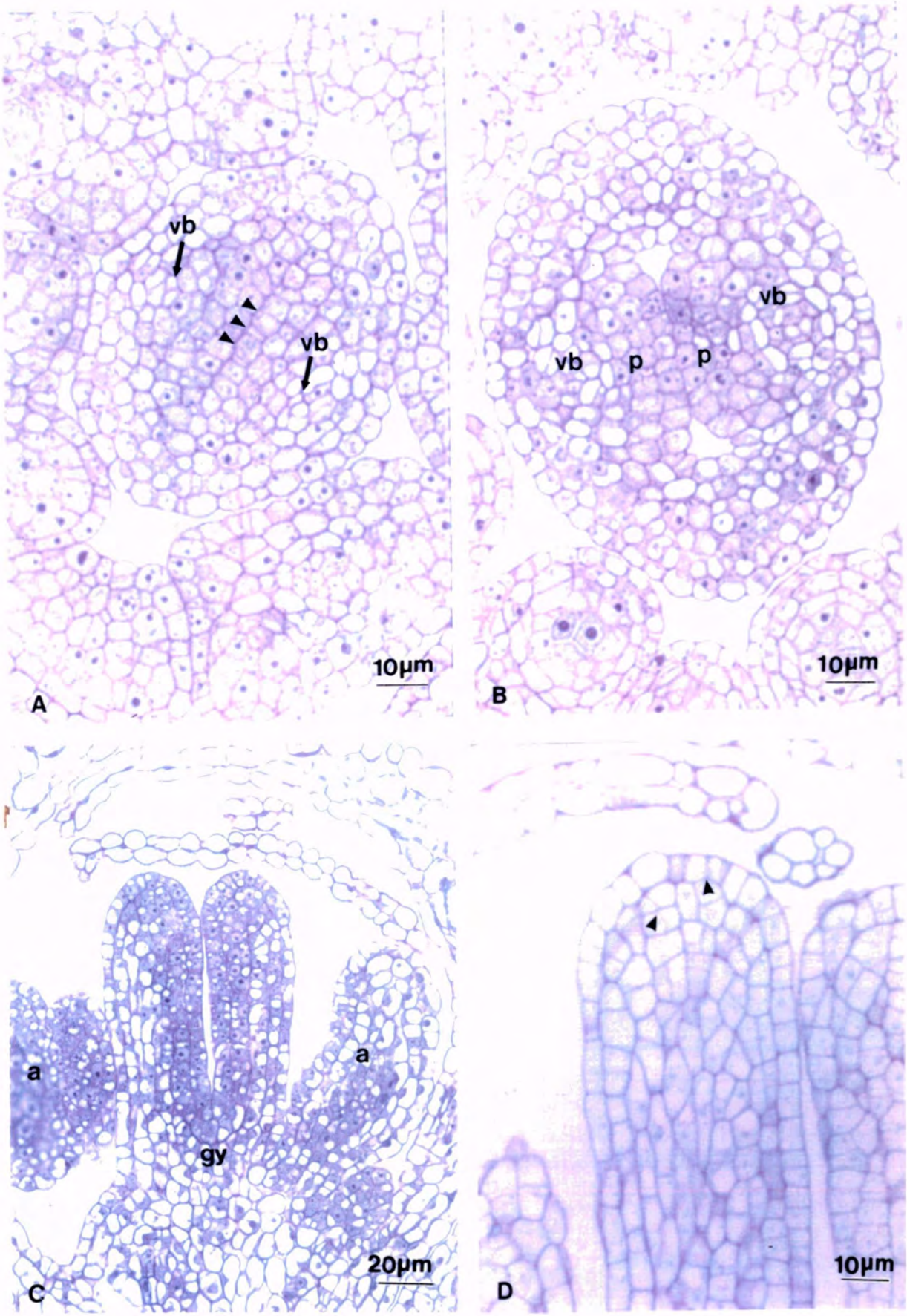

Figure 1.

Figure 2. Mid stages of gynoecial development.

The sections are stained with toluidine blue and photographed under bright field illumination.

[A] Transverse section of a stage 3 gynoecium showing the ovule primordia (ov) and the three carpel wall layers; (en) endocarp, (ex) exocarp, (me) mesocarp.

[B] Transverse section showing the distinction between the larger cells of the ovules (ov) and those of the placentae(p) in the stage three gynoecium.

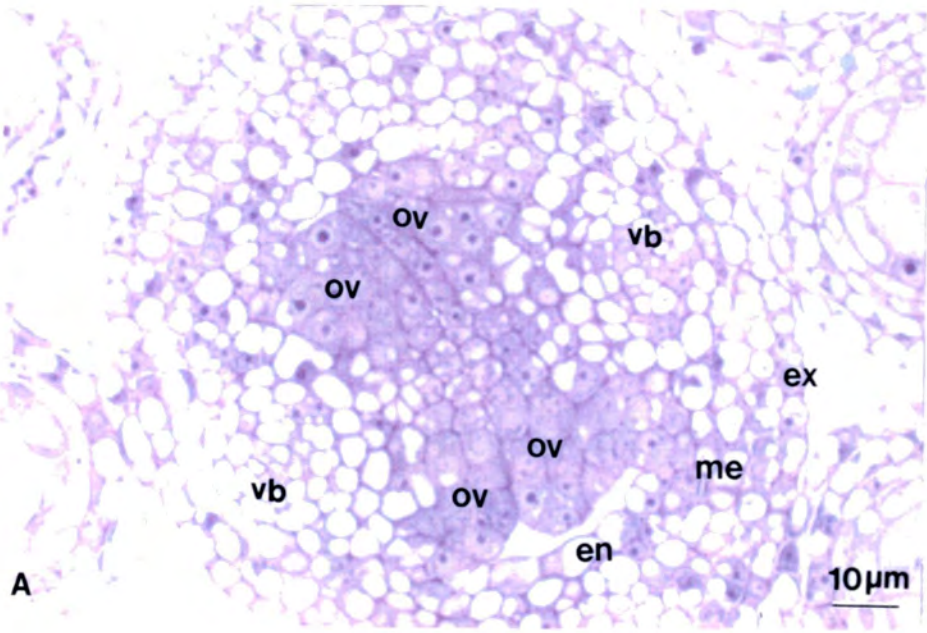

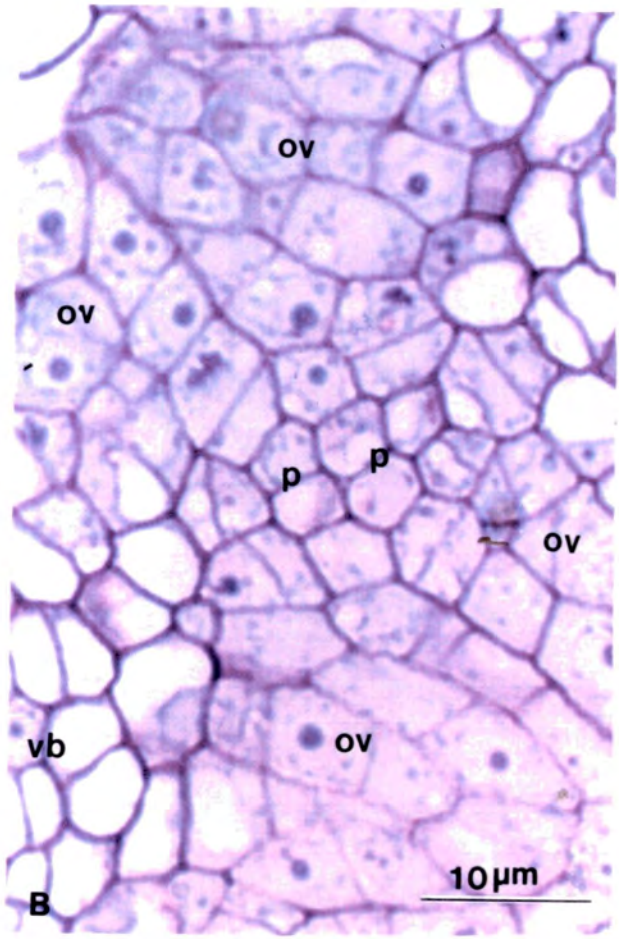

Figure 2.

The number of meristematic cells within the gynoecial wall decreases, but as can be seen in Fig. 1B, the meristematic layers lining the fissure wall begin to bulge into the centre of the fissure at stage two. Although this may be due to widening of the fissure margins (Hill & Lord 1989), it could also be attributed to the increase in the size of the primary vascular bundles, which are much larger and quite well differentiated by stage two (Fig. 1B).

The bulges or placentae produce two pairs of opposing ovule primordia at stage three, which protrude into the widening margins of the fissure (Fig. 2A). The ovular cells are much larger than those of the placentae as illustrated in Fig. 2B. The walls of the gynoecium, or carpel walls, adjacent to the fissure margins become distinct from the placental and vascular tissues, and three distinct cell types can be discerned in the wall (Fig. 2A). The layer lining the fissure margins, the endocarp, comprises a single layer of thin walled parenchymous cells. Adjacent to the endocarp there are four or five layers of slightly smaller parenchymous cells which form the mesocarp. Small intercellular spaces are present within the mesocarp layer. The outermost layer, the exocarp, forms a single continuous layer around the outside of the gynoecium. The exocarp cells are of a similar size to the mesocarp cells but have slightly thicker walls and are interspersed with guard cells and stomata. There are very few meristematic cells remaining in the carpel wall layers by stage three. A rudimentary vascular bundle begins to form in each carpel wall late in stage three, these we have termed secondary bundles. Both the primary and secondary vascular bundles extend from the pedical of the flower.

Late in stage three and certainly by stage four the gynoecium has almost doubled in diameter and the open, upper end of the gynoecium has closed. Periclinal divisions in the central area of the placentae, between the ovule primordia, produces two opposing pseudo-septa which fuse in the centre of the gynoecium forming a false partition and creating a bilocular ovary (Fig. 3A). The septum always runs parallel to the axis of the inflorescence. There is further differentiation of the carpel wall layers at stage four. The cell layer immediately adjacent to the endocarp undergoes many anticlinal divisions, which results in a distinct layer of small, thin, very tightly packed cells (Fig. 3A). For ease of interpretation we have classed this layer of cells as a 'sub' or secondary endocarp layer rather than a mesocarp layer. The first endocarp layer we have termed endocarp a (en*a*) and the second layer as endocarp b (en*b*). The primary and secondary vascular bundles branch out at the tip of the gynoecium and terminate just beneath the top surface of the stigma.

Figure 3. Late stages of gynoecial development

The sections are stained with toluidine blue and photographed under bright field illumination.

[A] Transverse section of a stage 4 gynoecium following differentiation of the second endocarp layer and carpel wall bundle; (en*a*) endocarp *a*, (en*b*) endocarp *b*, (vb) vascular bundle

[B] Transverse section showing the structure of the mature gynoecium and the major tissue types; (c) carpel walls, (s) septum, (vb) vascular bundle.

[C] Transverse section of the septum showing the extra cellular spaces (es) forming in the inner tissues and the point of fusion, indicated by small arrows.

[D] Transverse section of the carpel wall (c), the small arrows indicate the patterns of cell division in the mesocarp layer (me).

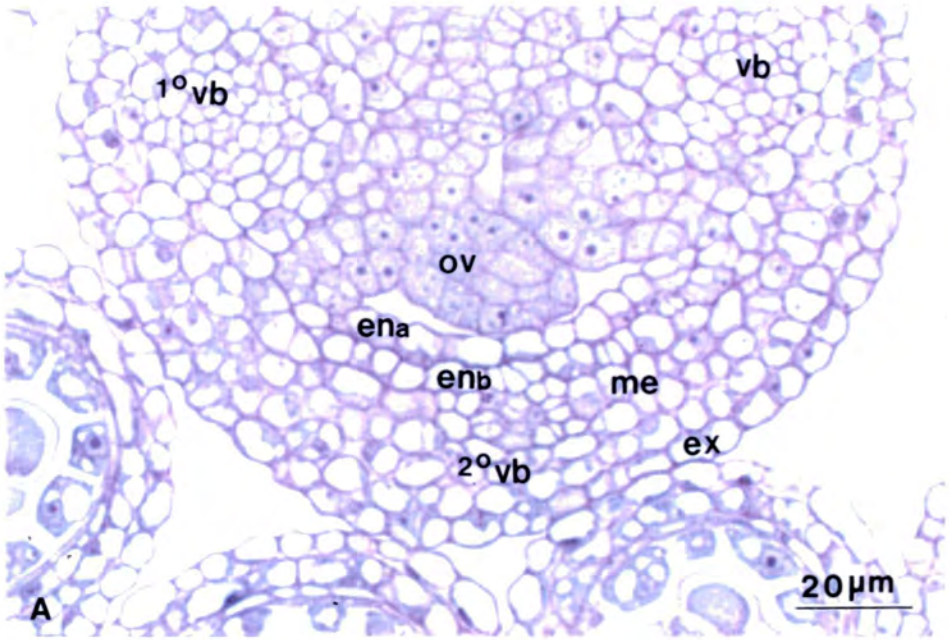
1°vb
vb
ov
ena
enb
me
ex
2°vb
20µm
A

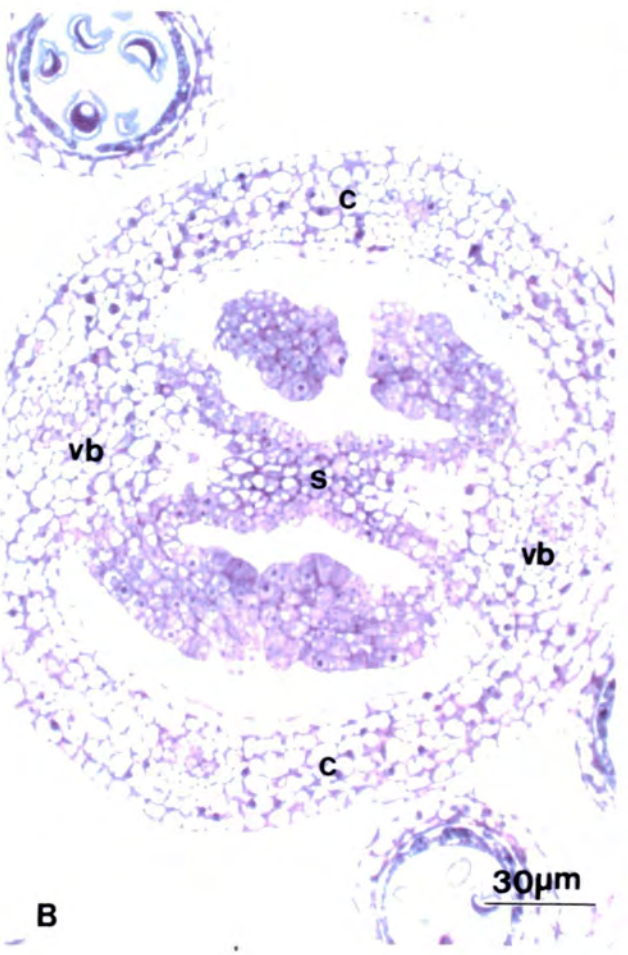
c
vb
s
vb
c
30µm
B

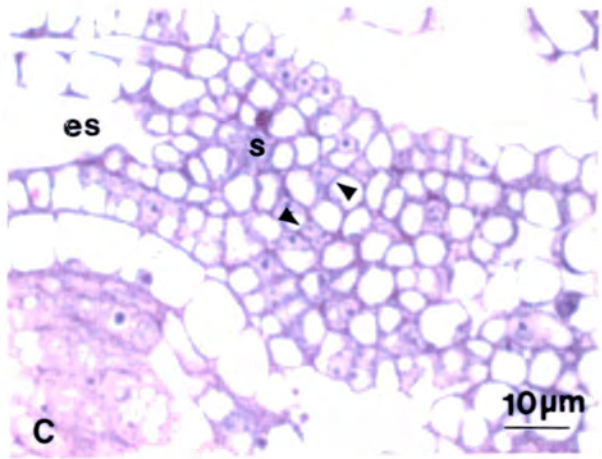
es
s
10µm
C

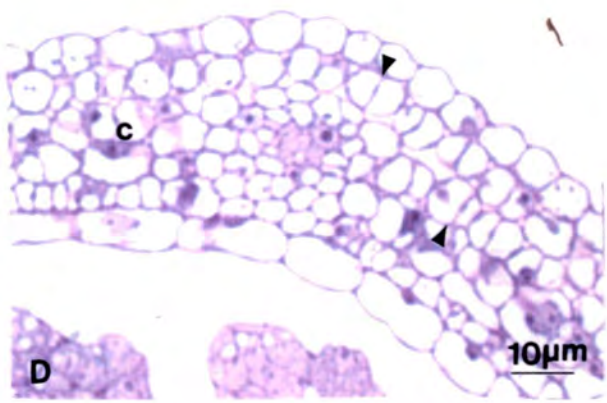
c
10µm
D

Figure 3.

Directly above the vascular bundles short papillae begin to form on the outside of the gynoecium. During stage four the ovules develop a funicle and appear stalked. As the major gynoecial tissue types have been established by the end of stage four, stage five is predominantly a growing phase. The locules greatly increase in size to accommodate the growing ovules (Fig. 3B), and the gynoecium elongates to reach the height of the mature anthers (Fig. 4A). There are continued anticlinal divisions in the exocarp and mesocarp layers indicated by arrows in Fig. 3D. The exocarp cells also begin to expand along the long axis while, as Fig. 3D illustrates, intercellular spaces increase in size and frequency within the mesocarp layers and there is little cell expansion. Within the endocarp, en*b* cells also show little cell expansion but anticlinal divisions occur at a much higher rate than in the rest of the carpel wall. In transverse section en*b* has many more cells than other carpel wall layers. En*a* cells on the contrary show less cell division but expand in all planes (Fig. 4B). These are the largest cells of the carpel walls.

The septum shows the most noticeable size increase during stage five and lengthens in the radial plane (Fig. 3B). This is achieved by anticlinal divisions of the outer cell layer. The fused cells in the centre of the septum do not divide. The inner septum cells show some cell division, however large intercellular spaces form in the inner septum as it elongates. These intercellular spaces are well illustrated in Fig. 3C. Late in stage five much of the intercellular spaces within the septum are filled with an amorphous, extracellular matrix which stains pink in toluidine blue stained sections (Fig. 4A). Okada *et al.* (1989) reported this matrix to stain pink with azure B. Acridine orange stained sections revealed bright red staining of this matrix which is indicative of a high pectin or RNA content. The papillae at the tip of the gynoecium elongate considerably during stage five producing a dry papillate stigma (Fig. 4A & 4C). The top of the gynoecium reaches the height of the mature anthers (Fig. 8B) and at the end of stage five the plant typically self fertilises.

Figure 4 The mature gynoecium

Sections in Fig. A & Fig. B are stained with toluidine blue and photographed under bright field illumination.

[A] Transverse section of the mature gynoecium showing the pink staining extracellular matrix in the central septum (s); (c) carpel wall, (st) stigma.

[B] Longitudinal section of the carpel wall of the mature gynoecium showing cell layers of the carpel wall; (en) endocarp, (me) mesocarp, (ex) exocarp.

[C] SEM view of the top of the wild type gynoecium (gy) showing the young stigmatic papillae (st).

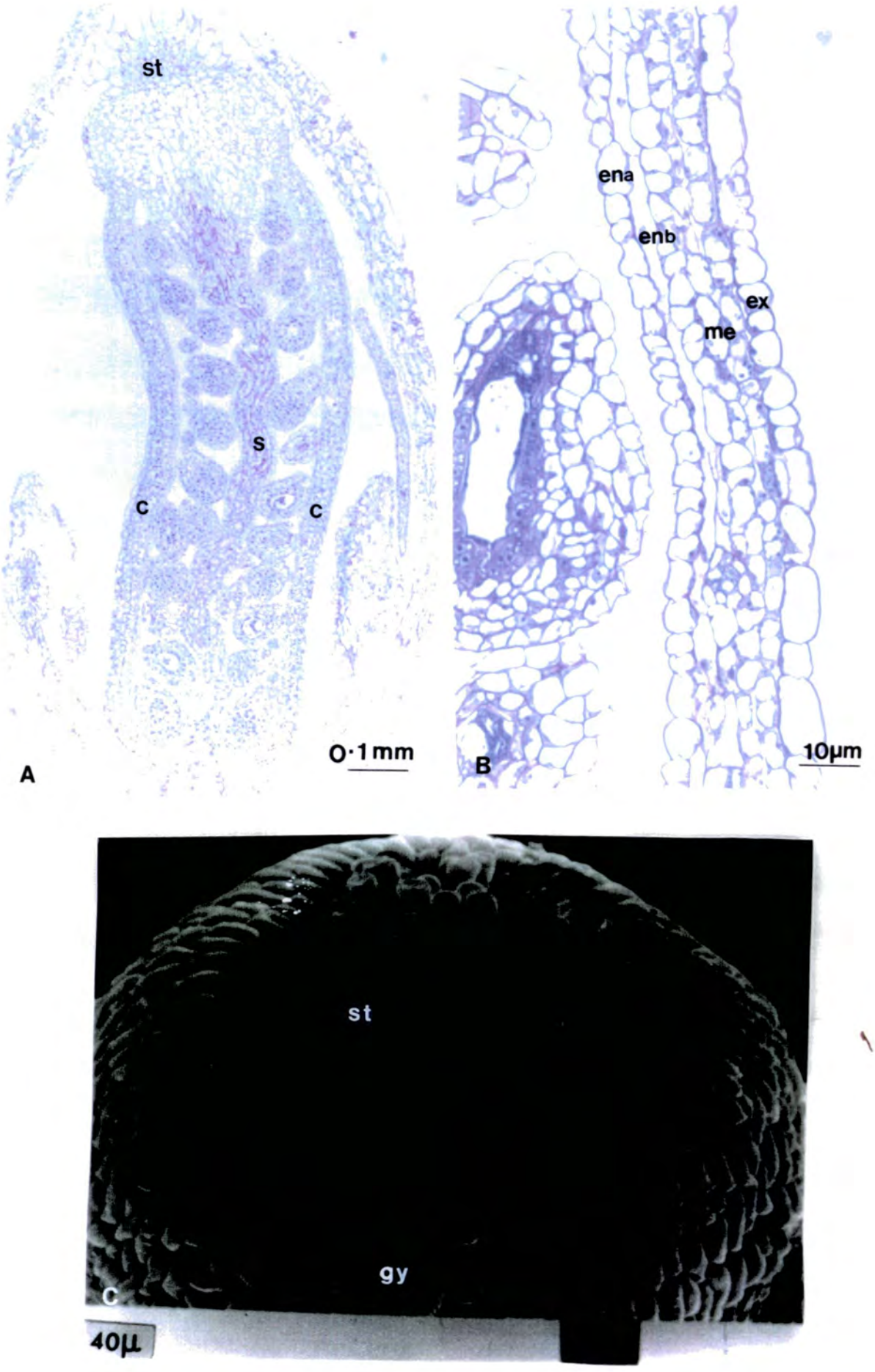

Figure 4.

HISTOCHEMISTRY OF THE PRE-FERTILISED FRUIT

ESTERASE

Esterase activity was detected as blue deposits on frozen tissue sections stained with fast blue BB, control sections showed no colour development. The differentiating vascular tissues show the highest esterase activity throughout all the stages of gynoecial development. During the initial two stages of development, all gynoecial tissues show esterase activity, as illustrated in Fig. 5A. However, following differentiation of the carpel wall at stage three, activity is completely absent from the exocarp layer and only a little residual activity remains in the mesocarp layers. Activity within the endocarp layer however remains constant during these stages. In the inner septum cells activity increases following placental fusion while those on the outer septum show very little or no activity (Fig. 5B). Following stage four, activity increases in the endocarp layer (Fig. 5D), however, activity is restricted to en*a*; no activity is detected in en*b*.

In the mature gynoecium en*a* is the only carpel wall layer still to exhibit any significant esterase activity. Just prior to and during fertilisation at stage five, activity is high in the mesodermal tissues of the stigma, as illustrated in fig. 5C, although no activity is detected in the stigmatic papillae or pollen grains. Activity in the inner septum has decreased significantly in the mature gynoecium by stage five however, this decrease could be a consequence of the increased intercellular spaces within the inner septal tissues.

PHENOL OXIDASE

Phenol oxidase activity was detected as blue deposits on frozen tissue sections stained with naphthol, control sections showed no colour development. The vascular tissues showed the highest activity throughout all the pre-fertilisation stages of development. During the first two stages of gynoecial development no phenol oxidase activity was detected in any of the gynoecial tissues. In late stage three gynoecia the primary vascular bundles only show a little activity, but by stage four activity in the primary vascular bundles has increased significantly (Fig. 6A). The secondary bundles also show some activity in stage four gynoecia. Following differentiation of the second endocarp layer, en*b*, a little activity within en*a* and the outer septum cells was observed (Fig. 6A). In the mature gynoecium phenol oxidase activity is very high in all of the mature vascular bundles however, the low activity

Figure 5 Histochemistry of the pre-fertilised fruit, esterase

Esterase activity is shown as blue deposits and photographed under Nomarski illumination.

[A] Transverse section of a young gynoecium (gy) showing the pattern of esterase distribution, the highest activity is in the anthers (a).

[B] Transverse section of the septum (s) of a mid stage wild type gynoecium showing esterase activity in the inner septum tissues; (c) carpel wall, (ov) ovule

[C] Longitudinal section of the top of the mature gynoecium (gy) showing esterase distribution in the stigma (st) and vascular bundles (vb). There is no activity in the stigmatic papillae or pollen grain (gr).

[D] Transverse section of the carpel wall (c) of a mature gynoecium. Esterase is restricted to the outer endocarp layer, indicated by arrows; (ov) ovule.

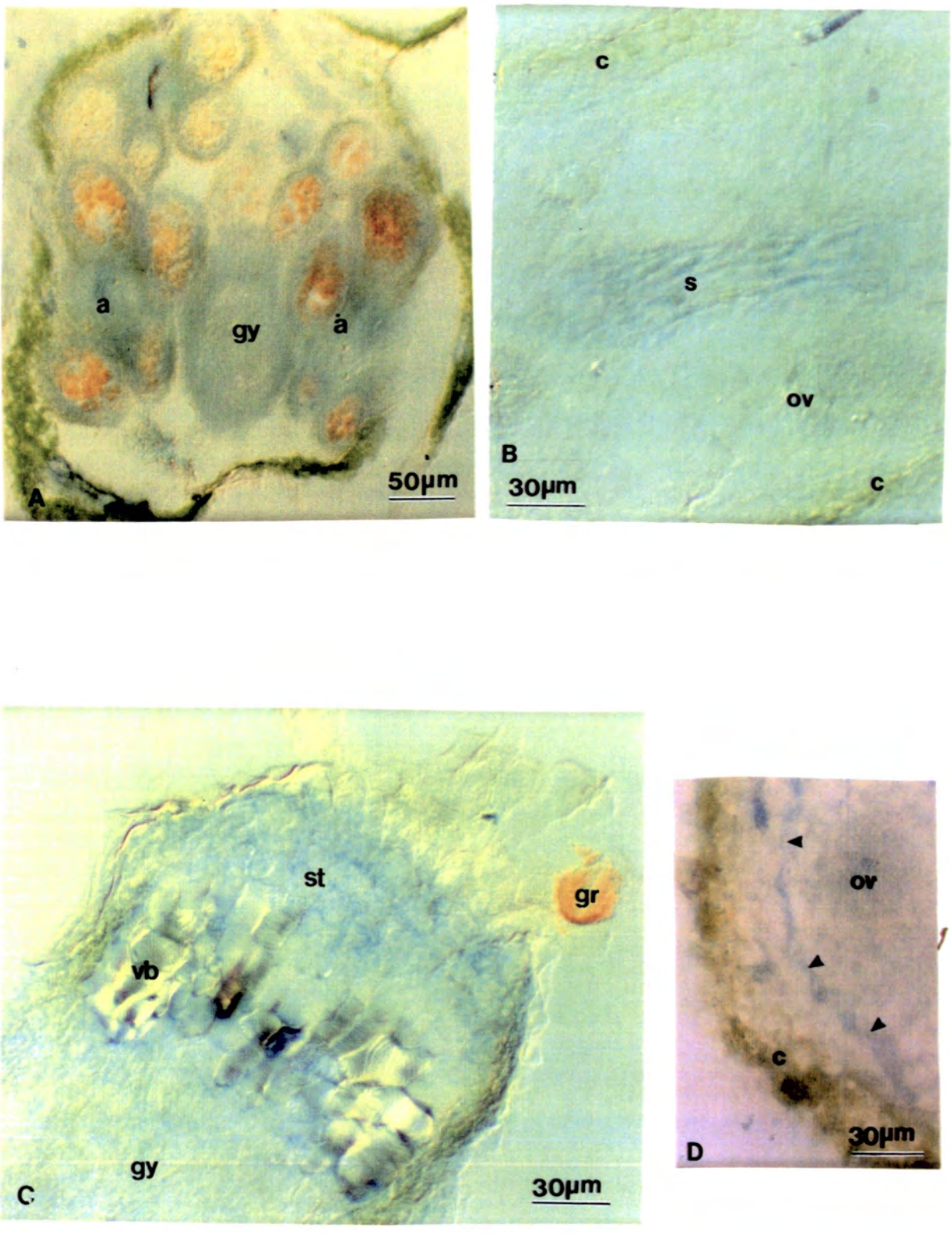

Figure 5.

within the outer septum cells and ena appears to be a significant feature. The vascular bundles within the pedicle also showed phenol oxidase activity (Fig 6B).

IMMUNOCYTOCHEMISTRY OF THE PRE-FERTILISED FRUIT

A panel of monoclonal antibodies raised in rat from cell wall isolates of *Daucus carrota* root (Knox *et al.* 1989, 1990, Pennell *et al.* 1989, Stacey *et al.* 1990) were kindly supplied by the John Innes Institute. An initial screen of ten antibodies six to arabinogalactan (AGP), two for glycoprotein and two for pectin was performed on sections from wax-embedded tissue. Fluorescein conjugated to a secondary antibody was used as the marker and specific localisations were detected as green fluorescence which was absent from control sections. Antibodies chosen for further study were detected using colloidal gold conjugated to a secondary antibody as the marker. Colloidal gold was silver enhanced and specific localisations were detected as either brown deposits under bright field illumination or bright silver/gold on a dark background under epi-polarising illumination.

PECTIN ANTIBODIES

The two pectin antibodies JIM5 and JIM7 bound to all tissue types within the gynoecium during all of the pre-fertilisation stages, results not shown, and are therefore probably detecting common structural constituents of the cell wall.

GLYCOPROTEIN ANTIBODIES

The two glycoprotein antibodies JIM11 and JIM16 did not show any significant binding to the gynoecium of the pre-fertilised fruit at any stage of development.

AGP ANTIBODIES

Five of the AGP antibodies, JIM4, JIM12, JIM14, JIM15 and MAC207 showed no significant binding to the gynoecium of the pre-fertilised fruit at any stage of development. During stage two when the placentae are formed, weak JIM13 binding is detected in the young placental tissues; this is more clearly demonstrated in the clv1 gynoecium (Fig. 6C) in which there are four placental primordia. JIM13 binds strongly to the anthers at this stage of development. JIM13 did not bind to the placental tissues after stage two or in any of the subsequent stages of gynoecial development.

Figure 6 Histochemistry of the pre-fertilised fruit, phenol oxidase and JIM13.

Phenol oxidase is shown as dark blue deposits and was photographed under Nomarski illumination. JIM13 binding is shown as bright silver deposits and photographed under epi-polarising illumination.

[A] Transverse section of a mid stage gynoecium showing phenol oxidase distribution. Very faint blue staining can just be discerned in the outer septum (s) and endocarp; (c) carpels wall, (vb) vascular bundle.

[B] Transverse section of a pedicle of a wild type flower showing phenol oxidase activity in the vascular bundles; (ed) exoderm.

[C] Transverse section of a stage 2 *clv1* gynoecium. The anthers (a) show very strong binding of JIM13 and the placentae (p) show some weak binding.

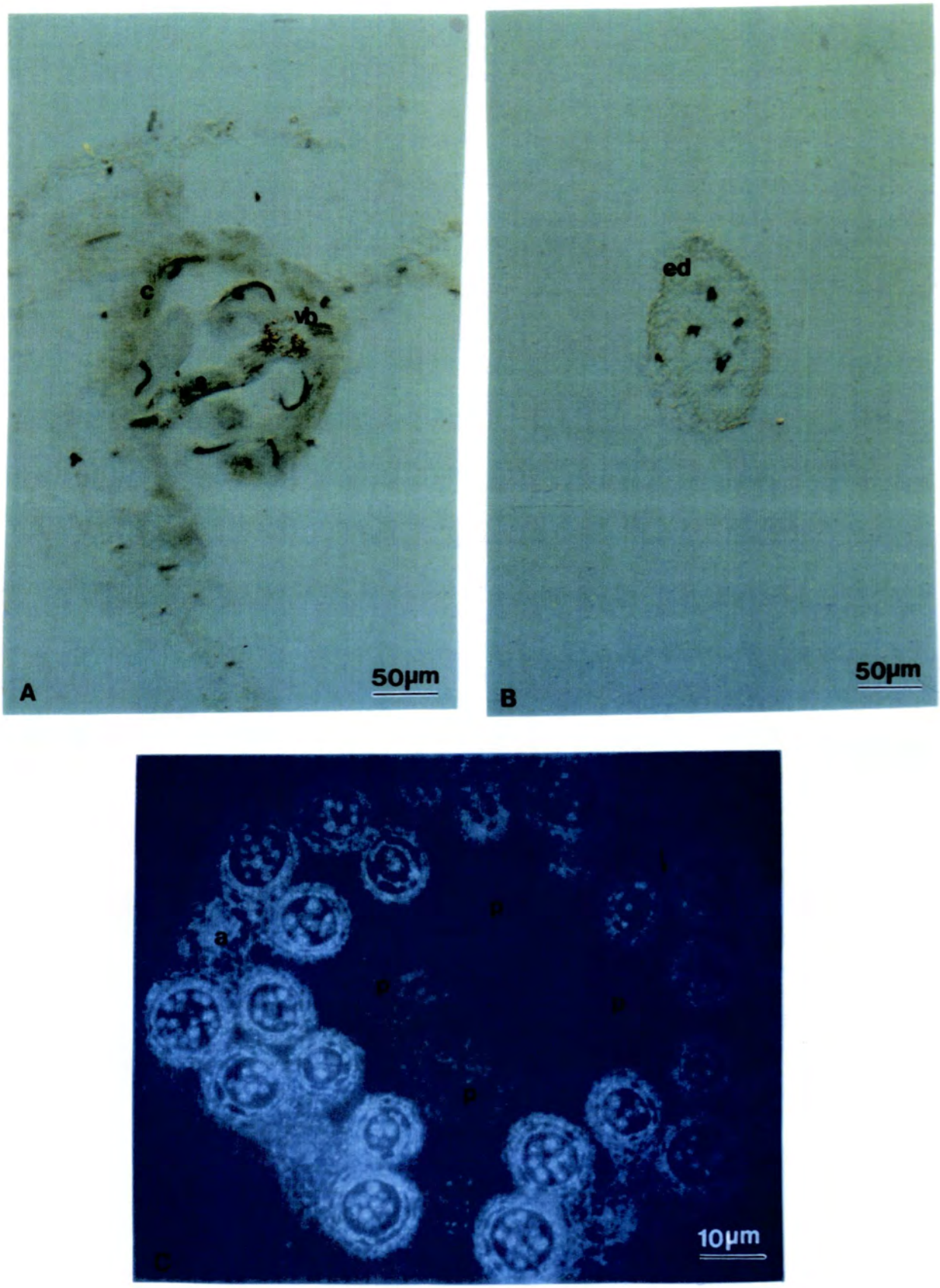

Figure 6.

PROTEASE

A pea protease with specific activity against Rubisco has been shown by immunolocalisation to be present in the exocarp of developing pea pods (Cercos & Carbonell 1993 in press). The rabbit antibody to pea pod protease was kindly donated by Dr. M. Cercos, and was localised by fluorescein conjugated to a secondary antibody. Protease distribution was detected as green fluorescence on wax-embedded tissue which was absent from control sections. There was no significant level of protease detected in the gynoecium at any stage of development of the pre-fertilised *Arabidopsis* fruit. Protease was however detected in the exodermal layers of the pedical and sepals.

RUBISCO (RIBULOSE 1, 5, BIS PHOSPHATE CARBOXYLASE)

Ribulose 1, 5, bis phosphate carboxylase is a major photosynthetic enzyme. A rabbit antibody to Rubisco was kindly donated by Dr. M. Cercos, and was localised by fluorescein conjugated to a secondary antibody. Rubisco distribution was detected as green fluorescence on wax-embedded tissue which was absent from control sections. There was no significant level of Rubisco detected in the gynoecium until the final stage of gynoecial development. Rubisco was localised in the chlorenchymous mesocarp layer of the gynoecial wall from completion of stage five. This pattern suggests that the mesocarp layer cells only begin to photosynthesise actively late in gynoecial development. The chlorenchymous mesophyll cells of the sepals also showed significant Rubisco levels throughout early gynoecial development.

MOLECULAR HISTOCHEMISTRY OF THE PRE-FERTILISED FRUIT

CELLULASE (ß 1, 4, GLUCANASE)

Cellulase mRNA was detected on sections from wax-embedded tissues by hybridisation of a digoxygenin labelled cDNA probe. After hybridisation the specifically bound probe was localised by anti digoxygenin conjugated to a alkaline phosphatase, the latter being detected histochemically as red deposits which were absent from control sections. A cDNA probe to tomato fruit cellulase was kindly donated by Dr. W. Schuch. Cellulase mRNA was first detected in the central septum tissues during the mid stages of gynoecial development, following fusion of the septa at stage four. Quite high levels of staining were detected though to the last

Figure 7 Histochemistry of the pre-fertilised fruit, cellulase and pectinesterase.

Cellulase and pectinesterase mRNA distribution is shown as red deposits and was photographed under Nomarski illumination.

[A] Transverse section of a mature wild type gynoecium showing cellulase mRNA distribution in the inner septum (s). There is no staining in the carpel wall (c) or stigma (st).

[B] Transverse section of a mid stage wild type gynoecium showing pectinesterase mRNA in the septum (s), there is no staining in the carpel wall (c) but there is some weak staining in the anthers (a).

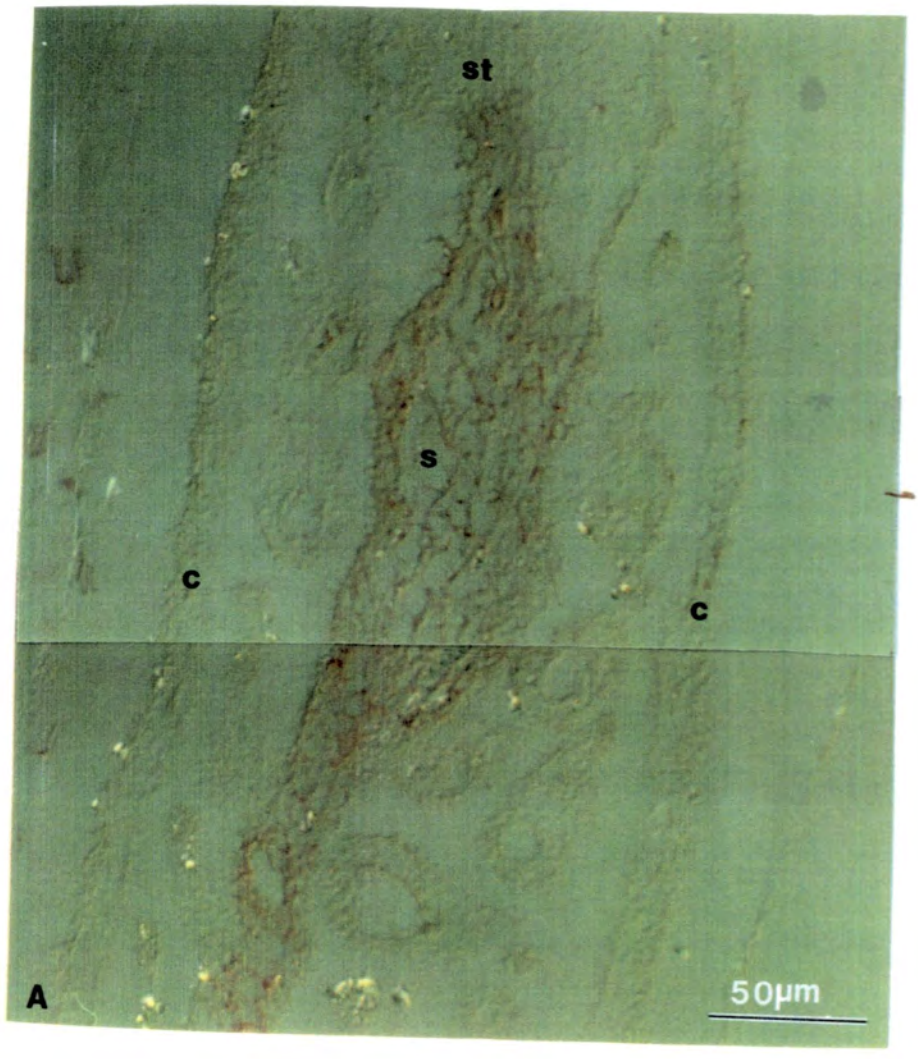

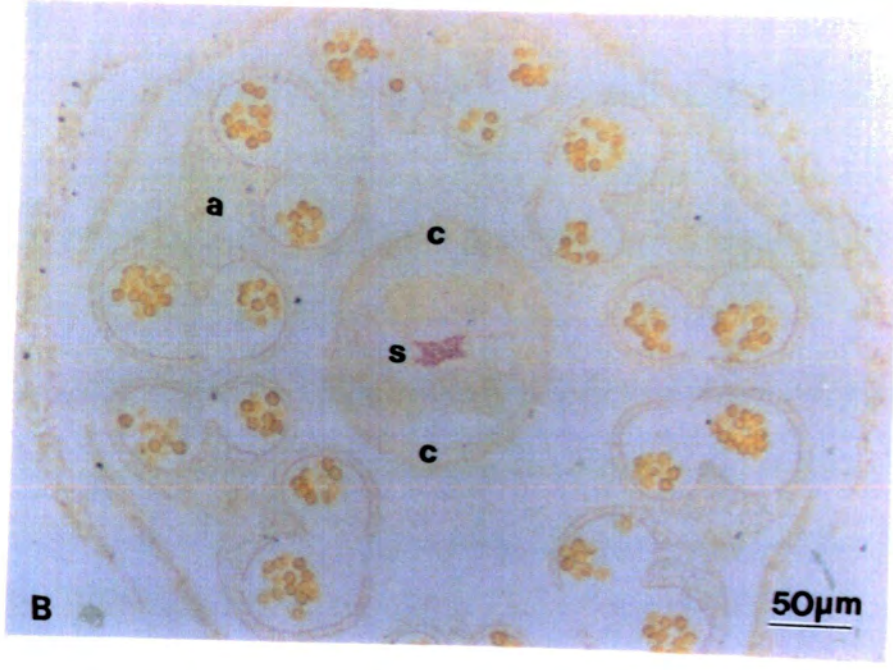

Figure 7.

stage of gynoecial development (Fig. 7A). There was no staining of tissues around the primary vascular bundles or the stigma. In control sections there was some non-specific binding of the probe to the central septum tissues, however, the signal was always much weaker than that of the test sections. Cellulase mRNA was also detected in the anthers, during dehiscence, and in the sepals and petals prior to abscission.

PECTINESTERASE

Pectinesterase mRNA was detected on sections from wax-embedded tissues by hybridisation of a digoxygenin labelled cDNA probe. After hybridisation the specifically bound probe was localised by anti digoxygenin conjugated to alkaline phosphatase, the latter being detected histochemically as red deposits which were absent from control sections. A cDNA clone to pea fruit pectinesterase was kindly donated by Dr. J Gatehouse and Mr. D. Bown. The role of pectinesterase in pea fruit ripening is currently under investigation (D. Bown personal communication) and its role in tomato fruit ripening has recently been studied (Ray *et al.* 1988).

The pattern of pectinesterase expression in the gynoecium was similar to that reported for cellulase. Binding was detected in the central septal tissues following septal fusion and remained through to the last stage of gynoecial development (Fig. 7B). Control sections also showed a little background deposit in the central septal tissues, however, this was much weaker than that in the test sections. Pectinesterase mRNA was also noted in the tapetum cells of the mature anthers and filaments (Fig. 7B).

POLYGALACTURONASE

Polygalacturonase mRNA was detected on sections from wax-embedded tissues by hybridisation of a cDNA probe. After hybridisation the specifically bound probe was localised by anti digoxygenin conjugated to alkaline phosphatase, the latter being detected histochemically as red deposits which were absent from control sections. A cDNA clone to tomato fruit polygalacturonase was kindly donated by Dr. W. Schuch. Polygalacturonase has been shown to be one of the major cell wall softening enzymes in the tomato fruit (Markovic & Jornvall 1986). No significant staining could be detected in the *Arabidopsis* gynoecium at any stage of pre-fertilisation development using the tomato fruit cDNA probe to polygalacturonase.

Figure 8 Gross morphology of wild type *Arabidopsis thaliana*.

[A] The mature *Arabidopsis thaliana* plant.

[B] The inflorescence of *Arabidopsis thaliana*.

[C] The gross morphology of the wild type silique during the five post fertilisation stages of development.

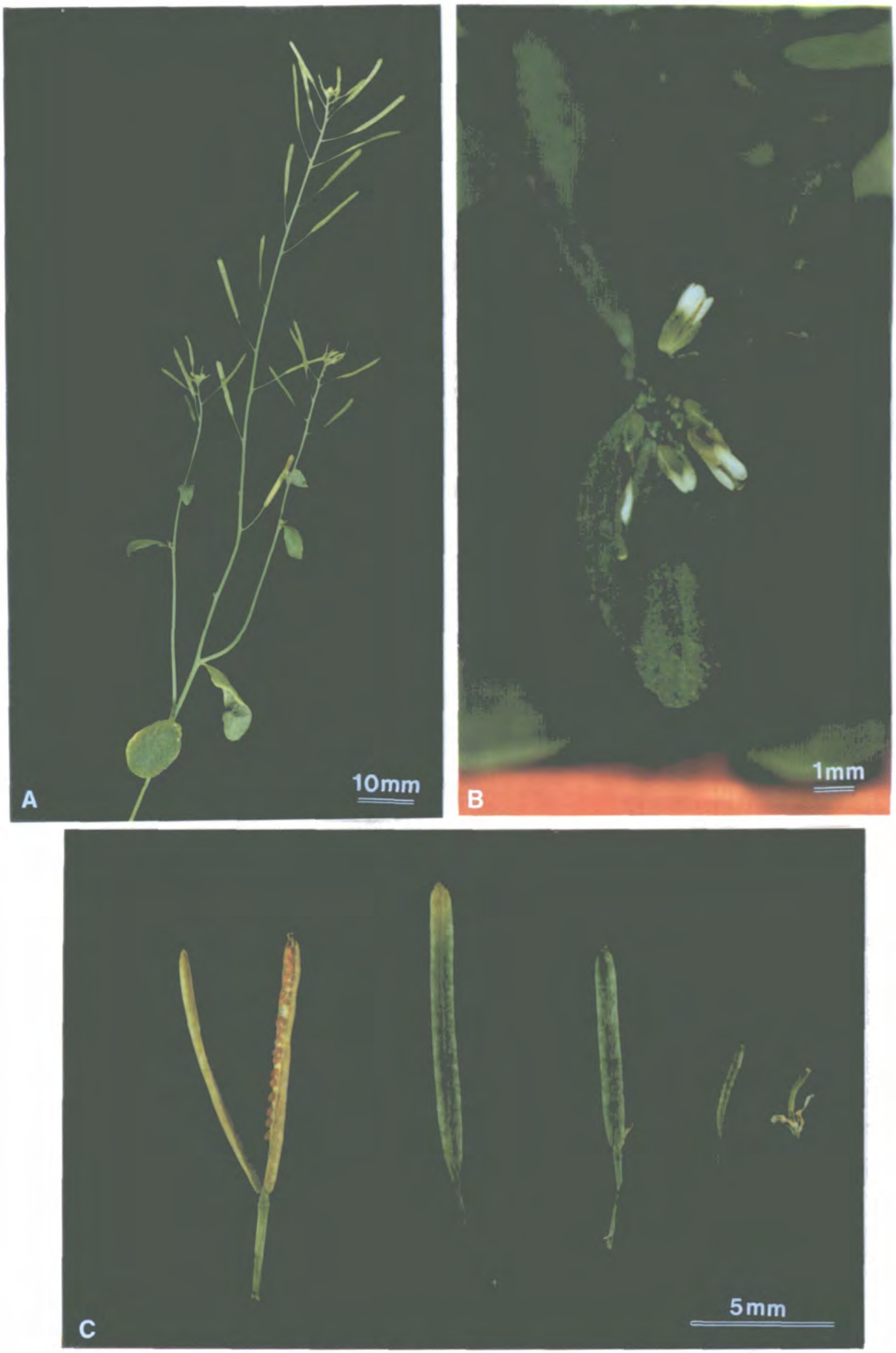

Figure 8.

DEVELOPMENT OF THE *ARABIDOPSIS* SILIQUE

We have been concerned mainly with the development of the carpel walls and the dehiscence zones during the later stages of fruit development. The post fertilised gynoecium is referred to as a silique and, following development of the dehiscence zones, regions of the carpel walls (referred to as valves) are isolated and eventually separate (Fig. 8C). This post-fertilisation development of the fruit may be divided into a further five stages (Table 3).

Following fertilisation there is a marked increase in the length of the silique but a comparatively small increase in the diameter. Macroscopically two opposing sutures become visible running the length of the silique. At stage six, the layer of cells forming the exocarp continue to divide and expand in all planes, but predominantly along the long axis, except for those adjacent to the primary vascular bundles. These show no expansion in transverse section. The outer tangential walls of exocarp cells thicken considerably during this stage. The cells of the mesocarp layer also continue to divide and expand in all planes, however, much size variation can be observed between cells within the mesocarp, and there is also an increase in the size and frequency of intercellular spaces between mesocarp cells. As Fig. 10A shows, mesocarp cells at stage six develop many chloroplasts which are concentrated around the edges of each cell. The most noticeable size difference between the mesocarp cells is evident at the carpel margins where about four rows of cells are distinctly smaller and do not contain chloroplasts.

STAGE	KEY EVENTS
6	carpel margins begin to constrict
7	dehiscence zone cells develop
8	mesocarp around dehiscence zone lignifies
9	En*a* lignifies, En*b* disintegrates
10	fruit dehisces

Table 3: Brief Summary Of Silique Development

The two endocarp layers become even more distinct during this growing phase. En*a* cells continue to divide and expand more along the short axis (Fig. 10A & 10B), and appear quite swollen in transverse section. In contrast en*b* cells continue to divide anticlinally early in stage six but then expand along the long axis to form

Figure 9 Early stages of silique development

Sections in Fig. A and Fig. B are stained with toluidine blue and photographed under bright field illumination. The section in Fig. C is stained with acridine orange and photographed under fluorescence illumination using a blue filter.

[A] Transverse section of a young silique showing the structure and major tissue types; (c) carpel wall, (s) septum, (vb) vascular bundle.

[B] Transverse section of the primary vascular bundle (vb) of the young silique The arrows indicate the slight constrictions of the marginal carpel walls (c).

[C] Transverse section of a young silique equivalent to Fig. 9B.

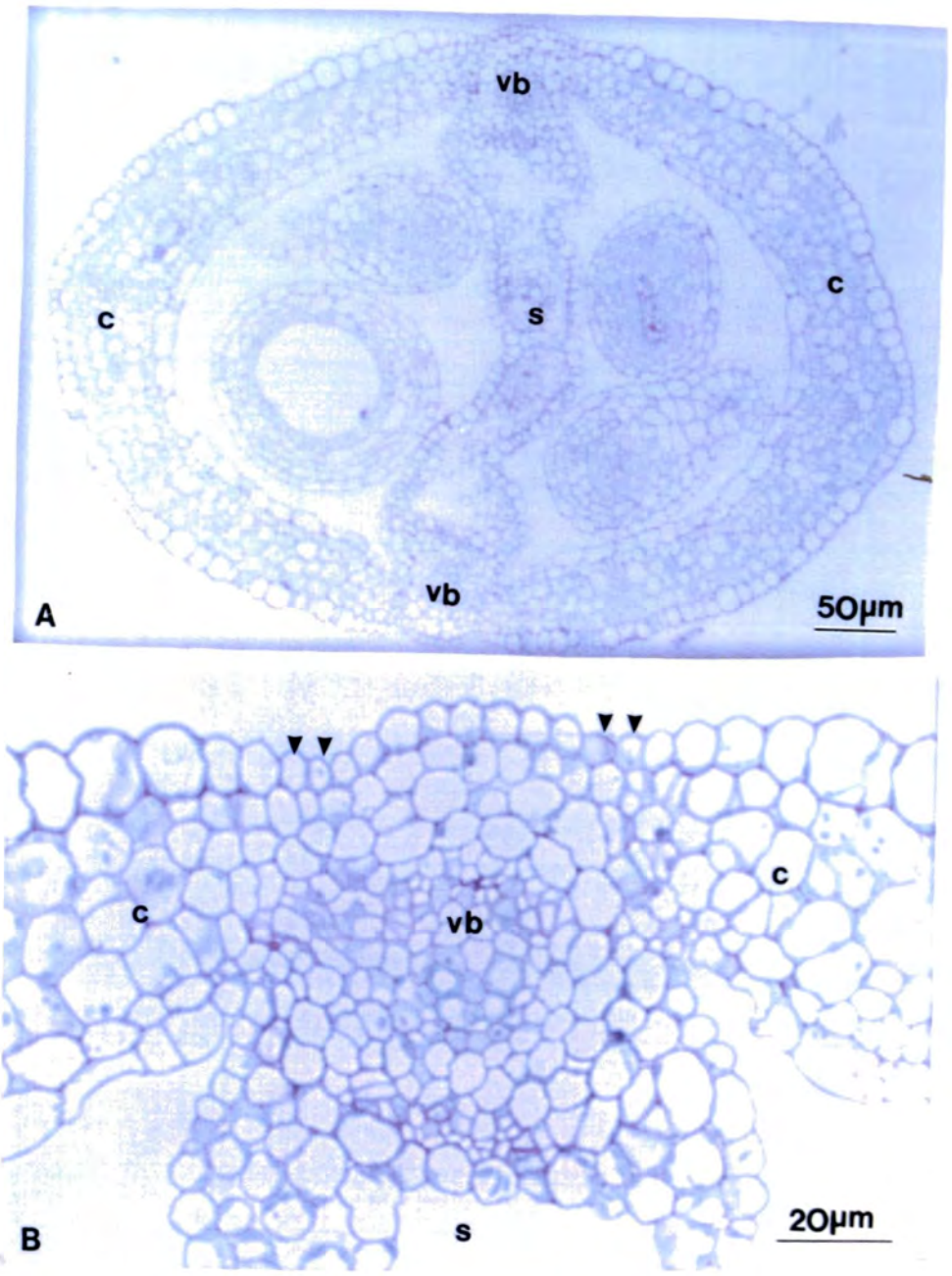

Figure 9.

long, thin, tapered cells (Fig. 10B). As with the other carpel wall layers endocarp cells on the margins of the carpels are much smaller. The differential increase in cell size between the carpel margins and the rest of the carpel wall causes a distinct constriction at each carpel margin (Fig. 9A, 9B & 9C).

The septum also increases in length during stage six as the outer septum cells continue to divide and expand mainly in the radial plane. The extracellular matrix is less apparent remaining only in the central area where fusion occurred (Fig. 10C). Intercellular spaces within the inner septum increase in size and frequency, and isolated cells which contain chloroplasts are often observed. The parenchymous cells which surround the primary vascular bundles contain chloroplasts and so resemble those of the mesocarp but they are smaller. The primary vascular bundles generally increase in size and the xylem elements lignify. The secondary bundles within the carpel walls also generally increase in size and form many branches which extend out through the mesocarp layers.

Two rows of the smaller cells on the extreme margins of the carpel walls begin to disintegrate during stage seven (Fig. 11B). These rows of disintegrating cells extend through all the layers of the carpel wall dehiscence zones and form the separation layers. This isolates the carpel wall from the primary vascular bundles and septum, forming two valves and a replum (Fig. 11A).

Valve wall exocarp cells continue to expand in all planes, but more along the long axis, and as Fig. 12A & 12B illustrate have very thickened outer walls which forms a cuticular coat. Much more size variation can be seen among cells within the exocarp layer. The replar and dehiscence zone exocarp cells remain small. Mesocarp cells also expand in all planes. En*a* cells continue to increase in size and by stage seven appear very swollen and 'empty', while en*b* cell walls thicken to form a typical sclerenchymous tissue layer.

The septum also increases in length during stage seven, however it is only the outer layer of cells which shows any growth or division. The outer layer of septum cells resemble those of en*a* and appear as quite swollen 'empty' cells while those in the central area do not seem to divide or grow at all and the inner septum appears almost empty (Fig. 11A & 12C). All of the silique vascular bundles continue to differentiate and are the only tissues showing further growth by the end of stage seven when the silique has reached its maximum length and diameter.

Figure 10 Carpel wall and septum structure of the young silique.

Sections are stained with toluidine blue and photographed under bright field illumination.

[A] Transverse section of the carpel wall showing the major tissue types. The cells of the exocarp (ex) have thickened outer tangential walls and are interspersed with guard cells (gc) and stomata. Cells within the mesocarp (me) contain many chloroplasts and the two endocarp layers (en*a* and en*b*) are very distinct.

[B] Longitudinal section of the carpel wall showing the two endocarp layers. Cells in endocarp *b* (en*b*) are long thin tapered cells with thickened tangential walls; (en*a*) endocarp *a*, (ex) exocarp, (me) mesocarp.

[C] Transverse section of the septum (s) showing the structure of the outer septum cells (os).

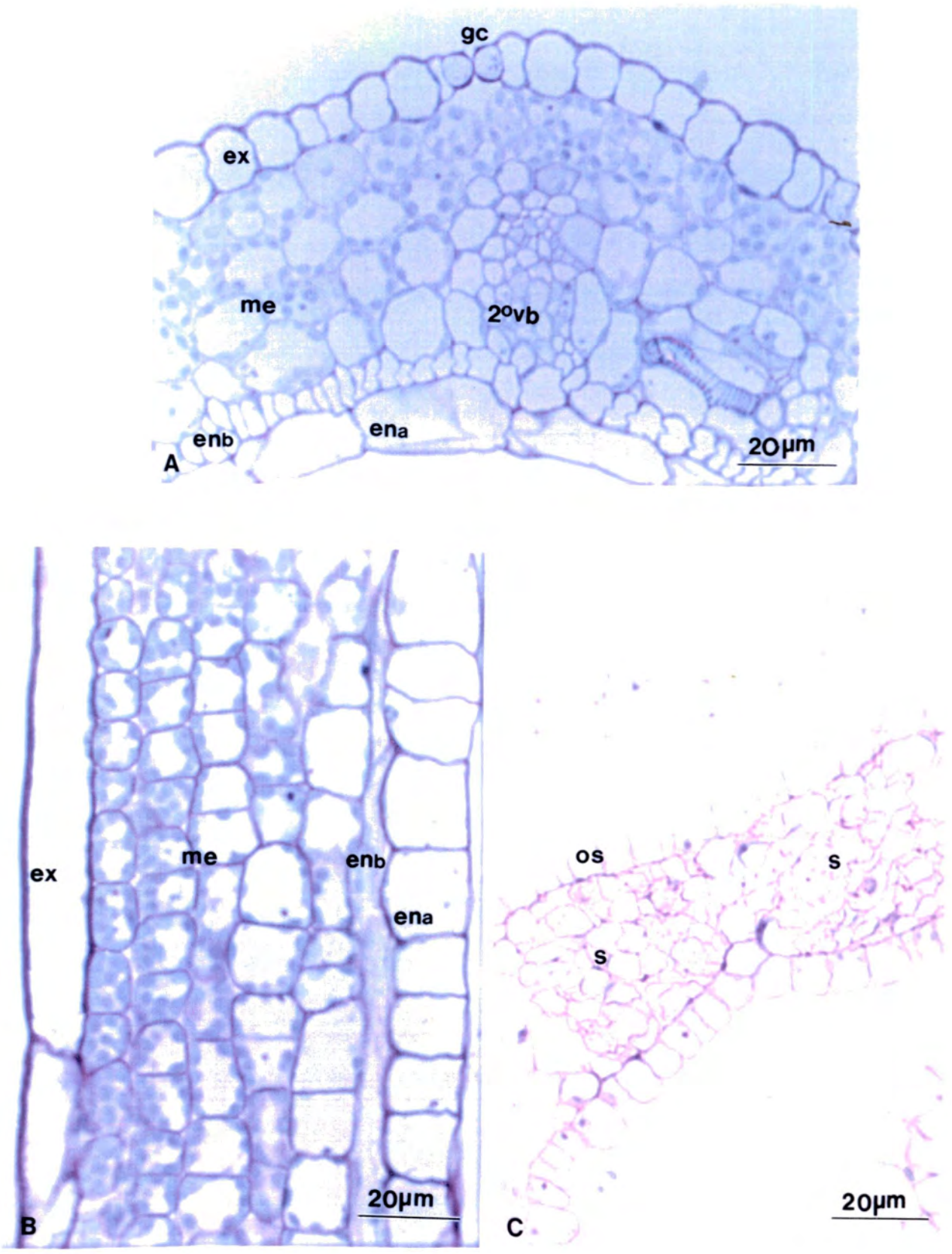

Figure 10.

Figure 11 The mature silique and dehiscence zones.

Sections in Fig. A and Fig. B are stained with toluidine blue and photographed under bright field illumination. The section in Fig. C is stained with acridine orange and photographed under fluorescence illumination using a blue filter.

[A] Transverse section of a mature silique showing the structure and major tissue types; (c) carpel wall, (s) septum, (vb) vascular bundle.

[B] Transverse section of the dehiscence zones of the mature silique. The arrows indicate the separation layer cells which show some degree of degradation, on either side of the vascular bundle (vb).

[C] Transverse section of the dehiscence zones equivalent to Fig. 11B showing the lignified cells of the valve wall (lme) and the vascular bundle (vb) which stain yellowish. The cells of endocarp *b* (enb) also show lignification.

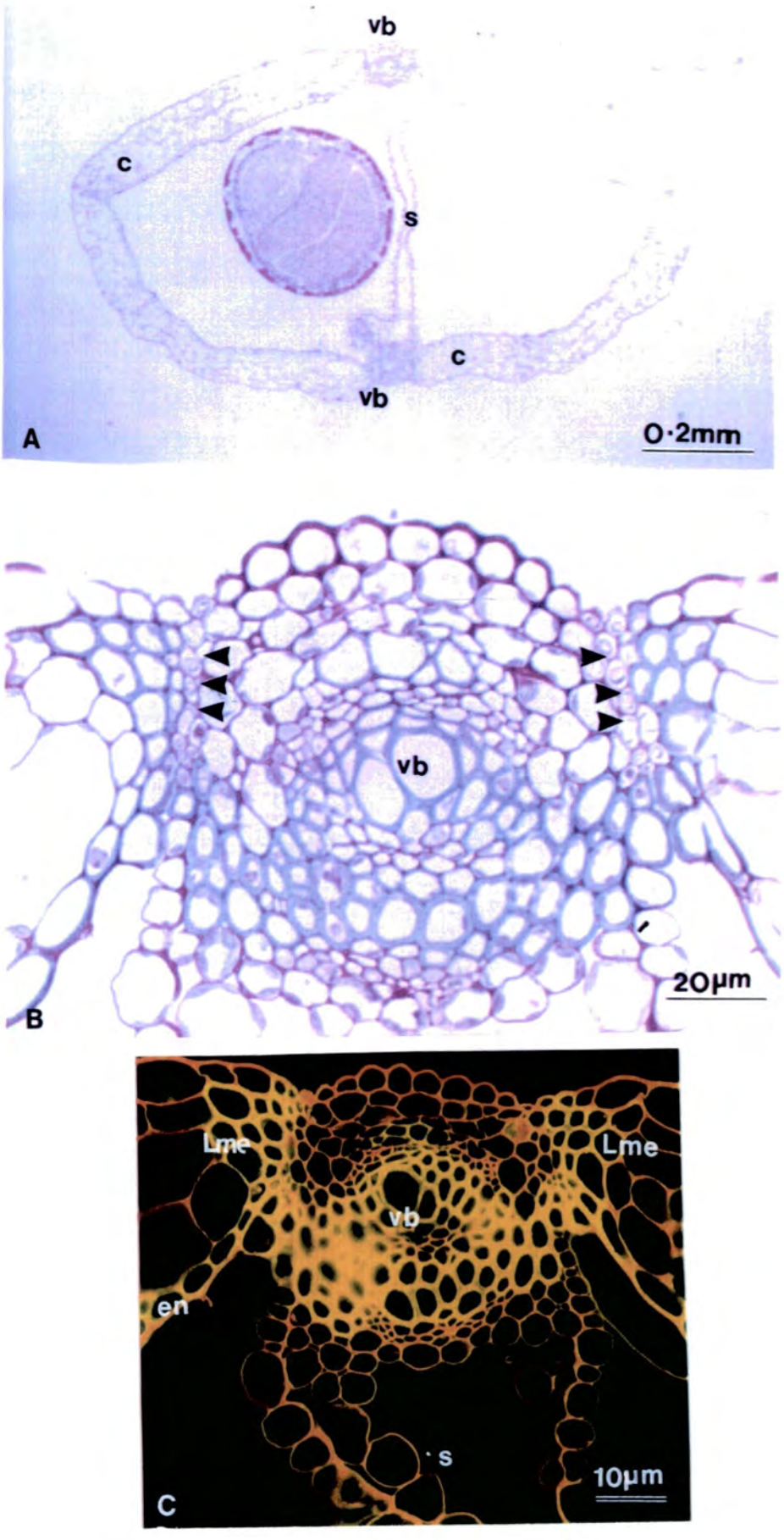

Figure 11.

The dehiscence zones differentiate further at stage eight as the few rows of small valve wall cells, adjacent to the separation layer, thicken and link the thickened endocarp and exocarp layers. As Fig. 11C illustrates these cells stain yellowish with acridine orange, indicative of lignifying tissue. The outer septum cells also thicken, but only along the inner edge. This forms a thick basement wall between the inner and outer septum tissues up to the replar bundles. The central septum appears almost empty due to the large intercellular spaces.

At stage nine the thickened enδ layer lignifies, as shown by acridine orange staining (Fig. 11C). Enα and the outer septum cell layers were never observed intact by stage nine, most cells appear to have collapsed (Fig. 12A, 12B & 12C). Although it is possible that these delicate cells are damaged during sectioning, it seems more likely that they do actually disintegrate. Macroscopically the silique begins to turn yellow from the tip to the base, (Fig. 8A & 8C), as the mesocarp begins to dry out.

At stage ten the valves split away from the replum at the separation layer. This appears to be due to lack of cell cohesion between separation layer cells, rather than cell disintegration, as whole cells were usually observed in section from dehiscing siliques.

Figure 12 Carpel wall and septum structure of the mature silique.

Sections are stained with toluidine blue and photographed under bright field illumination.

[A] Transverse section of the valve wall in a stage 9 silique. The arrows indicate the cell remnants of the first endocarp layer. Cells within the second endocarp layer (en*b*) show thickening of the tangential walls; (ex) exocarp, (me) mesocarp.

[B] Longitudinal section of the valve wall in a stage nine silique. The outer tangential walls of the exocarp (ex) show substantial thickening; (en*b*) endocarp *b*, (me) mesocarp.

[C] Transverse section of the septum (s) of a mature silique showing the basement wall and cell remnants, indicated by arrows, of the outer septum.

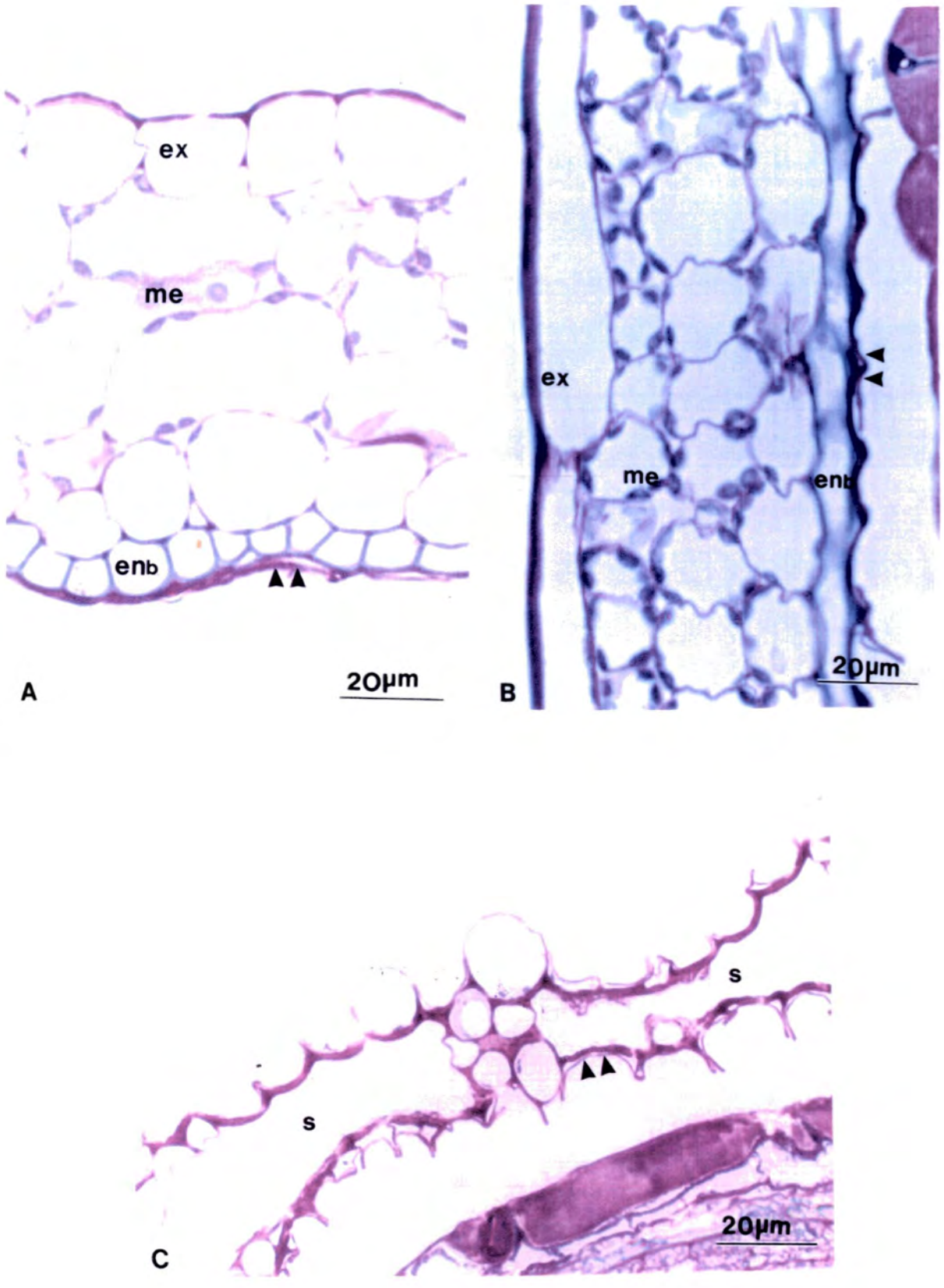

Figure 12.

HISTOCHEMISTRY OF THE POST FERTILISED FRUIT

ESTERASE

Esterase activity was detected as blue deposits on frozen tissue sections stained with Fast blue BB. Throughout all of the stages of silique development the differentiating vascular tissues showed the highest esterase activity. Following fertilisation, esterase activity within the carpel wall is restricted to en*a* and the vascular tissues, however, activity appears quite weak in the endocarp (Fig. 13A). The aerenchymous inner septum shows very little residual activity during stages six and seven however, as Fig. 13A illustrates, activity is very high in the outer septum layer. Activity declines gradually within the outer septum and endocarp layer and has completely gone by the end of stage seven when the separation layer cells have begun to disintegrate. Just prior to dehiscence, at stage nine, esterase activity is restricted to the vascular tissues. The valve wall vascular tissues still exhibit high activity but within the replar bundles activity is reduced compared to previous stages (Fig. 13C).

PHENOL OXIDASE

Phenol oxidase activity was detected as blue deposits on frozen tissue sections stained with naphthol. Throughout the stages of silique development the vascular tissues showed the highest activity. Following fertilisation a weak signal in the outer septum and en*a* gradually disappears, and, as illustrated in Fig. 14C, no signal can be detected by the end of stage six. Activity remains high and relatively constant in the silique vascular tissues throughout all the stages of silique development. Phenol oxidase activity is quite high within the cell walls of en*b* during stages eight and nine as the sclerenchymous tissue layer develops (Fig 14A & 14B). Activity within en*b* remains through to dehiscence of the silique.

IMMUNOCYTOCHEMISTRY OF THE POST-FERTILISED FRUIT

PECTIN ANTIBODIES

The two pectin antibodies JIM5 and JIM7 bound to all tissues types within the silique during all of the post fertilisation stages, results not shown. This pattern is the same as in the pre-fertilisation stages and therefore these antibodies are probably detecting common constituents of the cell wall.

Figure 13 Histochemistry of the post fertilised fruit, esterase.

Esterase activity is shown as blue deposits and photographed under Nomarski illumination.

[A] Transverse section of a young silique showing the strong staining in the cells of the outer septum (s). There is weak staining of the endocarp layer of the carpel wall (c); (vb) vascular bundle.

[B] Esterase control section equivalent to fig. 13A.

[C] Esterase staining in the primary vascular bundle of a mature silique showing the reduced signal compared to that in fig. 13A.

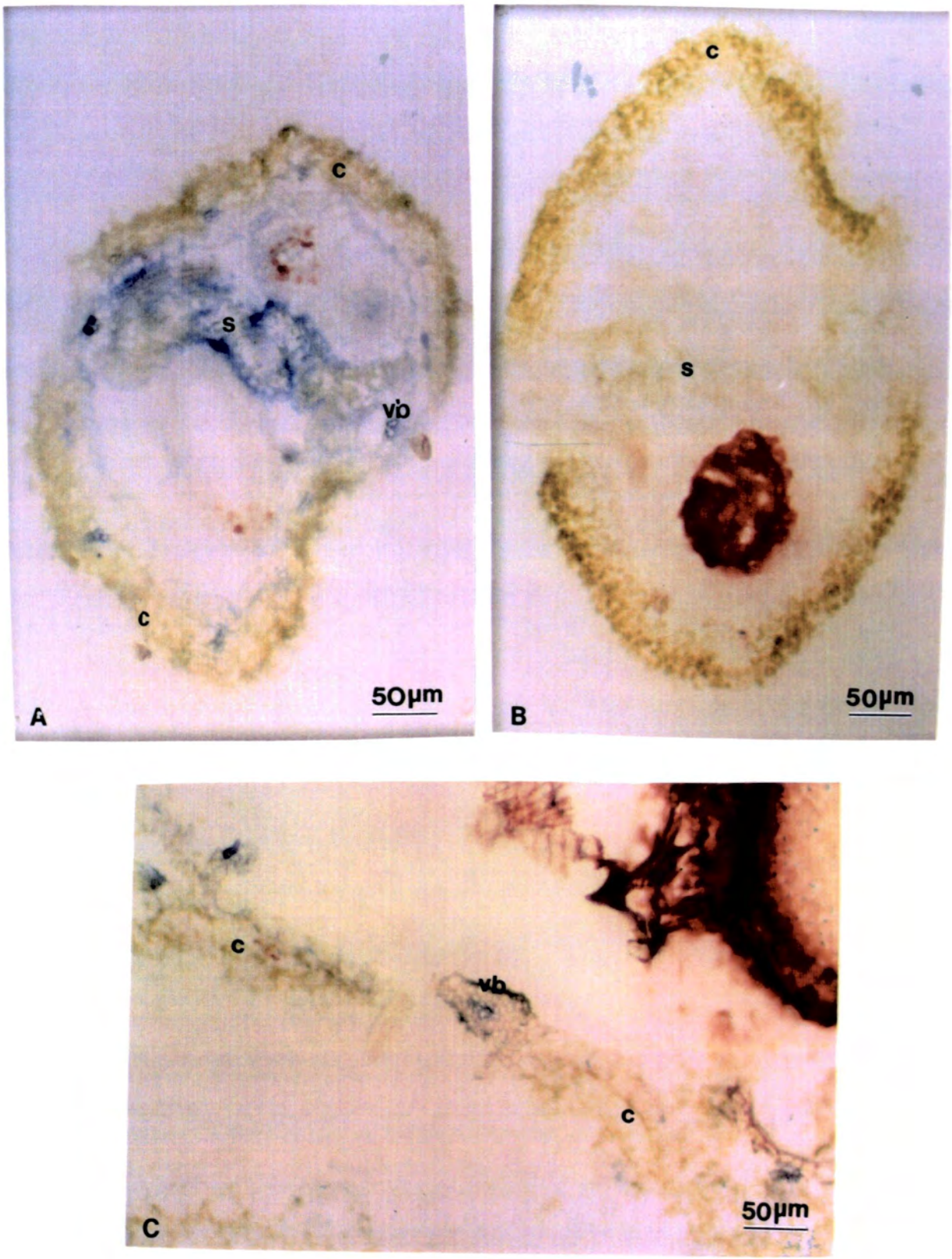

Figure 13.

Figure 14 Histochemistry of the post-fertilised fruit, phenol oxidase.

Phenol oxidase activity is shown as blue deposits and photographed under Nomarski illumination.

[A] Transverse section of a stage 9 silique showing phenol oxidase activity in the endocarp (en).

[B] Transverse section of a stage 9 silique showing phenol oxidase activity, indicated by arrows, localised to the thickened tangential walls of the endocarp (en) and vascular bundles (vb).

[C] Transverse section of a stage 6 six silique showing phenol oxidase activity in the vascular tissues; (c) carpel wall, (s) septum, (vb) vascular bundle.

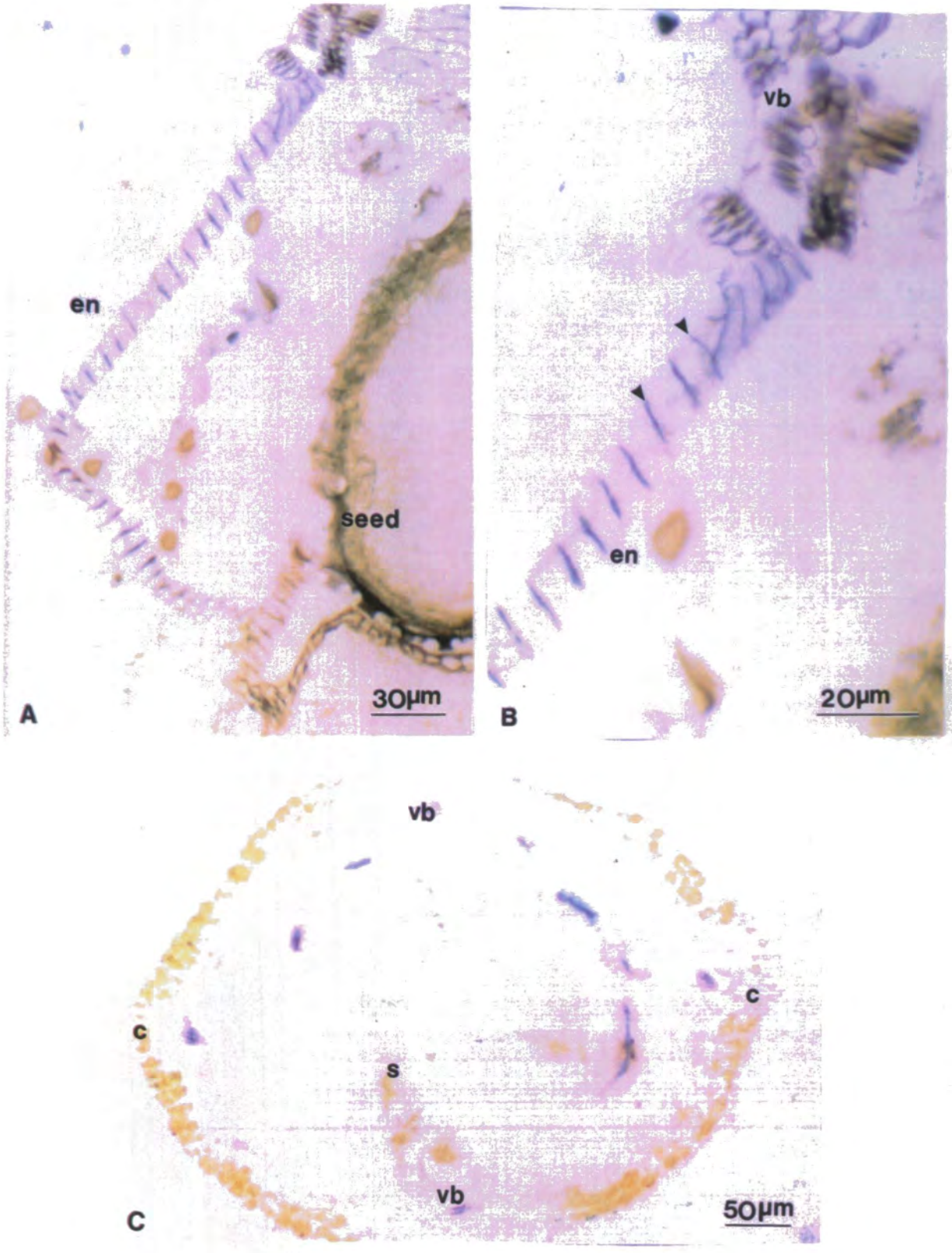

Figure 14.

GLYCOPROTEIN ANTIBODIES

The two glycoprotein antibodies JIM11 and JIM16 did not show any significant binding to component of the silique at any stage of development. As these two antibodies do not show any binding in the pre-fertilisation stages either it seems likely that neither of these glycoproteins is present in the *Arabidopsis* fruit.

AGP ANTIBODIES

Five of the AGP antibodies, JIM4, JIM12, JIM14, JIM15, and MAC207 showed no significant binding in the silique at any stage of development. As none of these antibodies showed any binding in the pre-fertilisation stages either it seems likely that non of these AGPs are present in the *Arabidopsis* fruit. In the closing stages of silique development, following disintegration of en*a* at stage nine, the second endocarp layer en*b* showed very high JIM13 binding (Fig. 15A & 15C). No JIM13 binding was detected in en*b* at any stage when en*a* was intact. Binding was also detected in the lignifying cells of the dehiscence zone and primary and secondary vascular bundles (Fig. 15B). This pattern of activity suggests that the JIM13 epitope is perhaps involved in the later stages of wall thickening.

PROTEASE

Protease was localised by fluorescein conjugated to a secondary antibody and was detected on wax-embedded tissue as green fluorescence which was absent from control sections. Following fertilisation at stage six, as the silique enlarges, protease binding was detected in the exocarp cells of the silique wall, although it was totally absent from the stomatal guard cells within the exocarp (Fig. 16A). Protease binding within the exocarp layer continued through all of the post fertilisation stages of development until dehiscence of the silique. Following development of the dehiscence zones and separation of the valves and replum, protease binding was only detected in the exocarp of the replum. The role of protease in parthenocarpic fruits and senescence is currently under investigation (Cercos *et al.* personal communication).

Figure 15 Histochemistry of the post-fertilised fruit, JIM13.

JIM13 binding is shown as brown deposits and photographed under Nomarski illumination or bright silver/gold on a dark background and photographed under epi-polarising illumination.

[A] Transverse section of a stage 9 silique showing the overall pattern of JIM13 binding to the endocarp (enb) and vascular bundles (vb); (c) carpel wall.

[B] Transverse section of the primary vascular bundle and dehiscence zones of a stage nine silique showing JIM13 binding to the vascular bundle (vb) and lignified cells of the dehiscence zone (lme).

[C] Transverse section of a stage 9 silique showing JIM13 binding to the second endocarp layer cells (enb).

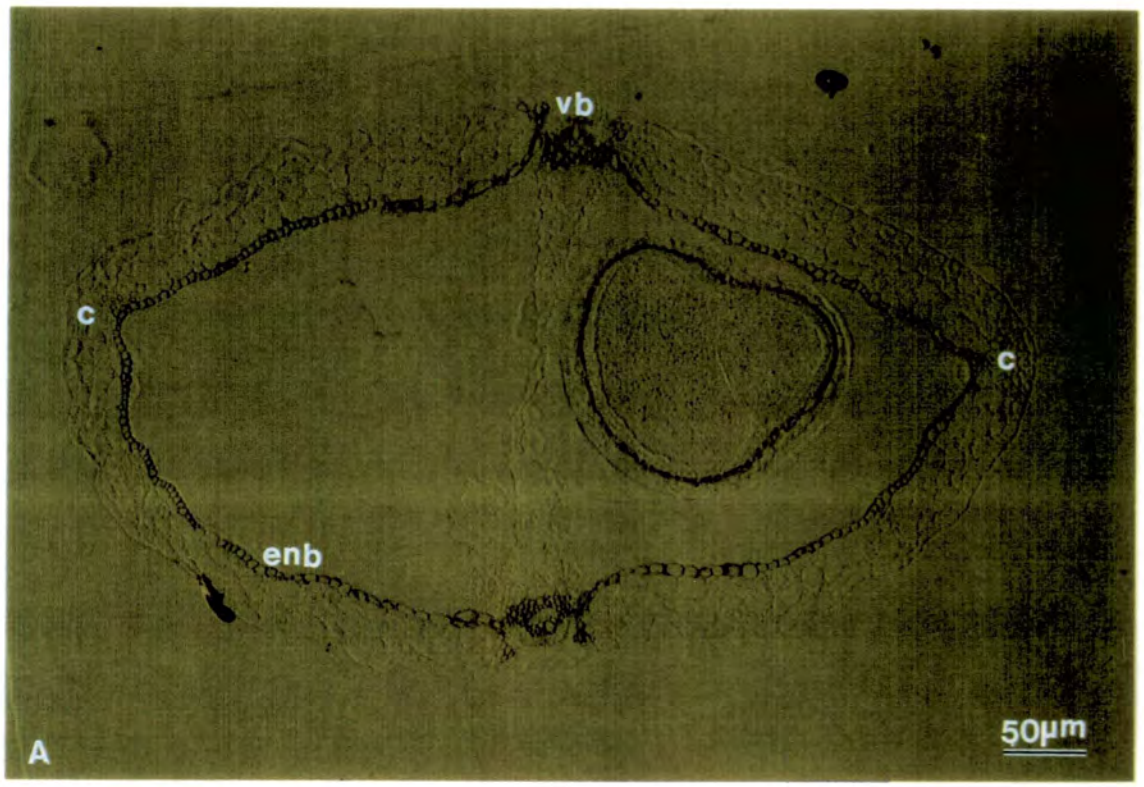

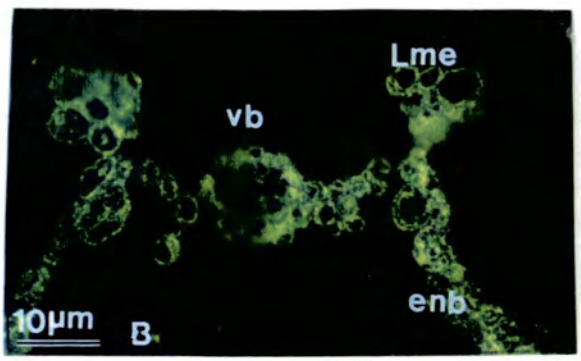

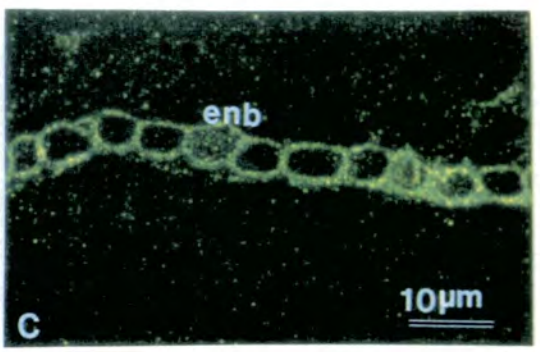

Figure 15.

RUBISCO

Rubisco was localised by fluorescein conjugated to a secondary antibody and was detected as green fluorescence on wax-embedded tissue which was absent from control sections. Rubisco was first present in the mesocarp layer of the mature gynoecium, and in the post fertilisation stages binding increased within this layer. Rubisco was detected in the mesocarp layer, (Fig. 16B), until late in stage nine when the mesocarp layer has begun to dry and collapse. Just prior to dehiscence at stage ten no Rubisco was detected in the mesocarp layer. The inner septum cells also showed a little binding during the early post fertilisation stages, however, due to the aerenchymous nature of the tissue binding was not very strong and proved difficult to photograph.

MOLECULAR HISTOCHEMISTRY OF THE POST-FERTILISED FRUIT

CELLULASE

Cellulase mRNA was detected on sections from wax-embedded tissues by hybridisation of a digoxygenin labelled cDNA probe which was localised by anti digoxygenin conjugated to alkaline phosphatase, the latter being detected histochemically as red deposits which were absent from control sections. Cellulase mRNA in the developing silique was detected in the central septal tissues following fertilisation, however, staining decreased as the tissue became more aerenchymous. Following development of the dehiscence zones at stage seven cellulase mRNA was detected in about five rows of mesocarp cells adjacent to the lignifying cells of the dehiscence zone (Fig. 17A) and remained through to dehiscence. There was no staining above background in other mesocarp cells of the valve wall. Cellulase has also been reported to be involved in the dehiscence of oilseed rape (Meakin & Roberts 1990b) and the pattern of activity in the dehiscence zone of the *Arabidopsis* silique is similar to that reported during bean leaf abscission (Tucker *et al.* 1991).

PECTINESTERASE

Pectinesterase mRNA was detected on sections from wax-embedded tissue by hybridisation of a digoxygenin labelled cDNA probe. Following hybridisation the specifically bound probe was localised by anti digoxygenin conjugated to a alkaline phosphatase, the latter being detected histochemically as red deposits that were absent from control sections. Pectinesterase mRNA remained in the central septum

Figure 16 Histochemistry of the post-fertilised silique, Protease and Rubisco.

Protease and Rubisco binding is shown as bright yellow/green and photographed under fluorescence illumination using a blue filter.

[A] Transverse section of a young silique showing protease binding to the exocarp cells, indicated by arrows; (c) carpel wall (vb) vascular bundle.

[B] Transverse section of a mature silique showing Rubisco binding to the cells of the mesocarp layer (me); (en) endocarp, (ex) exocarp, (vb) vascular bundle.

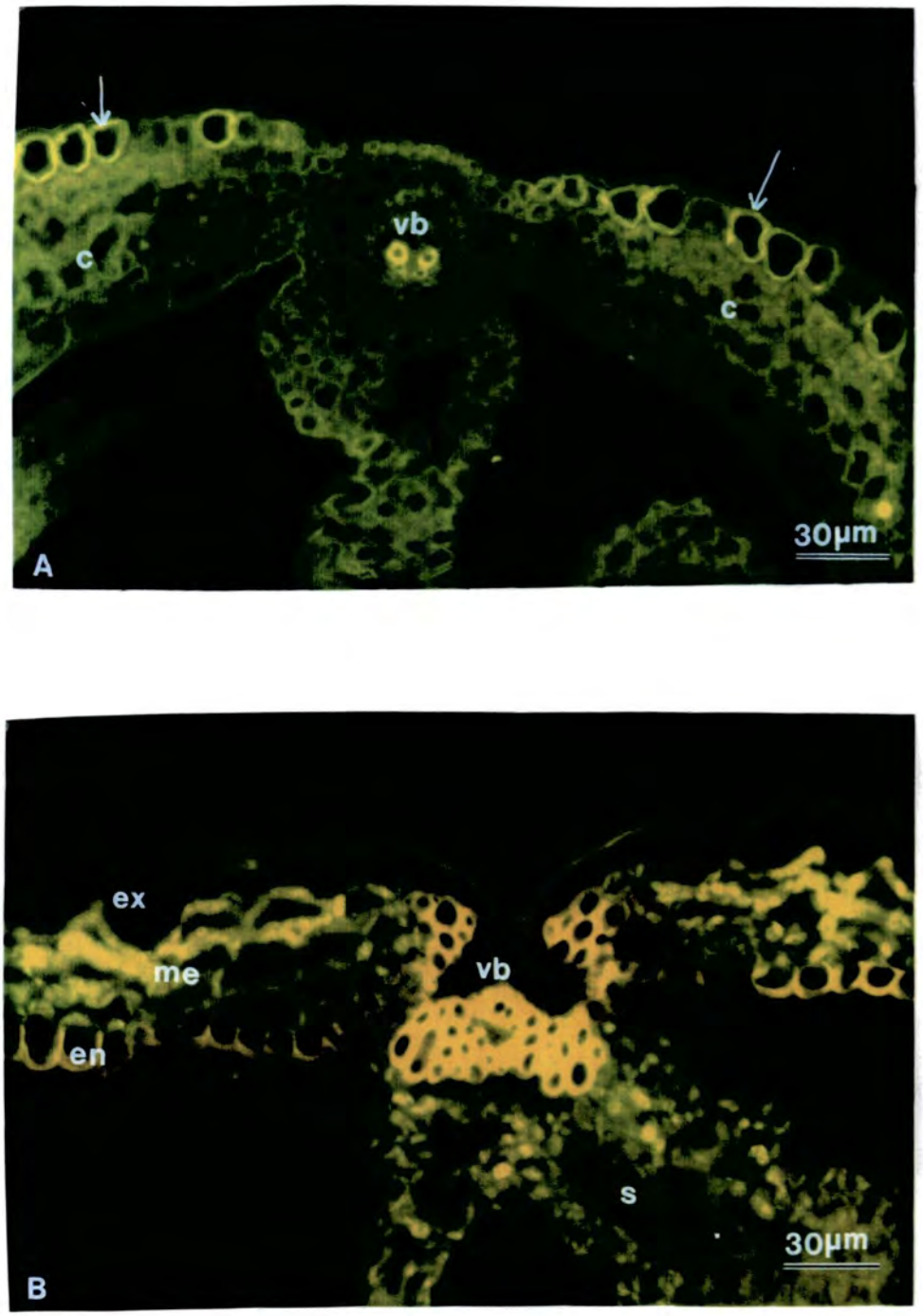

Figure 16.

following fertilisation of the fruit, however staining decreased as the tissue became more aerenchymous. Following thickening of the outer septal cells staining was also be detected in the basement wall. In the post fertilisation stages staining was present in the mesocarp cells of the valve walls (Fig. 17B), and remained through to dehiscence. En*b* showed pectinesterase mRNA in the later stages of silique development following thickening of this cell layer (Fig. 17B); it was not detected in the lignifying cells of the dehiscence zone.

POLYGALACTURONASE

Polygalacturonase was detected by hybridisation of a digoxygenin labelled cDNA probe. The probe was localised by anti digoxygenin conjugated to alkaline phosphatase, the latter being detected histochemically. As in the pre-fertilisation stages of development, polygalacturonase mRNA was not detected in any of the post-fertilisation stages of development. This result is in accordance with those of Meakin & Roberts (1990b) who found no significant polygalacturonase activity in oilseed rape pods.

Figure 17 Histochemistry of the mature silique, cellulase and pectinesterase.

Cellulase and pectinesterase mRNA distribution is shown as red deposits and photographed under Nomarski illumination.

[A] Transverse section of a mature silique showing cellulase mRNA in the cells of the mesocarp adjacent to the dehiscence zones; (en) endocarp, (ex) exocarp, (me) mesocarp, (vb) vascular bundle.

[B] Transverse section of a mature silique showing pectinesterase mRNA in the carpel wall; (en) endocarp, (ex) exocarp, (me) mesocarp.

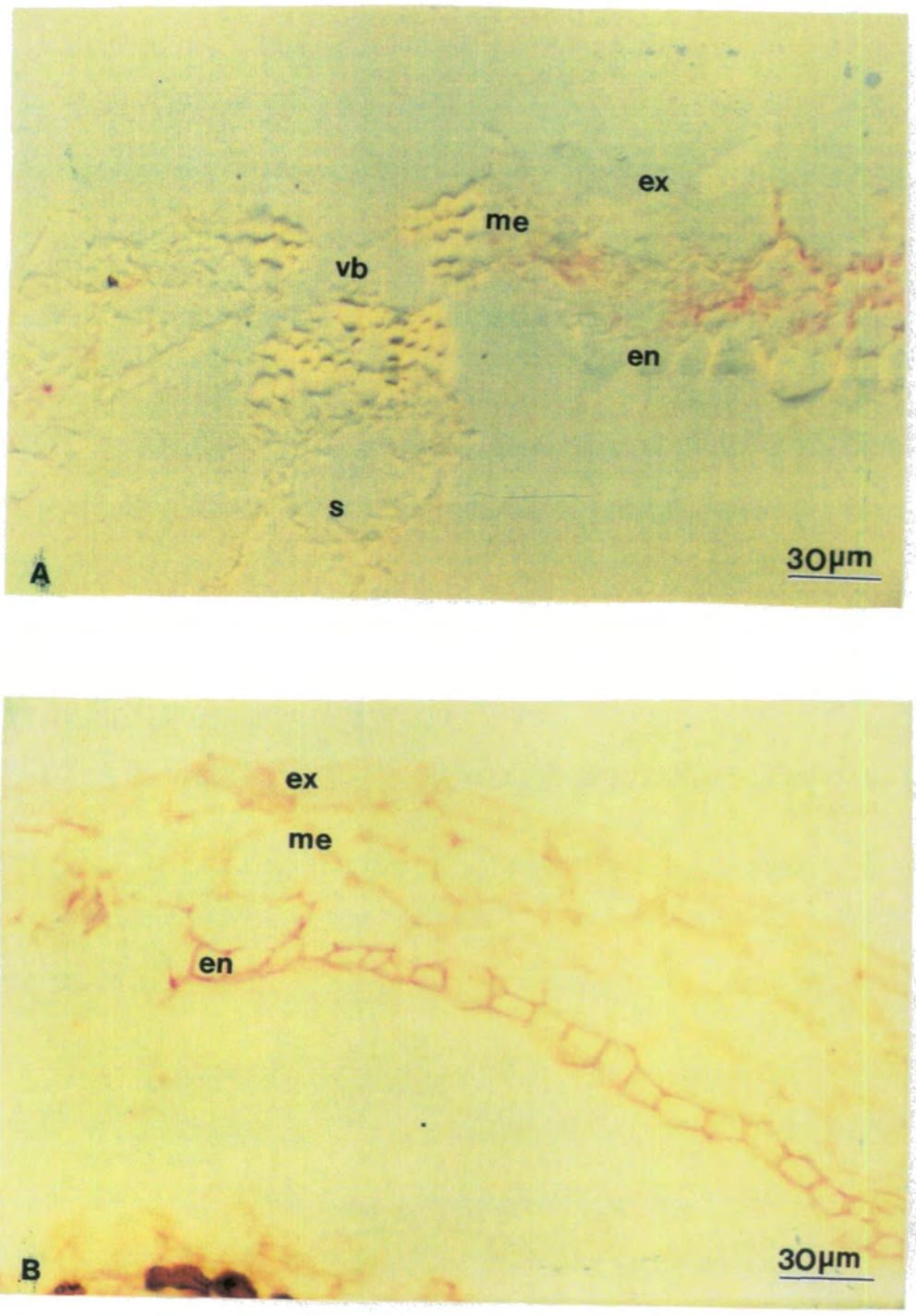

Figure 17.

Figure 18 Gross morphology of the *clavata* mutant plant.

[A] The gross morphology of the *clavata* mutant plant.

[B] *Clv1* silique showing split vascular bundle.

[C] The gross morphology of the *clv1* silique during the five post fertilisation stages of development.

Figure 18.

DEVELOPMENT OF THE *CLAVATA1* (*CLV1*) MUTANT SILIQUE

The *clv1* mutation has been mapped to chromosome 1 (Koorneef *et al.* 1983) and is allelic to flo5, renamed clv1-2, (Haughn & Sommerville 1988) and FASCIATAL3 (fas3), renamed clv1-3. The phenotype of the clv1 mutant plant (Fig. 18A) is characterised by stem fasciations, club shaped siliques (Fig. 18C) and additional floral organs. The additional floral organs may arise in any or all of the floral whorls, although all of the floral organs are wild type.

The club shaped siliques result from an increase in the number of carpels or locules within the silique, and although four loculed siliques are the most frequently observed (Fig. 20B, 21A & 23C) (Haughn & Sommerville 1988, Komaki *et al.* 1988, Okada *et al.* 1989, Ottoline leyser in press) three is not uncommon (Fig. 19B) and occasionally *clv1* siliques may possess two (fig. 22A) or five locules (Fig. 19C & 21B). The number and position of two, three and five loculed siliques on the mature plant appears to be totally random. *Clv* siliques are in general shorter and broader than those of the wild type and most siliques contain an extra organ (Fig. 23A) which we have termed a vestigial gynoecium, and which may occlude one of the locules and often possesses stigmatic papillae. As four-loculed siliques are the most common, and seem to result from a simple duplication of the carpels, we have considered the development of the four loculed silique as the model system. The development of the *clv* silique is described below based on the ten stages of wild type development previously described.

MODEL DEVELOPMENT OF THE CLV1 SILIQUE

The *clv1* gynoecium arises temporally and spatially as in the wild type. As Fig. 19A illustrates, the stage one gynoecium is more rounded than that of the wild type and generally possesses four opposing rudimentary primary vascular bundles. The gynoecial wall tissues develop as in the wild type at stage two, however, an increased number of placentae develop, one adjacent to each primary vascular bundle (Fig. 19A). Anticlinal divisions in the gynoecial wall layers between the placentae define the number of carpel walls which differentiate as in the wild type at stage three to form the exocarp, mesocarp and en*a* layers (Fig. 20A). Each placenta develops two opposing ovule primordia (Fig. 20A) and a rudimentary secondary vascular bundle develops in each of the carpel walls.

Figure 19 Early stages of *clv1* gynoecial development.

The sections are stained with toluidine blue and photographed under bright field illumination.

[A] Transverse section of a stage 2 *clv1* gynoecium showing development of 4 placentae (p).

[B] Transverse section of a stage 3 *clv1* gynoecium showing development of 3 placentae (p).

[C] Transverse section of a stage 2 *clv1* gynoecium showing development of 5 placentae (p).

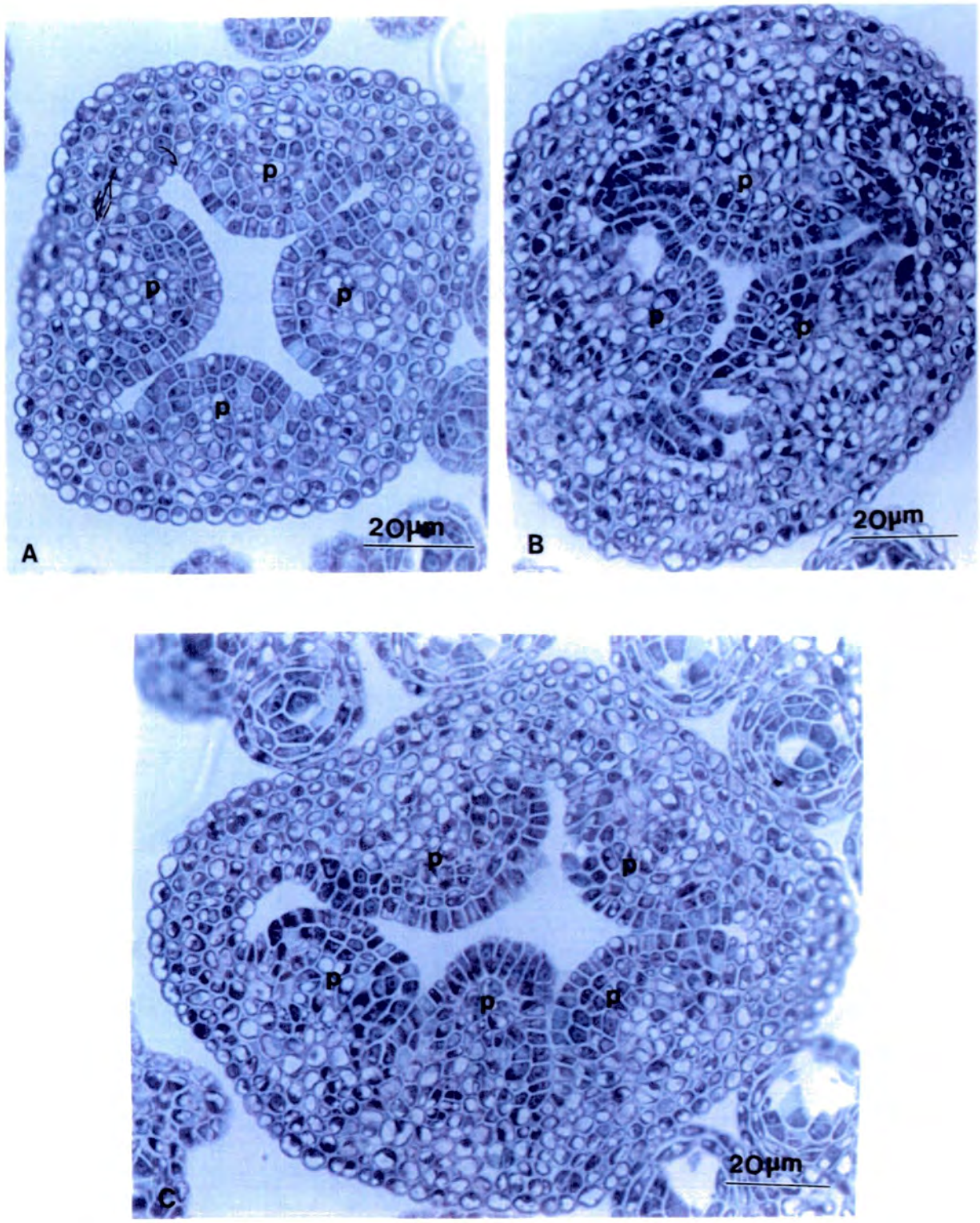

Figure 19.

Figure 20 Late stages of *clv1* gynoecial development.

Fig. 20A is stained with toluidine blue and photographed under bright field illumination.

[A] Transverse section of a *clv1* gynoecium showing normal development of the carpel wall (c) tissues and septa (s).

[B] SEM view of the *clv1* gynoecium. The young gynoecium is not club shaped like the mature silique.

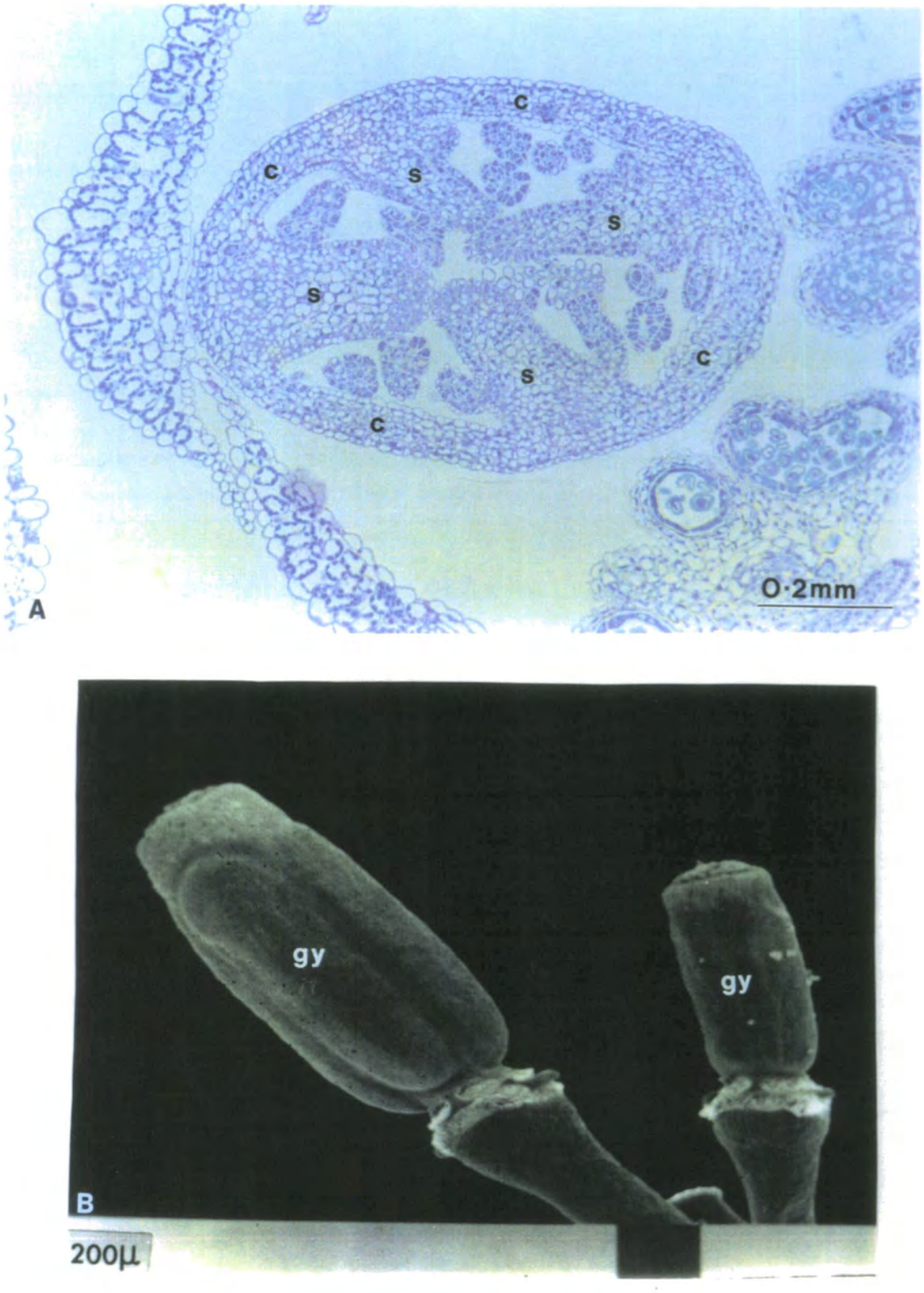

Figure 20.

The placentae elongate at stage four and fuse in the centre of the gynoecium usually producing an ovary with four locules. Sections from whole inflorescences reveal that the septa in wild type gynoecia always run parallel to the axis of the inflorescence, however, there does not appear to be any such positional uniformity to the septa in the *clv* mutant. The carpel wall differentiates at stage four to form the second endocarp layer en*b*. The cell layers within the carpel wall appear identical to those in the wild type. The major tissue types of the gynoecium continue to differentiate as in the wild type at stage five and the gynoecium increases in length to reach the height of the mature anthers and the plant typically self fertilises.

After fertilisation the *clv1* silique increases in length and as in the wild type the dehiscence zones develop. The pattern of development of the dehiscence zones is identical to that of the wild type (fig. 21C). There is constriction of each marginal carpel wall at stage six followed by development of the separation layer cells at stage seven to form four valves. The few rows of mesocarp cells adjacent to the separation layer lignify at stage eight and at stage nine en*b* lignifies and en*a* disintegrates. The mesocarp layer begins to dry and collapse and the silique dehisces at stage ten (Fig. 18C).

The *clv1* gynoecium arises from a larger gynoecial primordia. Within the enlarged primordia there is a duplication of the primary vascular bundles which may initiate a duplication of the placental primordia. The carpel walls and septa of the *clv1* gynoecium are cytologically identical to those in the wild type gynoecium. The dehiscence zones are also positionally and cytologically identical to those in the wild type silique. All histochemical immunocytochemical and molecular tests which were performed on the wild type gynoecium were also carried out on the *clv1* gynoecium. The *clv1* gynoecium shows the same binding patterns as the wild type for all probes utilised (results not shown).

GYNOECIAL FASCIATIONS

Although the model system possesses four primary vascular bundles, the number of primary bundles in the gynoecial primordia of *clv1* plants does vary. These fasciations appear to be totally random and often cause the young gynoecium to have a more exaggerated shape in the early stages of development, as illustrated in Fig. 19C where there are five primary bundles and five placentae are initiated. However, it does not always follow that the number of primary bundles present at

Figure 21 Late stages of *clv1* silique development.

The sections are stained with toluidine blue and photographed under bright field illumination.

[A] Transverse section of a mature *clv1* silique with 4 carpels (c).

[B] Transverse section of a mature *clv1* silique with 5 carpels (c).

[C] Transverse section of a mature *clv1* silique showing the structure of the dehiscence zones.

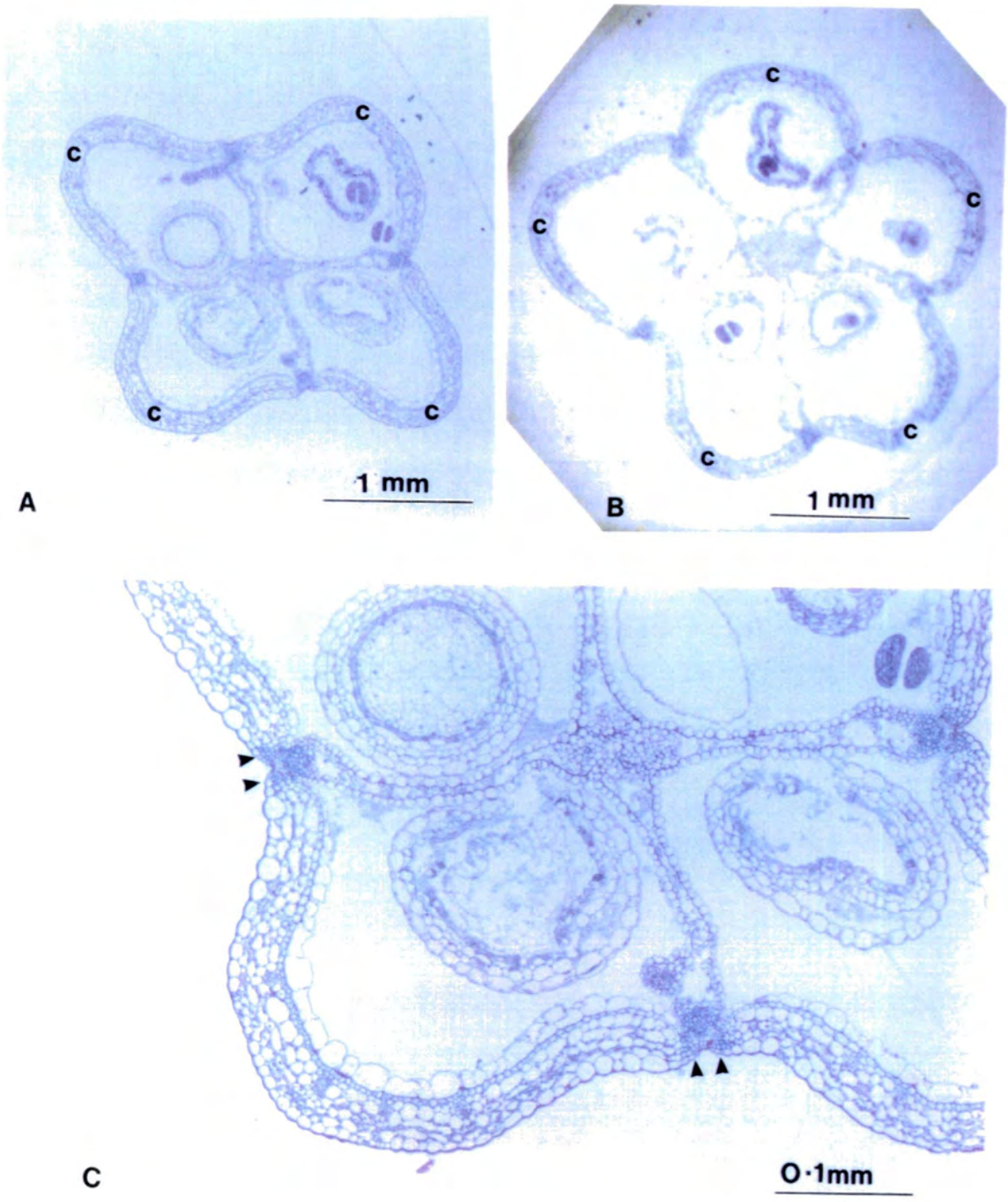

Figure 21.

Figure 22 Anomalies in *clv1* gynoecial development.

Sections are stained with toluidine blues and photographed under bright field illumination.

[A] Transverse section of a stage 3 *clv1* gynoecium showing how 2 vascular bundles indicated by arrows may be split by differentiation of adjacent mesocarp cells; (p) placenta.

[B] Transverse section showing a young vestigial gynoecium (vg) in the centre of a stage 3 *clv1* gynoecium; (p) placenta.

[C] Transverse section showing the vestigial gynoecium (vg) in the centre of a mature *clv1* gynoecium, the arrows indicate where the septa (s) have fused.

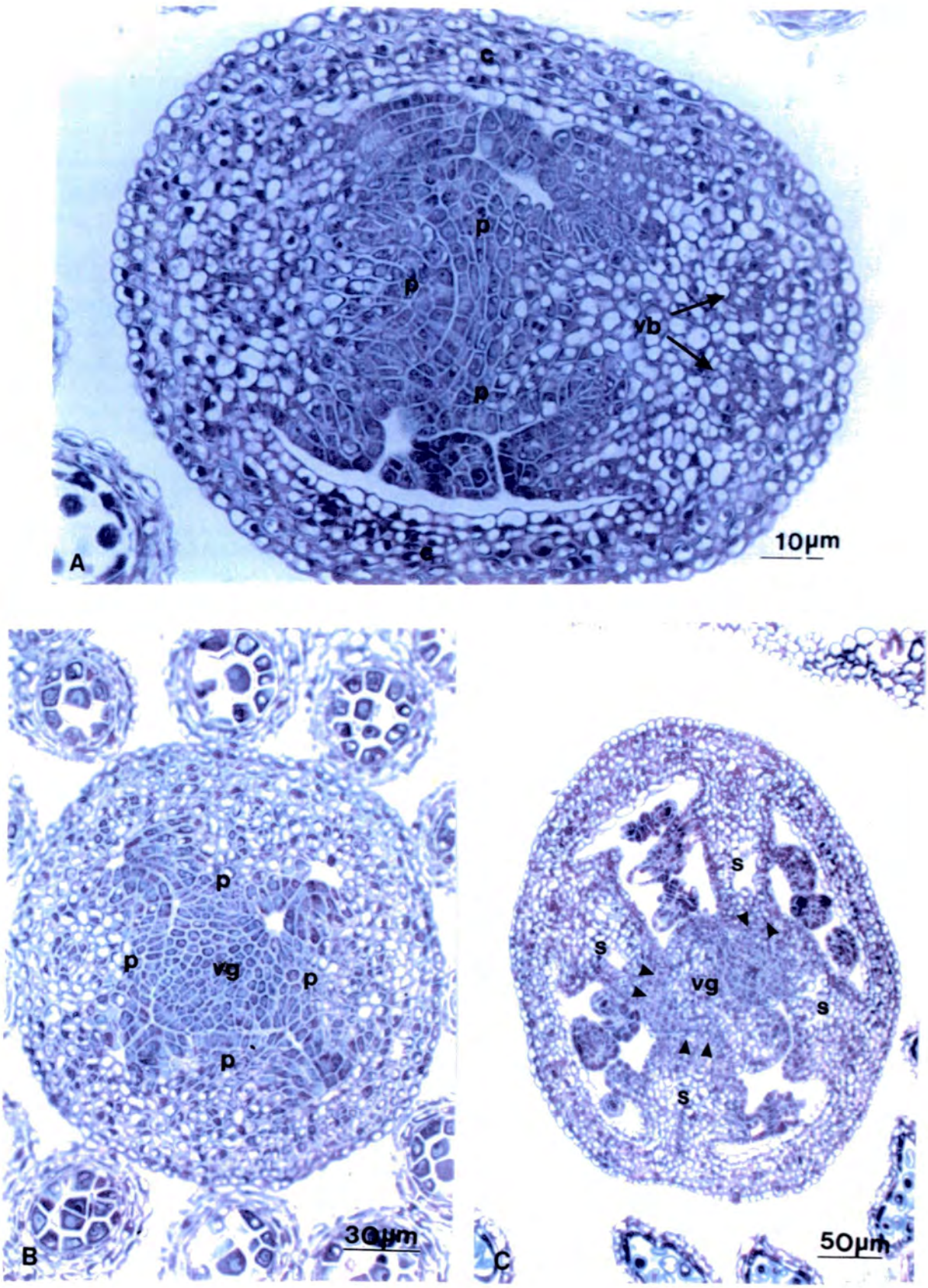

Figure 22.

Stage one di ctates the number of placentae that are initiated at stage two. Sometimes two or three placentae may develop, even though there are four or more primary bundles (Fig. 23B). When three placentae develop, usually one slightly broader placenta will develop adjacent to two primary bundles. Anticlinal divisions in the gynoecial wall layers between the bundles, in some instances, splits these two bundles and the placenta resulting in development of a fourth placenta (Fig. 18B). As Fig 22A illustrates this same phenomenon may occur to increase the number of placentae in gynoecia which first develop two placentae. Post fertilisation the dehiscence zones develop in the normal position at the margin of each carpel wall adjacent to the primary vascular bundles irrespective of the increase in the number of carpels.

Although rare short thin septa, which we have termed 'inferior septa', may also develop adjacent to what appear to be secondary vascular bundles (Fig. 25A & 25B). These apparent carpel wall bundles are unusually large and show more lignification than other carpel wall bundles. The precise time of development of the 'inferior placenta' is as yet unknown but no dehiscence zone has yet formed around the inferior septal bundle in what is otherwise a fully developed *clv1* silique with dehiscence zones around the primary bundles (Fig. 25C). This seems to indicate that the 'inferior placenta' develops much later than usual, perhaps when the secondary bundles increase in size.

THE VESTIGIAL GYNOECIUM

The majority of *clv1* siliques contain a vestigial gynoecium which is visible from the first stage of development as a clump of meristematic cells in the centre of the gynoecium and which occludes the fissure (Fig. 22B). As illustrated in Fig. 22C, development of the placental and ovule primordia, at stages two and three, is not affected by the presence of this extra organ, and the carpel wall differentiates normally. However, placental elongation and fusion at stage four is disrupted and the placentae may either fuse to the vestigial gynoecium (Fig. 22C & 24D) or fuse to each other laterally around it (Fig. 24C). Frequently the vestigial gynoecium obstructs the elongation of one or more of the septa. As the *clv1* gynoecium lengthens and elongates at stage five, the vestigial gynoecium also lengthens, widens and differentiates. The outer cell layer comprises a single layer of parenchymous cells which resemble those of the outer septum in size and shape and have thickened walls. The core of the structure comprises thin walled parenchymous

Figure 23 Anomalies in *clv1* silique development.

The section in Fig. 23B is stained with acridine orange and photographed under fluorescence illumination using a blue filter.

[A] Gross morphology of the vestigial gynoecium (vg).

[B] Transverse section showing a *clv1* silique with 2 locules (l) and four primary vascular bundles.

[C] SEM view of a *clv1* silique with 4 carpels.

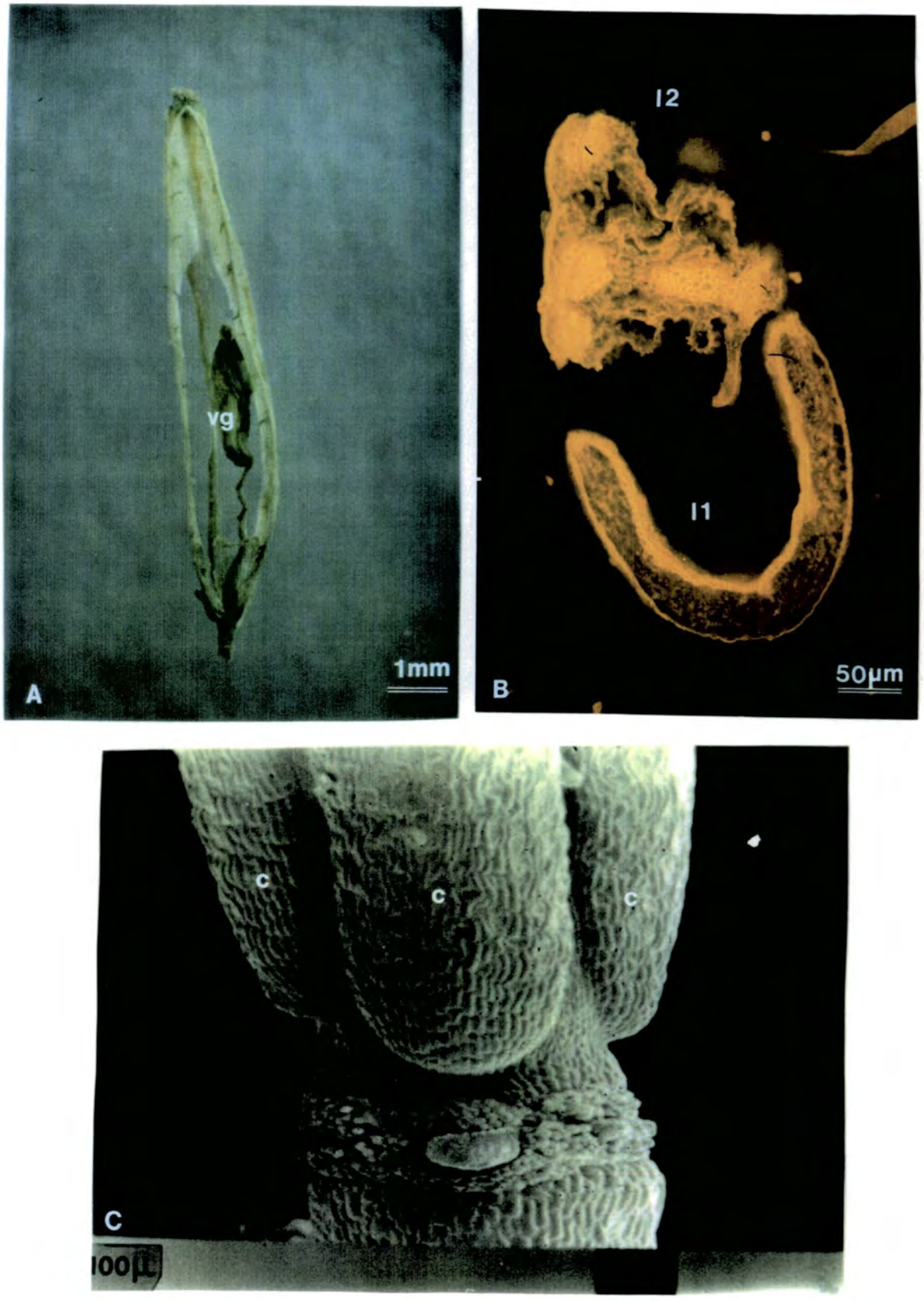

Figure 23.

Figure 24 The vestigial gynoecium.

Sections are stained with toluidine blue and photographed under bright field illumination.

[A] Transverse section of the base of a mature *clv1* silique showing the disruption of septal fusion and elongation; (c) carpel wall, (s) septum, (se) seed, (vg) vestigial gynoecium.

[B] Transverse section of the base of a mature *clv1* silique showing the morphology of the vestigial gynoecium (vg).

[C] Transverse section of the top of a mature *clv1* silique showing disruption of the septa, the arrows indicate the position of septal fusion.

[D] Transverse section of a mature *clv1* silique showing a vestigial gynoecium (vg) and disruption of septal fusion indicated by arrows.

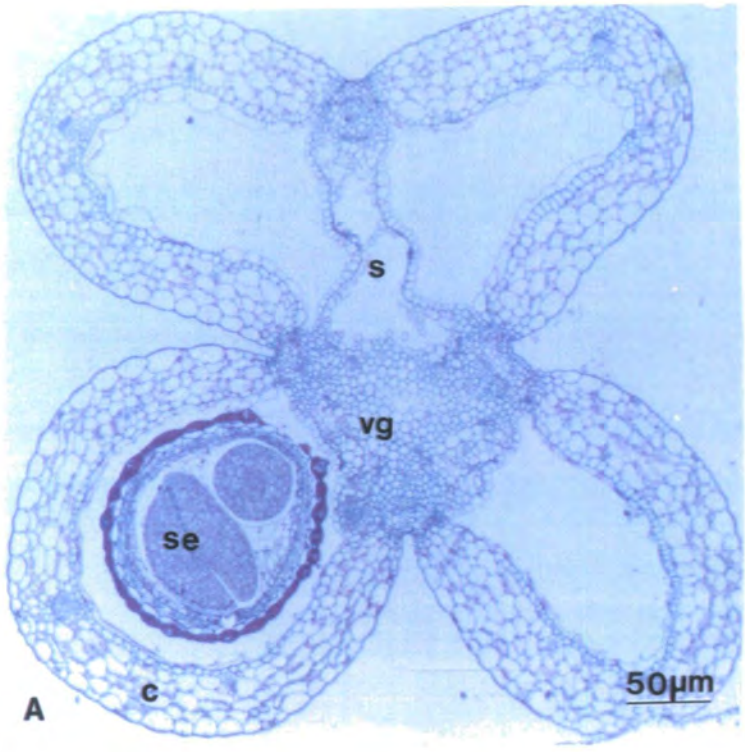

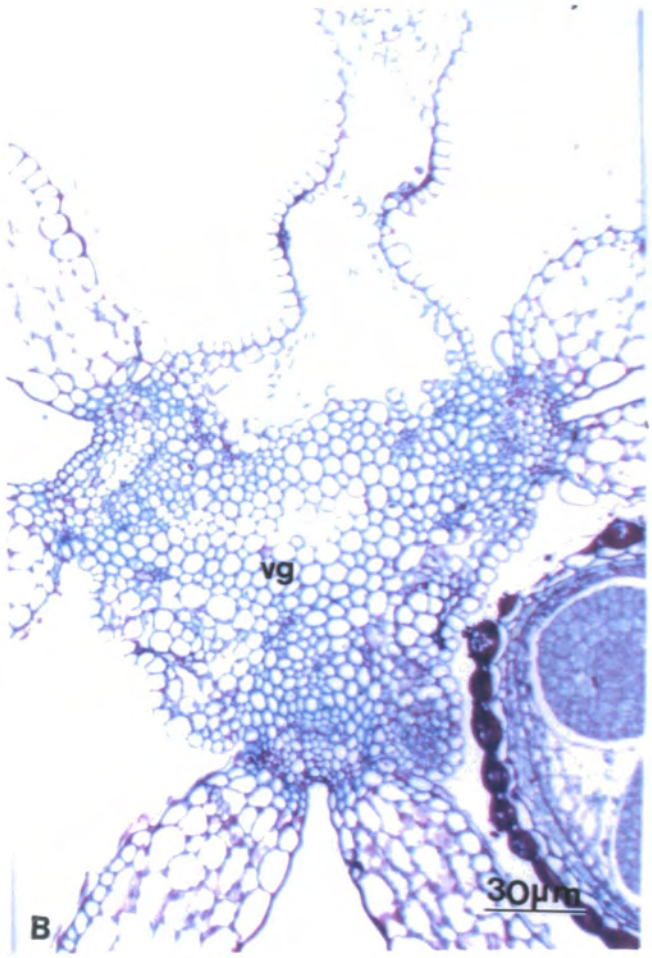

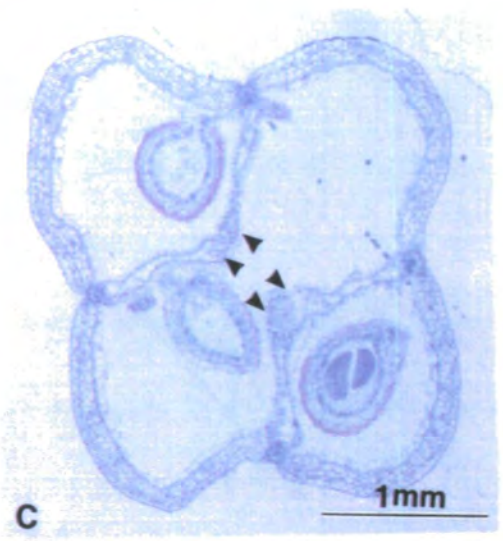

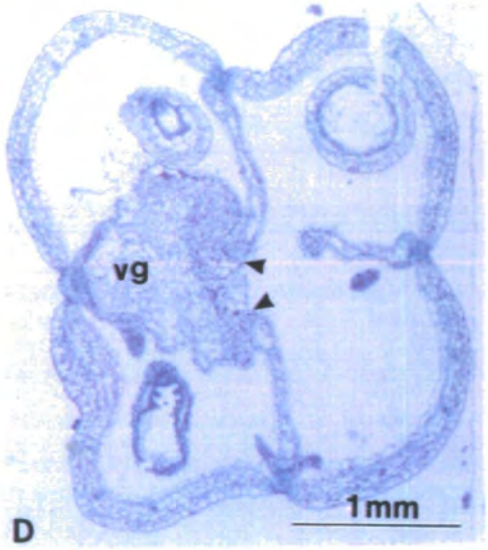

Figure 24.

cells and there is a large, central vascular strand. The presence of the vestigial gynoecium is independent of the number of carpels within the *clv1* gynoecium. After fertilisation, as the silique elongates, the vestigial gynoecium also elongates and frequently develops stigmatic papillae. Lengthening of the septa is disrupted especially near the base of the silique where there is frequently little septal elongation. Carpel wall differentiation is not affected and consequently, as Fig. 24A & 24B shows, the carpel walls still expand. Underdeveloped seeds are often found near the base of the *clv1* silique. Although the precise reason for this is unclear it is most likely caused by obstruction of the pollen tubes due to septal abnormalities.

In the fully mature *clv1* silique the vestigial gynoecium usually reaches about two thirds the length of the silique. Although sometimes located centrally, as illustrated in Fig. 25A, more usually one of the locules of the silique is partially or totally obstructed. Development of the tissues of the dehiscence zones is not usually affected by the presence of the vestigial gynoecium, however, it was noted that often *clv1* siliques dehisced more unevenly than those of the wild type. The valves of the *clv1* silique remain attached at the base for much longer, after they have separated at the tip. Although the reason for this is unclear it may be a consequence of underdeveloped seeds in the base of the silique. Developing seeds produce ethylene a hormone which has been implicated in the control of dehiscence (Sexton & Roberts 1982, Meakin & Roberts 1990b).

The two major contributing factors which are instrumental in producing the characteristic club shape of the *clv1* silique are; an increase in the number of carpels, and the presence of a vestigial gynoecium. Both of these factors are a result of the fasciations within the *clv1* gynoecial primordia.

Figure 25 The 'inferior septum'.

Sections are stained with toluidine blue and photographed under bright field illumination.

[A] Transverse section of a mature *clv1* silique with 2 'inferior' septa developed from apparent carpel wall vascular bundles (cwb).

[B] Transverse section of an 'inferior' septum (is) from Fig. 25A showing that no dehiscence zone has formed around the vascular bundle (cwb).

[C] Transverse section of one of the primary vascular bundles (vb) from Fig. 25A showing normal development of the dehiscence zones indicated by arrows.

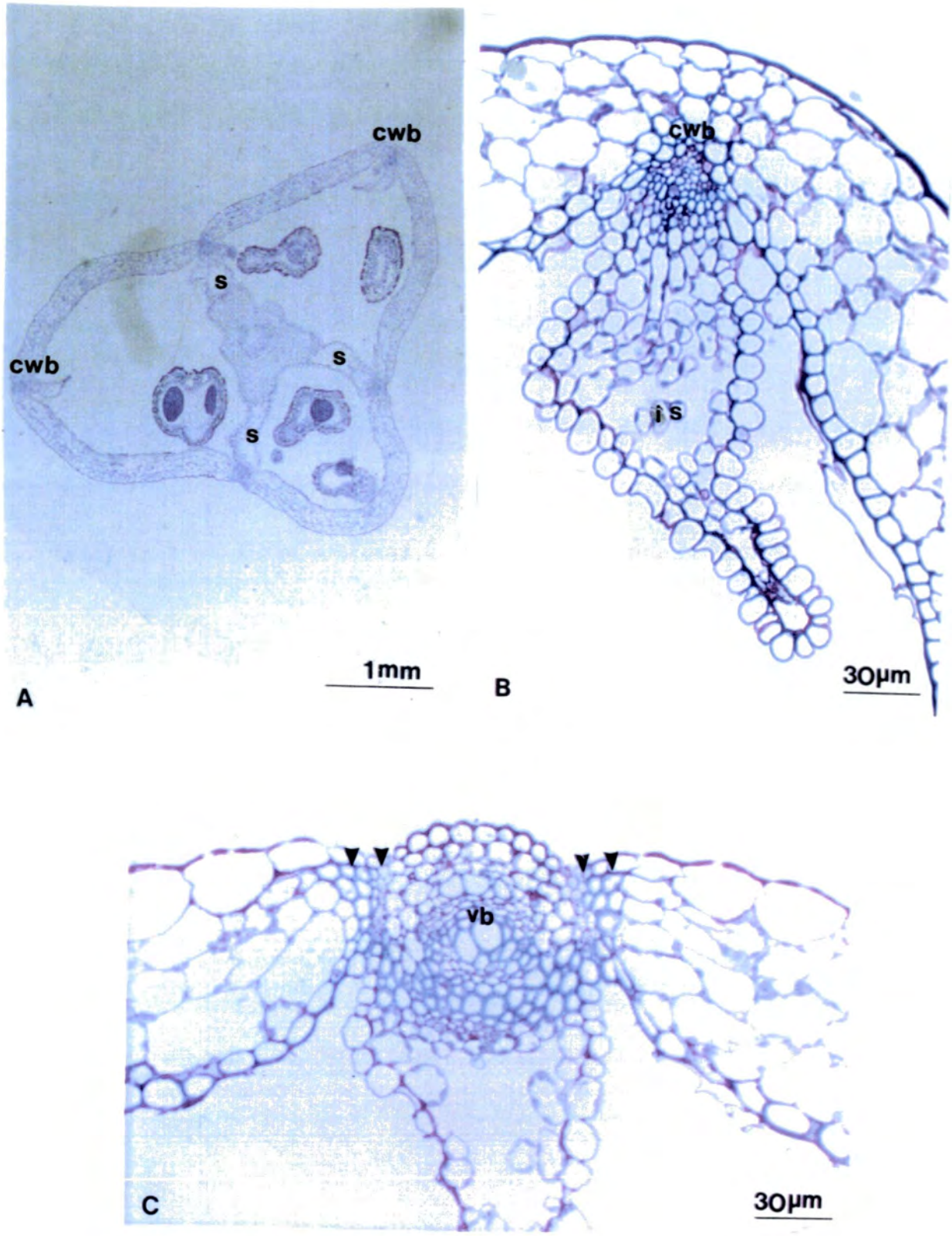

Figure 25.

EMS GENERATED MUTANTS

EMS treated Landsberg erecta seeds were obtained from Lehle Seeds, Tuscon U.S.A. and planted on a regular basis. Plants were screened for interesting mutants which were isolated and numbered sequentially. Seed stocks were built up from selected mutants for future study. The characterisation of selected mutants is not a main concern of this thesis, however a brief description of each is given below.

MUTANT 003

The phenotype of the 003 plant (Fig. 26B) is characterised by stem fasciations, additional floral organs and some siliques which are club shaped and consequently it phenotypically resembles the clv mutant. The mature plant reaches a height of 20-30 cm and exhibits the same temporal growth pattern as the wild type plant. The rosette of leaves at the base of the stem appear be wild type. The 003 plant may develop normal lateral branches and inflorescences, however, compacted inflorescences may be produced in which the flowers never open and stem elongation is halted.

The additional floral organs in the 003 plant are wild type and have thus far only been observed in the petal and gynoecial whorls. All of the petals are often broader and shorter than those of the wild type and, as Fig. 27A illustrates, the orientation of extra petals is often disturbed and one or more petals may appear to develop in a laterally opposed orientation. Although rare, two gynoecia may develop from a single flower. One of the gynoecia is usually larger, but both may develop fully into siliques and produce viable seeds. These siliques have independent pedicles but both pedicles are attached at the same point to the stem.

The clubish shape of some of the 003 siliques is due to an increase in the number carpels or locules within these siliques. In the 003 plant siliques with two or three carpels (Fig 27B) have only so far been identified. The number and position of three loculed siliques varies per plant. Preliminary studies seem to indicate that the increase in locule number is due to an increase in the number of vascular bundles within the gynoecial primordium as reported for the *clv1* plant. Although individual plants show variations, the racaemic pattern of the siliques along the length of the stem is usually lost in the 003 plant and up to four siliques may occupy the same vertical position along the stem.

Figure 26 EMS generated mutants.

[A] Gross morphology of mutant 006 showing extended internodes and desiccated siliques, indicated by arrows, which are still attached to the plant.

[B] Gross morphology of mutant 003. The arrow indicates the loss of the racaemic pattern of the siliques along the length of the stem.

[C] Gross morphology of mutant 007.

[D] Gross morphology of the inflorescence of the 007 mutant showing the spoked formation of the siliques.

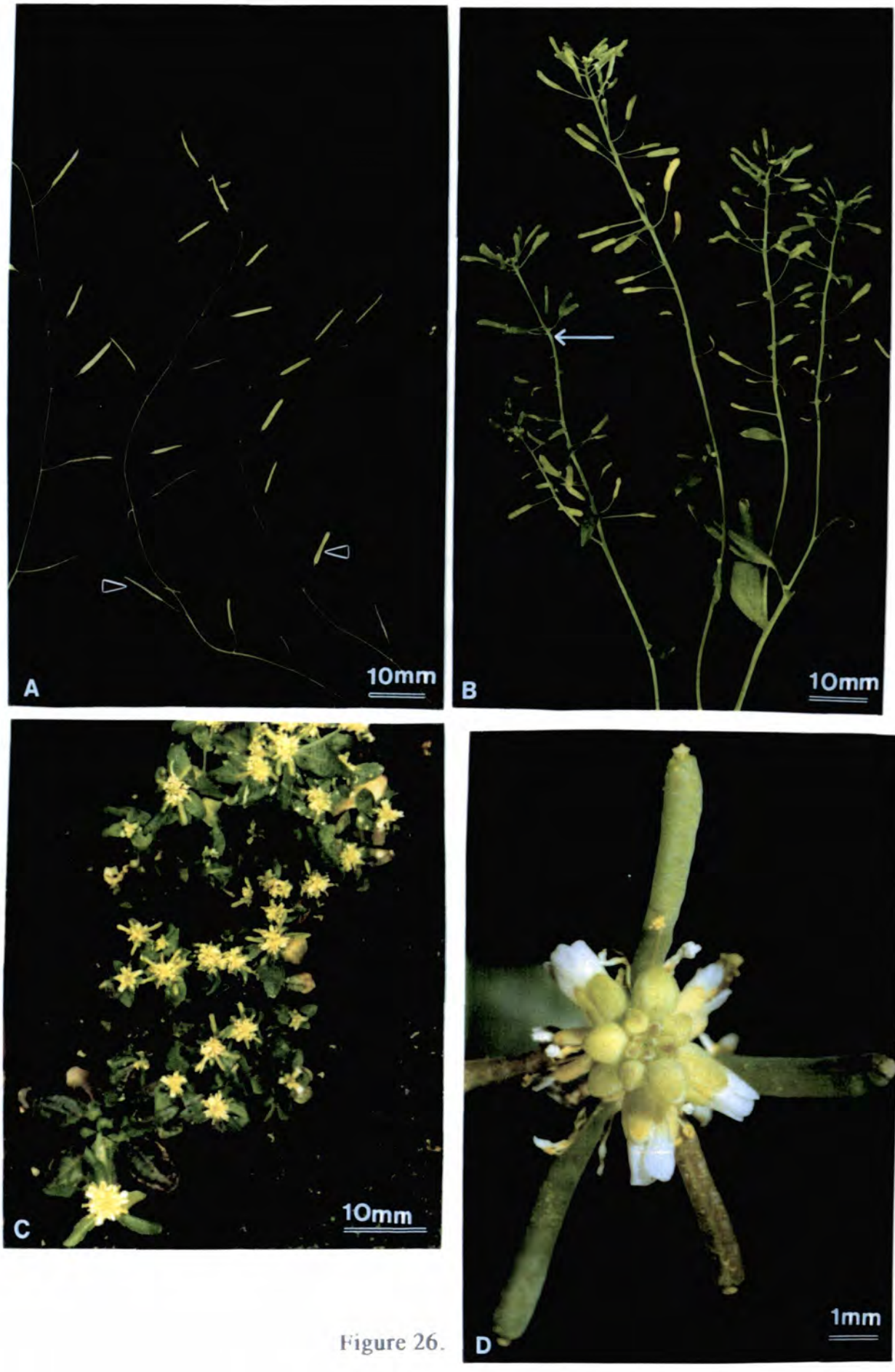

Figure 26.

Degenerate flowers can also be found within the inflorescence of the main stem as well as the lateral branches. Preliminary microscopic examination showed degeneration of all the floral organs in degenerate flowers prior to opening of the sepals. The main vascular bundles of the floral organs in these degenerate flowers are poorly developed, being small and showing no or very little lignification of the xylem elements (Fig. 27C & 27D).

MUTANT 006

The phenotype of the 006 mutant (Fig. 26A) is characterised by extended internodes, hairless leaves and long pointed siliques, which frequently remain attached to the plant following desiccation, and only shatter if a mechanical stimulus is applied. The mature 006 plant reaches a height of 50-60 cm and has a very thin stem but exhibits the same temporal growth pattern as the wild type plant. The inflorescence is usually small containing fewer flowers than the wild type, however, all of the floral organs examined were phenotypically wild type.

Preliminary microscopic examination of the mature 006 silique revealed a very poorly defined separation layer in the dehiscence zone of many siliques (Fig. 28A) although, as Fig. 28C shows, there is normal lignification of the adjacent mesocarp and replar cells as seen in the wild type (Fig. 28B). The valve wall and septum cells appear to differentiate normally. Following a mechanical stimulus to detach the valves they separate from the replum at the appropriate position although there is either no, or only a very poorly defined separation layer (Fig. 28C).

The increased stem and internode length of the 006 plant would seem to indicate that there is an imbalance of some growth hormone. Various plant growth hormones such as gibberellins and auxins have also been implicated in the control of abscission (Sexton & Roberts 1982) and an imbalance may also affect the temporal and/or spacial development of cells within the dehiscence zone of the 006 silique. Further characterisation of the 006 mutant is currently under investigation in this laboratory.

MUTANT 007

The 007 phenotype (Fig. 26C & 26D) is characterised by several very short stems which bear a compacted inflorescence at the tip and produce siliques in spoked formation (Fig. 26D). Beneath the inflorescence there are usually three to five dark

Figure 27 Mutant 003.

Sections are stained with toluidine blue and photographed under bright field illumination.

[A] Transverse section of a 003 flower showing a gynoecium (gy) with 2 carpels and an extra petal, indicated by an arrow, which appears to have developed in a laterally opposed orientation.

[B] Transverse section of a mature 003 silique with 3 carpels and 3 locules (l).

[C] Transverse section of a 003 gynoecium (gy) showing degeneration of the tissues. The arrows indicate the primary vascular bundles which are not very well developed.

[D] Transverse section of a 003 anther showing poor development of the vascular bundle indicated by arrows.

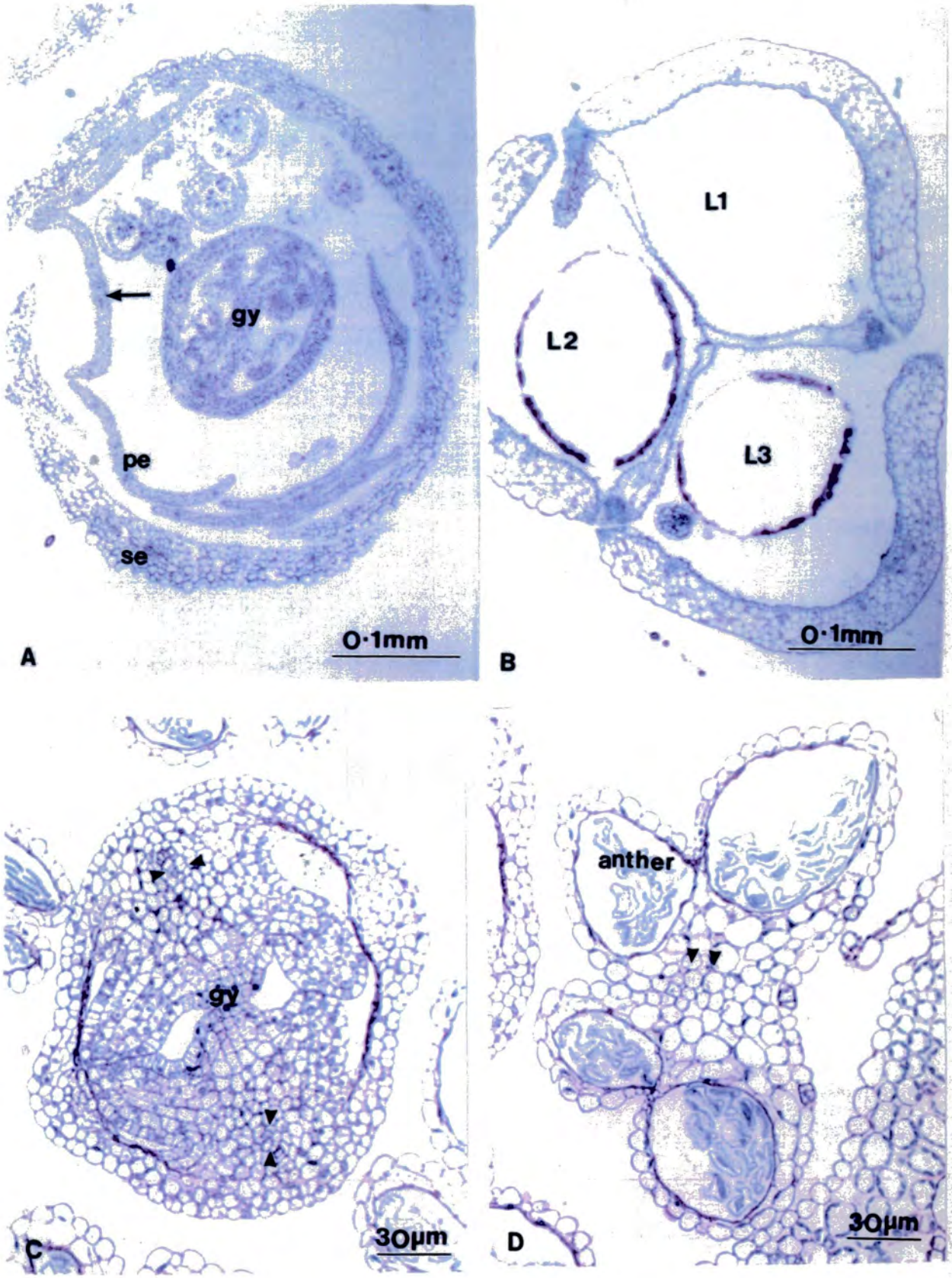

Figure 27.

slightly curled leaves. The 007 plant is slow growing and the mature plant reaches a height of only 3-7 cm. The rosette at the base of the stem comprises dark green or purple pigmented leaves which bear trichromes. The first inflorescence can be seen in the centre of the rosette before the stem is visible and there is little stem elongation following development of the inflorescence. The presence of the leaves under the inflorescence seems to indicate that stem elongation is occurring well below the inflorescence.

Usually more than one 'main' stem develops from the base rosette but all produce the same domed compacted inflorescence. Frequently there are also many small inflorescences around the base of the 'main' stems, these appear to be produced from stems which do not elongate at all. These develop later than the main inflorescences and the flowers may still be unopened when the main inflorescence has degraded. Lateral branches develop directly beneath the main inflorescence.

Microscopic examination reveals that all the flowers within the 007 inflorescence are phenotypically wild type although usually only the outermost flowers produce siliques which develop and dehisce normally. The peripheral zone of the apical meristem gives rise to the floral primordia whilst the central zone gives rise to the stem and Shannon & Meeks-Wagner (1991), have reported a mutant termed tfl in which the central zone of the apical meristem is converted into a floral meristem. The short stem, compacted inflorescence and spoked formation of the siliques seem to indicate that it is the central zone of the apical meristem which is also affected in the 007 mutant. Further characterisation of the 007 mutant is currently under investigation in this laboratory.

Figure 28 Mutant 006.

Fig. 28A and 28B are stained with toluidine blue and photographed under bright field illumination, Fig. 18C is stained with acridine orange and photographed under fluorescence illumination using a blue filter.

[A] Transverse section of the dehiscence zone of a silique of mutant 006. The mesocarp has lignified as normal (lme) but the arrows indicate poor development of the separation layer cells.

[B] Transverse section of the dehiscence zones of a wild type silique of comparable age to Fig 28A, the arrows indicate the degrading separation layer cells; (lme) lignified mesocarp cells.

[C] Transverse section of a dehiscing 006 mutant silique. The arrows indicate the point of separation but there are no obvious separation layer cells.

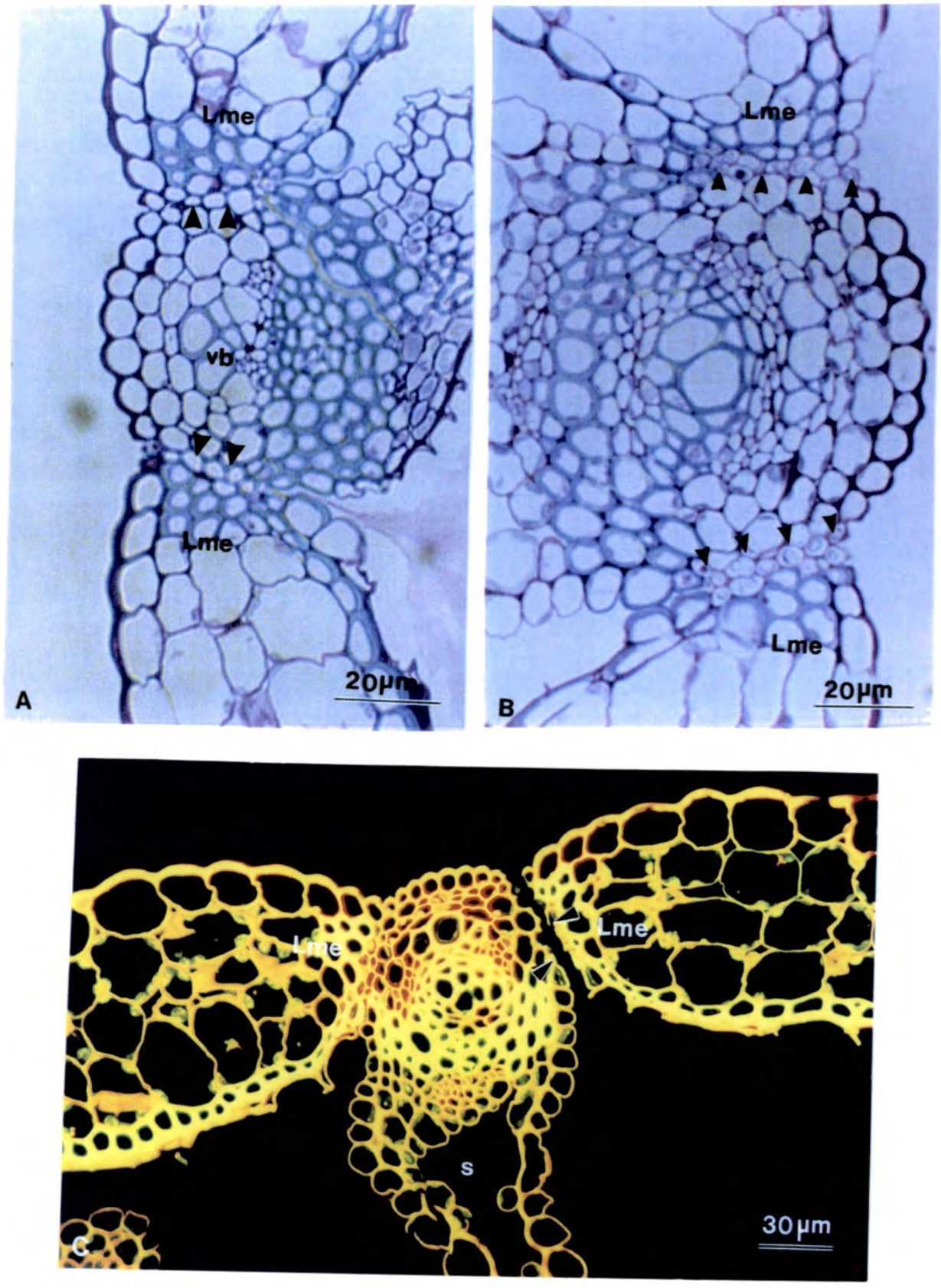

Figure 28.

DISCUSSION

Light microscopical studies have enabled us to determine a series of changes in form and pattern in the developing *Arabidopsis* silique. The major changes have been assigned to ten stages of development, five pre- and five post fertilisation. Stages one to five describe the development of the major tissue types of the gynoecium from inception until fertilisation. Stages six to ten are mainly concerned with the development of the dehiscence zones. In keeping with others we have supposed the *Arabidopsis* gynoecium to consist of two joined carpels. However, it was not obvious from the earliest stages what constituted a carpel as the gynoecium arises as a cylinder comprising amorphous meristematic tissue.

Following inception of the gynoecium, the first tissue type to differentiate within the meristematic cells are the primary vascular bundles. There are always two primary bundles in the wild type, however in the clv1 gynoecium the number varies. The clv1 phenotype includes enlargement of the central zone of the apical meristem, and this size increase has been associated with the fasciations in the clv1 stem (Ottoline Leyser in press). Similarly, the centre of the floral meristem is enlarged in the clv1 mutant and consequently this probably leads to the increased number of vascular bundles within the gynoecial primordia. The phenotype of the clv1 plant also includes extra floral organs. The vestigial gynoecium is such an extra organ, which does not develop fully, and is a consequence of the enlarged, fasciated floral meristem.

As the vascular tissue begins to enlarge and thicken, the placentae develop. In both the wild type and clv1 gynoecium the placentae always develop adjacent to the primary bundles and in the wild type the placentae are always parallel to the axis of the inflorescence. In the clv1 gynoecium, more than one bundle may be associated with one placenta in which case the placenta is usually much broader and there is no pattern to the position of the placentae. This loss of septal phyllotaxy in the clv1 gynoecium may also be attributed to the fasciations within the gynoecial primordia. It seems likely that the placentae are positionally determined and that the presence of the primary vascular bundles may in some way be involved. The inferior septa produced in the clv1 gynoecium may be formed if an apparent carpel wall bundle dramatically increases in size. The vascular bundles may perhaps influence placental development through hormone gradients, although much further work is required to prove this assumption.

The three carpel wall layers are established as early as stage three when the ovule primordia develop. The putative exocarp layer did show a highly ordered

appearance in earlier stages and is probably the first layer to be established. The exocarp differentiates to form a protective layer of thick-walled cells, which in the mature silique secrete a cuticular outer layer and are interspersed with guard cells and stomata. Protease activity was high in exocarp cells of the mature silique when the cuticular coat was being secreted and was first detected at about the same time as Rubisco appeared in the mesocarp layer. Although the precise role of the protease is not yet understood, the enzyme is also present in the exocarp of peas where it may serve a similar function (Cercos & Carbonell 1993 in press). The mesocarp comprises chlorenchymatous cells and supplies the photoassimilates for the developing silique. Rubisco was not detected in the mesocarp until about the time of fertilisation. This would suggest that up until then all photoassimilates were supplied via the vascular bundles. Mesocarp cells enlarge in all planes as the silique grows and during the major growing phase, post fertilisation, pectinesterase mRNA was detected in the mesocarp layer. Pectinesterase remained in the mesocarp layer until dehiscence of the silique when the mesocarp dries and collapses. This is seen as a visible yellowing of the silique.

The endocarp lines the locules of the gynoecium and at stage five differentiates to form two very distinct layers. The outermost layer lining the locule, en*a*, differentiates first and comprises a single layer of thin walled, isodiametric cells which divide and generally increase in size during the growing phases and appear almost swollen in the mature silique. The inner endocarp directly adjacent to the mesocarp, en*b*, comprises small, tightly packed, columnar cells. During gynoecial development these cells increase in size and elongate along the long axis. after fertilisation en*b* cells thicken and, prior to dehiscence, lignify; phenol oxidase activity was high at the time of lignification. This lignification may be instrumental in the degradation of en*a* as it may decrease the amount of assimilates reaching these cells. Esterase activity was weak but uniform throughout the endocarp during early development and increased slightly after fertilisation but just prior to the major growing phase. Post-fertilisation such activity was localised to the outermost endocarp layer en*a*. Esterase has been associated with cells destined to undergo elongation in pea fruits (Vercher & Harris in press). In the *Arabidopsis* fruit it is the cells within en*b* which elongate, however, it is possible that en*a* disintegrates before a major elongation phase has taken place. Following en*a* disintegration, en*b* showed significant accumulation of the JM13 epitope. Although this may be indicative of subtle changes within the endocarp layer, its function is unknown.

The septum of the *Arabidopsis* fruit is derived from the meristematic placentae which grow towards the centre of the gynoecium and usually fuse between stages two and four. The outer septum cells which line the locules develop morphologically similar to, but smaller than, those of ena and also disintegrate prior to dehiscence. However, esterase activity is slightly different in these two tissues. Strong esterase activity was detected in the outer septum cells just following fertilisation. During the growing phase the inner septum cells continually form aerenchymous tissue and there appears to be a little cell growth but no cell division. Prior to fertilisation, the inner septum cells are surrounded by an extracellular matrix which is stained red by acridine orange, indicative of a high pectin or RNA content. At the time of fertilisation the matrix showed high binding of both cellulase and pectinesterase cDNA probes although there are few cells in the aerenchymous central septum tissue. The extracellular matrix gradually disappears post fertilisation.

In the mature silique a basement wall is formed by thickening of the inner walls of the outer septum cells. When the cells disintegrate the basement wall is left intact, and appears macroscopically in dehisced siliques as a thin translucent membrane. In the early stages of septal development cells are biologically active however, in the late stages the role of the septum appears to be only supportive. Disruption of septal development by the vestigial gynoecium in the *clv1* silique appears only to affect fertilisation and does not affect development of the carpel walls or the dehiscence zones.

Dehiscence of the *Arabidopsis* silique involves a sequence of cytological and biochemical changes which occur within defined regions of the silique. These changes have many features in common with leaf abscission (Sexton & Roberts 1982) and dehiscence of *Brassica napus* pods (Meakin & Roberts 1990 a & b). The similarity to leaf abscission lends support to the early hypothesis that the fruit is a modified leaf. Prior to fertilisation it was not possible to determine cytologically or biochemically those cells which would eventually form the dehiscence zones. This suggests that some process during or after fertilisation may be a trigger for dehiscence zone formation. Just prior to and following fertilisation there is a marked increase in the size of the primary vascular bundles. Although the bundles are less likely to be involved in the induction of dehiscence, the increased lignification may be involved later in causing increased tensions within the dehiscence zones.

After fertilisation the dehiscence zones can first be distinguished cytologically on the basis of cell size, those of the putative dehiscence zones being the smallest, and consequently causing constrictions of the marginal carpel walls. No biochemical changes within the putative dehiscence zones are evident at this early stage, however, protease was first detected in the exocarp at stage six. The exocarp cells enlarge and secrete an outer cuticular layer. Differentiation of the exocarp is also likely to be involved in causing tensions within the dehiscence zones.

A major stage in the development of the dehiscence zone is the formation of the separation layers. The two to three layers of cells which form the separation layer begin to degrade prior to lignification of the adjacent cells which represent the edges of the valves. This suggests that the degradation is genetically or hormonally determined rather than being due to a decrease in the amount of assimilates reaching these cells. Although cell changes were not studied at an ultrastructural level, it is reasonable to presume that degradation is caused by middle lamellar breakdown as reported for *Brassica napus* pods (Meakin & Roberts 1990). Dehiscence zone formation in these two members of the Brassicacea show many histological similarities.

A cDNA probe to 9.5 cellulase, an enzyme long associated with abscission, identified cellular mRNA distribution in the septum of the mature gynoecium and the silique, and in 3-4 rows of valve wall mesocarp cells adjacent to the separation layer cells in the mature silique. Bean (*Phaseolus vulgaris*) has been used as a model to study leaf abscission. Immunocytochemical studies using an antibody to 9.5 cellulase, localised the protein to the separation layer cells and vascular tissue of the bean leaf abscission zone (Campillo *et al.* 1990). Cellulase was also localised in the dehiscence zone of *Brassica napus* (Meakin & Roberts 1990b). Hybridisation studies on bean leaf using a cDNA 9.5 cellulase probe identified cellulase mRNA activity in 2-3 layers of cells either side of the fracture plane and in the parenchymous cells of the stele (Tucker *et al.* 1991). Although cellulase has been proposed to be involved in dehiscence its actual function and its precise substrate are still unknown. We did not find cellulase mRNA in the separation layer cells. However, it is possible that if the enzyme is involved in degradation of the separation layer cells, it might diffuse from the cellulase-synthesising cells to act upon those in the separation layer.

Polygalacturonase mRNA was not detected in the *Arabidopsis* fruit even though it has been implicated by many authors as a major cells wall hydrolytic enzyme. Although this result is in agreement with those of Meakin & Roberts (1990b), who

found no relationship between polygalacturonase activity and dehiscence in oilseed rape, tomato fruit polygalacturonase has been shown to differ from that involved in tomato leaf abscission (Taylor *et al.* 1990). It is, therefore, possible that the tomato fruit enzyme shows no homology to polygalacturonase in the *Arabidopsis* fruit.

During development of the silique cells of the exocarp and endocarp undergo significant asymetric thickening. Lignification of 2-3 rows of cells on the valve side of the separation layer links these thickened cells of the endocarp and exocarp prior to valve detachment. This is likely to cause major tensions in the valves as the mesocarp dehydrates during senescence, with a consequent stress on the separation layer cells. Degradation of these cells causes a lack of cell cohesion and these tensions probably facilitate valve detachment. Separation layer cells were observed intact and adhered to the lignified valve edge and replum in dehisced siliques indicating that separation occurs along cell walls, possibly the middle lamella, rather than by rupture of cells. It is likely that, as proposed for oilseed rape, (Meakin & Roberts 1990), ethylene produced from the developing seeds may be instrumental in dehiscence. The uneven dehiscence of the clv1 silique may be a result of the underdeveloped seeds in the base of the silique.

We have described the histological development of the gynoecium and silique of *Arabidopsis thaliana* and identified tissue specific developmental processes which may result in the shatterable phenotype. We have identified histochemical markers associated with each of the major tissue types of the fruit wall. Protease has been identified in the exocarp, Rubisco in the mesocarp and esterase in the endocarp. We have also described and compared the histological development of the *clv1* mutant silique. Finally we have isolated EMS-induced mutants which show variation in silique development and structure.

FUTURE WORK

This thesis has mainly been concerned with the histological development of the major tissues of the developing *Arabidopsis* silique. We have identified the major tissue types concerned with the development of a shatterable fruit and its dehiscence mechanism, however, most of the control mechanisms involved are still unknown. Future study will include investigations into many of these possible control factors. We will continue to screen EMS treated stock for appropriate mutants and further characterise those mutants whose phenotype have been briefly described in this thesis.

APPENDIX 1

TISSUE PREPARATION

An aldehyde fixation protocol was used for all embedded material as this gave the best morphological preservation, providing the fixation time was long enough to allow penetration of whole tissue blocks. This was difficult with whole siliques as the outer cuticular layer is not very permeable, so the closed ends of each silique were excised, or siliques were cut in half to allow circulation of fixative to the inner tissues. Drews *et al.* (1991) reported that aldehyde fixation had proved unsuitable for *in situ* hybridization studies and formal acetic acid alcohol, FAA, gave superior results. We found that the time required for adequate fixation was at least double using FAA, tissue morphology was generally poor due to excessive shrinkage, and no significant increase in signal was observed with hybridization studies when compared to aldehyde fixed tissue.

L.R. White medium grade acrylic resin was chosen as the embedding medium for morphological studies for its low toxicity, excellent semi- and ultra-thin sectioning qualities, and its permeability to histochemical and immunohistochemical markers. A problem was encountered with this resin when tissues were post fixed in osmium tetroxide, the resin usually (but not always) partially polymerised to a gel during the first infiltration step. Post fixation was therefore avoided when using L.R. White. Resin sections were not suitable for all histochemical studies at L.M. level. This was probably due to either the impermeability of the resin to certain substances, the small amount of tissue present in 1μm sections, or the high temperatures used to polymerise the resin causing loss or changes in cellular composition. Paraplast wax was used to embed tissue for most histochemical studies. PEG was found to be an unsuitable embedding medium as various organs within flowers became mobile when the sections were floated out onto drops of water and frozen tissue sections were grossly distorted, even at 20 μm in thickness, likely caused by the inherent variations in the "hardness" of the tissue. However the wax infiltration step required long incubation times when hand processing and an unacceptable loss of cellular enzyme activity was often observed. One reason for this may have been inconsistencies in the temperature of the wax (by up to 12 ^{o}C) during infiltration depending upon the position of the sample in the laboratory oven. Dehydration and wax infiltration may be standardised by the use of an enclosed, automatic tissue processor which also reduces incubation times by processing under vacuum.

DETECTION METHODS

Due to the nature of aldehyde fixation (ALDEHYDE are cross-linking fixatives) tissue autofluorescence levels were high and at L.M. level masked weaker signals from fluorescent markers such as fluorescein which made photographing some signals very difficult. Immunocytochemical studies were performed on L.R. White sections using colloidal gold as the immunological conjugate with subsequent silver enhancement. We often experienced unacceptably high background silver deposition on wax embedded tissue and chose to use fluorescein conjugates. For *in situ* hybridisation studies alkaline phosphatase conjugates were used. Histochemical studies showed no endogenous alkaline phosphatase activity in tissue embedded in wax. NAMP/Fast Red TR were used as the substrates as the red reaction product is more readily distinguished using image analysis than the blue NBT/BCIP product.

REFERENCES

Albani D., Altosaar I., Arnison P. G. & Fabijanski S. F. (1991)
A gene showing sequence similarity to pectin esterase is specifically expressed in developing pollen of Brassica napus. Sequences in its 5' flanking region are conserved in other pollen specific promotors
Plant Molecular Biology 16: 501-513

Bowman J. L., Drews G. N., & Meyerowitz E. M. (1991)
Expression of the *Arabidopsis* floral homeotic gene AGAMOUS is restricted to specific cell types late in flower development
The Plant Cell 3: 749-758

Bowman J. L., Smith D. R., Meyerowitz E. M. (1989)
Genes directing flower development in *Arabidopsis*
The Plant Cell 1: 37-52

Bowman J. L., Smyth D. R., Meyerowitz E. M. (1991)
Genetic interactions among floral homeotic genes of *Arabidopsis*
Development 112: 1-20

Campillo E., Reid P. D. & Lewis L. N. (1990)
Occurrence and localisation of a 9.5 cellulase in abscising and nonabscissing tissues
The Plant Cell 2: 245-254

[Cercos M. & Carbonell J. (1993) in press]

Coen E. S. (1991)
The role of homeotic genes in flower development and evolution
Annual Review of Plant Physiology & Molecular Biology 42: 241-279

Coen E. S. & Meyerowitz E. M. (1991)
The war of the whorls: genetic interactions controlling flower development
Nature 353: 31-37

Coen E. S., Romero J. M., Doyle S., Elliott R., Murphy G. & Carpenter M. (1990)
Floricaula: a homeotic gene required for flower development in *Antirrhinun majus*
Cell 63: 1311-1322

Drews G. N., Bowman J. L., Meyerowitz E. M. (1991)
Negative regulation of the *Arabidopsis* homeotic gene agamous by the apetala2 product
Cell 65: 991-1002

Estelle M. A. Somerville C. R. (1986)
The mutants of *Arabidopsis*
Trends in Genetics 2: 89-93

Fisher R. L. & Bennett A. B. (1991)
Role of cell wall hydrolases in fruit ripening
Annual Review Plant Physiology & Plant Molecular Biology
42: 675-703

Gahan P. B. (1981)
An early cytochemical marker of commitment to stelar differentiation in meristems from dicotyledonous plants
Annuals of Botany 48: 769-775

Haughn G. W., Somerville C. R. (1988)
Genetic control of morphogenesis in *Arabidopsis*
Developmental Genetics 9: 73-89

Hill J. P., Lord E. (1989)
Floral development in *Arabidopsis thaliana*: a comparison of the wild type and the homeotic pistillata mutant
Canadian Journal of Botany 67: 2922-2936

Irish V. F., Sussex I. M. (1990)
Function of the apetala-1 gene during *Arabidopsis* floral development
The Plant Cell 2: 741-753

Jack T., Brockman L. L., Meyerowitz E. M. (1992)
The homeotic gene APETALA3 of *Arabidopsis thaliana* encodes a MADS box and is expressed in petals and stamens
Cell 68: 683-697

Jossefsson E. (1968)
Investigations into shattering resistance of cruciferous oil crops
Zeitschrift fur Pflanzenzuchtung 59: 384-396

Kadkol G. P., Beilharz V. C., Halloran G. M., Macmillan R. H. (1986)
Anatomical basis of shatter resistance in the oilseed *Brassicas*
Australian Journal of Botany 34: 595-601

Knox J. P. , Day S. Roberts K. (1989)
A set of cell surface glycoproteins forms an early marker of cell position, but not cell type, in the root apical meristem of *Daucus carota* L.
Development 106: 47-56

Knox J. P., Linstead P. J., King J., Cooper C., Roberts K. (1990)
Pectin esterification is spacially regulated both within cell walls and between developing tissues of root apices
Planta 181: 512-521

Komaki M. K., Okada K., Nishino E., Shimura Y. (1988)
Isolation and characterisation of novel mutants of *Arabidopsis thaliana* defective in flower development
Development 104: 195-203

Kunst, Klenz, Martinez-Zapater, Haughn (1989)
AP2 gene determines the identity of perianth organs in flowers of *Arabidopsis thaliana*
The Plant Cell 1: 1195-1208

Lord E. M. (1991)
The concepts of heterochrony and homeosis in the study of floral morphogenesis
Flowering News Letter 11: 4-13

Ma H., Yanofsky M. F., Meyerowitz E. M. (1991)
AGL1-AGL6, an *Arabidopsis* gene family with similarity to floral homeotic and transcription factor genes
Genes & Development 5: 484-495

Macmillan R. H. (1986)
Anatomical basis of shatter resistance in the oilseed *Brassicus*
Australian. Journal of Botany 34: 595-601

Marcus A., Greenberg J., Averyhart-Fullard V. (1991)
Repetitive proline-rich proteins in the extra cellular matrix of the plant cell
Physiologia Plantarum 81: 273-279

Markovic O. & Jornvall H. (1986)
Pectineseterase, the primary structure of the tomato enzyme
European Journal of Biochemistry 158: 455-462

Meakin P. J., Roberts J. A. (1990)a
Dehiscence of fruit in oilseed rape (*Brassica napus* L.)
1. anatomy of pod dehiscence
Journal of Experimental Botany 41: 995-1002

Meakin P. J., Roberts J. A. (1990)b
Dehiscence of fruit in oilseed rape (*Brassica napus* L.)
2. the role of cell wall degrading enzymes and ethylene.
Journal of Experimental Botany 41: 1003-1011

Meyerowitz E. M. (1989)
Arabidopsis, A useful weed
Cell 56: 263-269

Meyerowitz E. M., Pruitt R. E. (1985)
Arabidopsis thaliana and plant molecular genetics
Science 229: 1214-1218

Meyerowitz E. M., Smith D. R., Bowman J. L. (1989)
Abnormal flowers and pattern formation in floral development
Development 106: 209-217

Miksche J. P., Brown J. A. M. (1965)
Development of vegetative and floral meristems of *Arabidopsis thaliana*
American Journal of Botany 52(6): 533-537

Okada M., Komaki M. K. and Shimura Y. (1989)
Mutational analysis of pistil structure and development of *Arabidopsis thaliana*
Cell Differentiation and Development 28: 27-38

Ottoline Leyser H. M. & Furner I. J. (1992)
Characterisation of three shoot apical meristem mutants of *Arabidopsis thaliana*
Development (in press 1992)

Pennell R. I., Knox J. P., Scofield G. N., Selvendran R. R., Roberts K. (1989)
A family of abundant plasma membrane-associated glycoproteins related to the arabinogalactan proteins is unique to flowering plants
Journal of Cell Biology 108: 1967-1977

Polowick P. L., Sawhney V. K. (1986)
A scanning electron microscopic study on the initiation and development of floral organs of *Brassica napus* (cv. westar)
American Journal of Botany 73(2): 254-263

Ray J., Knapp J., Grierson D., Bird C. & Schuch W. (1988)
Identification and sequence determination of a cDNA clone for tomato pectin esterase
European Journal of Biochemistry 174: 119-124

Redei G. P. (1975)
Arabidopsis as a genetic tool
Annual Review of Genetics 9: 111-127

Schopfer P. (1990)
Cytochemical identification of arabinogalactan protein in the outer epidermal wall of maize coleoptiles
Planta 183: 139-142

Schultz E. A. & Haughn G. W. (1991)
LEAFY, a homeotic gene that regulates inflorescence development in *Arabidopsis*
The Plant Cell 3: 771-781

Schultz E. A. Pickett F. B. & Haughn G. W. (1991)
The FLO 10 gene product regulates the expression domain of homeotic genes AP3 and PI in *Arabidopsis*
The Plant Cell 3: 1221-1237

Schwartz-Sommer S., Hue E., Huijser P., Flor P. J., Hansen R., Tetens F., Lonnig W., Saedler H. & Sommer H. (1992)
Characterisation of the *Antirrhinum* floral homeotic MADS-box gene *Deficiens*: evidence for DNA binding and autoregulation of its persistent expression throughout flower development
The Embo Journal 11 251-263

Schwartz-Sommer S., Huijser P., Nacken W., Saedler H. & Sommer H. (1990)
Genetic control of flower development by homeotic genes in *Antirrhinun majus*
Science 250: 931-936

Sexton R. & Roberts J. A. (1982)
Cell biology of abscission
Annual Review Plant Physiology 33: 133-162

Shannon S. & Meeks-Wagner D. R. (1991)
A mutation in the *Arabidopsis* TFL1 gene affects inflorescence meristem development
The Plant Cell 3: 877-892

Smyth D. R., Bowman J. L., Meyerowitz E. M. (1990)
Early flower development in *Arabidopsis*
The Plant Cell 2: 755-767

Sommer H., Beltran J., Huijser P., Pape H., Lonnig W., Saedler H., & Schwartz-Sommer S. (1990)
Deficiens, a homeotic gene involved in the control of flower morphogenesis in *Antirrhinun majus*: the protein shows homology to transcription factors
The Embo journal 9: 605-613

Stacey N. J., Roberts K, Knox J. P (1990)
Patterns of expression of the JIM 4 arabinogalactan-protein epitope in cell cultures and during somatic embryogenesis in *Daucus carota* L.
Planta 180: 285-292

Taylor J. E., Tucker G. A., Lyssett Y., Smith C. J. S., Arnold C. M., Watson C. F., Schuch W., Grierson D. & Roberts J. A. (1990)
Polygalacturonase expression during leaf abscission of normal and transgenic tomato plants
Planta 183: 113-138

Tayto T. O., Morgan D. G. (1979)
Factors influencing flower and pod development in oilseed rape
Journal of Agriculture and Science 92: 363-373

Tucker M. L., Baird S. L. & Sexton R. (1991)
Bean leaf abscission: tissue specific accumulation of a cellulase mRNA
Planta 186: 52-57

[Vercher Y. & Harris N. (1993) in press]

Yanofsky M. F., Ma H., Bowman J. L., Drews G. N., Feldman K. A., Meyerowitz E. M. (1990)
The protein encoded by the *Arabidopsis* homeotic gene agamous resembles transcription factors
Nature 346: 35-39